

The Hydrochemical Fate and Transport of Treated Domestic Wastewater
Contaminants During a Wastewater Polishing Experiment in a Sub-Arctic Ladder
Fen Peatland

by

Colin Patrick McCarter

A thesis
presented to the University of Waterloo
in fulfillment for the degree of
Doctor of Philosophy
in
Geography

Waterloo, Ontario, Canada, 2016

© Colin Patrick McCarter 2016

Author's Declaration

This thesis consists of material all of which I authored or co-authored: see Statement of Contributions included in the thesis.

This is a true copy of the thesis, including any required final revisions, as accepted by my examiners

I understand that my thesis may be made electronically available to the public.

Statement of Contributions

This thesis is structured in accordance with the manuscript option. Chapters two, three, and four will be submitted for review; as such, the published papers may differ from the chapters presented here based on the comments from the peer review process.

Colin McCarter designed and executed the experiments and collected the resulting data. Colin McCarter wrote the first draft of all chapters herein, where Dr. J. Price, who acted as the advisor for this thesis, provided editorial comments on each chapter or manuscript. As the thesis advisor Dr. Price provided guidance on the research approach, field methods, experimental design, and comments and suggestions in the writing. Dr. Branfireun has provided guidance on the research approach, field methods, and experimental design throughout this thesis. Additionally, Dr. B. Branfireun is a co-author on Chapter 4 and as such, provided editorial comments to improve the manuscript. Dr. M. Kompanizare is a co-author on Appendix A and developed the mathematical solution for the single well transmissivity tests and provided editorial comments on Appendix A.

Abstract

Protecting northern aquatic ecosystems is critical to ensuring the sustained use of these environments; however, with increasing industrial and residential development pressures in this region the safe and effective treatment of domestic wastewater is becoming a concern. Globally, peatlands have been used successfully to treat and polish domestic wastewater in northern environments but there is a dearth of knowledge on contaminant transport in peatlands, specifically reactive contaminants; such as the constituents of domestic wastewater. Ladder fens act as the conveyers of water, and likely solutes, from the bog peatlands to the aquatic ecosystems and similar systems have been used for domestic wastewater treatment. Ladder fens consist of a pool-rib-pool topography where the flow of water is governed by the peat ribs and their associated microtopography. Within a given rib, there are two distinct microtopographies: topographically high ridges that impede water flow and topographically low preferential flow paths that enhance water flow during periods of high water tables. Thus, the hydrological, and potentially solute, connectivity is thought to be controlled by the surface elevation of the low-lying preferential flow paths. However, the mechanisms governing the hydrological connectivity of these systems is still relatively unknown. Furthermore, there is limited knowledge on the processes and mechanisms that govern the fate and transport of contaminants, such as domestic wastewater, in ladder fens. Understanding the processes and mechanisms governing the hydrology, solute transport, and contaminant removal is critical to safely and effectively using these systems for domestic wastewater treatment or polishing; thus, is the primary objective of this thesis.

To elucidate these processes and mechanisms in ladder fens, a continuous experimental simulated-domestic wastewater release occurred in 2014 (day of year 192 – 243) with an associated hydrological load (2014 – $38 \text{ m}^3 \text{ day}^{-1}$ and 2015 – $30 \text{ m}^3 \text{ day}^{-1}$) in a small sub-arctic ladder fen (EXP Fen) in the James Bay Lowland, Ontario, Canada approximately 100 km west of Attawapiskat. Typical domestic wastewater contaminants, nitrate (7.6 mg L^{-1}), ammonium (9.1 mg L^{-1}), and phosphate (7.4 mg L^{-1}), were injected into the EXP Fen, along with sulphate (27.2 mg L^{-1}), sodium (25.3 mg L^{-1}), and chloride (47.2 mg L^{-1}) to better mimic local domestic wastewater conditions. Given that sulphate can enhance the methylation of mercury in peatlands, total dissolved mercury (THg) and methylmercury (MeHg) concentrations were measured at the EXP

Fen in addition to the hydrological and biogeochemical conditions throughout the summers of 2014 and 2015. Prior to the experimental loading the background geochemical and hydrological conditions were monitored in 2013 at the EXP Fen and at 3 nearby reference sites (2013 – 2015).

The flow of water and solutes in ladder fens depends on the hydraulic conductivity and transmissivity distributions within the peat ribs and the surface elevation of the low-lying preferential flow paths. The low-lying preferential flow paths typically had higher hydraulic conductivity within the upper 0.1 m of the saturated peat than equivalent elevation in the ridges. Yet, overland flow events vastly increased the hydrological connectivity and runoff ratios exceed 1 during these events (when excluding the pumped water). Once overland flow occurred, the rate of water movement from the top of the system to the bottom decreased from weeks to hours. However, when the water table resides within the upper peat layers rapid conservative solute (chloride) transport was observed. The high hydraulic conductivity ($16 - 598 \text{ m day}^{-1}$) in upper peat layers resulted in high conservative solute velocities (1.9 m day^{-1}), while adsorptive (sodium) solute velocities were only slightly lower (1.1 m day^{-1}). Although the solute velocities were high, it was still lower than the average linear groundwater velocity (2.1 m day^{-1}), resulting in a retardation factor of 1.2 for chloride and 2.1 for sodium. The retardation factor for chloride, a conservative solute, greater than 1 was likely due to diffusion into the inactive porosity of the peat (0.29 – 0.44). This processes likely influenced all contaminants studied.

Similar to other treatment or polishing peatlands, the EXP Fen was highly effective at removing all contaminants from the pore water and no contaminants were detected at the site outflow. Nitrate was only transported 0.5 m into Rib 1, while ammonium (0.3 m day^{-1}) and phosphate (0.2 m day^{-1}) were transported further, yet were still relatively immobile. Initially, phosphate was completely immobile but the system saturated towards phosphate, resulting in a mobile contaminant. Sulphate, unlike the other contaminants, was very mobile (1.3 m day^{-1}) within the EXP Fen, more similar to chloride and sodium. Additionally, within the sulphate plume elevated THg and MeHg concentrations were observed compared to background and reference site concentrations. Methylmercury, as a percentage of THg, comprised 80 -100 % in the pore water but no MeHg was observed at the site outflow. The enhanced generation of MeHg and THg is potentially a concern when using ladder fens as wastewater polishing or treatment peatlands due

to the high mobility of sulphate. However, the efficient removal of all contaminants from the pore water suggests that ladder fens may be suitable for domestic wastewater treatment. Nevertheless, ensuring the water table is below the high hydraulic conductivity layers would greatly decrease the transport rates, thus increasing treatment, allowing for the safe operation of ladder fens as treatment wetlands.

Acknowledgements

Since starting at the University of Waterloo 11 years ago I have had an enormous amount of support from family, friends, and colleagues. Without your support over these many years I would not have gotten here.

To the Environment Department at the De Beers Group of Companies Victor Diamond Mine, thank you for providing me with the support and hospitality over the last 4 years. Your support has made the entire thesis possible and I cannot thank the entire Victor Mine, and specifically the Environment Department, enough. Additionally, I would like to thank the chefs and cooking staff at the Victor Mine for keeping me so well fed, allowing me to concentrate on field work, science, and billiards with Owen and Jake.

To my friends and colleagues Peter Whittington and Scott Ketcheson, thank you for guiding me through my graduate career and becoming good friends along the way. I appreciate everything you have done for me and want to thank you both for all your support, guidance, beers, and laughs over the years and I look forward to all the future beers and laughs. To James Sherwood and Corey Wells, you two have been integral over these long years either in the lab or the Grad House, thank you. I would like to thank everyone past and present in the Wetlands Hydrology Lab for their support, help, comradery, and beers over the last seven years.

Seven years ago I had the pleasure of meeting Dr. Jonathan Price in an undergraduate class. Since then, Jon has become a mentor, and more importantly, a good friend. Over that time you have pushed me to become a better academic, scientist, and person and for that I am eternally grateful. Most importantly, I would be remiss not to mention your thorough tutelage in scotch and cigars, it has been a most enjoyable and illuminating experience. I would additionally like to thank my committee members Dr. Brian Branfireun, Dr. Merrin Macrae, and Dr. William Quinton for all your help and guidance.

To my parents, thank you for everything you have done for me, I cannot put it into words how much I love you. Katie and John, I have a few cold IPA's waiting for you, I cannot wait to meet "nugget". Last but certainly not least, my fiancé Katharine, without you I would not be here today, doing what I love. I cannot wait to "take the plunge" with you and am so excited to spend the rest of my life with you talking about wetlands, planning, bees, and everything else under the sun. I love you so much.

Dedication

To my soon to be wife, Katharine, I cannot wait to continue our adventure together.

Table of Contents

Author's Declaration.....	ii
Statement of Contributions	iii
Abstract.....	iv
Acknowledgements.....	vii
Dedication.....	ix
Table of Contents.....	x
List of Figures	xiii
List of Tables	xvii
1 Introduction.....	1
1.1 Objectives.....	5
1.2 Organization of Thesis	6
2 Experimental hydrological forcing to illustrate water flow processes of a ladder fen in the James Bay Lowland, Canada	7
2.1 Summary	7
2.2 Introduction	7
2.3 Study Site	9
2.4 Methods.....	11
2.4.1 Field Methods	12
2.4.2 Hydraulic Conductivity and Transmissivity	14
2.5 Results	17
2.6 Discussion	22
2.7 Conclusions	26
2.8 Acknowledgements	27
3 The transport dynamics of chloride and sodium in a ladder fen during a continuous wastewater polishing experiment.....	28
3.1 Summary	28

3.2	Introduction	28
3.3	Study Site	31
3.4	Methods	33
3.4.1	Field Methods	34
3.4.2	Water Sampling and Analysis.....	35
3.4.3	Physical Soil Parameters.....	35
3.4.4	Pool Residence Times.....	36
3.4.5	Retardation Factors	37
3.5	Results	38
3.5.1	Solute Transport.....	41
3.6	Discussion	46
3.7	Conclusions	52
3.8	Acknowledgements	54
4	The transport and treatment of domestic wastewater contaminants enhances net methylmercury production in an undisturbed sub-arctic ladder fen peatland.....	55
4.1	Summary	55
4.2	Introduction	55
4.3	Study Site	59
4.4	Methods	60
4.4.1	Water and Soil Temperature	61
4.4.2	Water Sampling and Analysis.....	61
4.4.3	Treatment Efficiency (TE).....	63
4.5	Results	63
4.5.1	Contaminant Transport	66
4.5.2	Treatment Efficiency	69
4.5.3	Mercury.....	71
4.6	Discussion	72
4.6.1	Sulphate and Mercury	76
4.6.2	Ladder Fens as Wastewater Treatment Wetlands.....	77

4.7	Conclusions	79
4.8	Acknowledgements	80
5	Conclusions and Recommendations	81
	References.....	87
	Appendix A.....	97
	Rational	97
	Methods.....	98
	Results.....	101
	Discussion and Conclusions	102

List of Figures

Figure 2-1 A map of the EXP Fen with all relevant measurement points. Pools number increases to the south from Pool 1, where the hydrological loading occurred. Ribs are also numbered sequentially towards the south, where Rib 1 is the rib directly south of Pool 1. Hydraulic and elevation gradients are from north to south.....	10
Figure 2-2 Hydraulic conductivity distribution at the EXP Fen. The difference in maximum elevation is due to the differing surface elevations at the EXP Fen. Ribs 1-3 surface elevation is ~ 87.4 m asl, while the rest of the site is ~87.0 m asl.....	17
Figure 2-3 Water table elevations for Pool 1 (black), Pool 2 (grey), and at the end of the site (flume measurement point, dark grey) for the EXP Fen (top) and the three average water tables for the reference sites. Note no data at the reference sites in 2015 due to instrumentation limitations.	20
Figure 2-4 Total horizontal hydraulic gradients at the EXP Fen between water tables at Pool 1 and the flume measurement point. More negative indicates an increased hydraulic gradient.	20
Figure 2-5 Surface water discharge measured at the flume measurement point for all three years at the EXP Fen.....	21
Figure 2-6 A conceptual diagram of flow and connectivity in a typical pool-rib-pool sequence. The solid blue line is the high water table and the dashed blue line the low water table in 2014. The blue arrows represent idealized flow paths, where the longer the arrow the greater proportion of flow occurs in that region. The inset of is the hydraulic conductivity distribution determined for Rib 1 at the EXP Fen. The hydraulic conductivity within the upper few centimeters of peat governs the majority of flow during high water table periods.....	23
Figure 3-1 Map of the EXP Fen, adapted from Chapter 2.	32
Figure 3-2 Water table, precipitation (secondary y-axis) and C/C ₀ for chloride and sodium during the study period. Experimental loading occurred between the dashed lines (DOY 192 – 243). In-between the vertical dashed lines is the pumping period. The left column of graphs represents the pre-identified PFP's, while the right are the ridges. The approximate location of each microform within the site is represented by P (PFP) and R (ridge).	40

Figure 3-3 Bulk density, specific yield and effective porosity the EXP Fen divided into the northern half (north) and southern half (south). Shallow and deep refer to the depth of each sample: shallow = at the top of the water table and deep = ~ 1.5 m below the top of the water table. *** and * indicates significantly different at $p < 0.001$ and $P < 0.05$, respectively. Specific yield data presented by McCarter and Price (in review). 41

Figure 3-4 Chloride concentration iso-concentration map of the EXP Fen generated from the well water sample data during the experimental loading. Note the highly irregular plume development. 42

Figure 3-5 Sodium concentration iso-concentration map of the EXP Fen generated from the well water sample data during the experimental loading. Note the highly irregular plume development. 43

Figure 3-6 Chloride concentration in the pore water within the peat profile before (172), during (221) and after (257) experimental loading. Background chloride concentration (2013 and DOY 172) was $< 1 \text{ mg L}^{-1}$. The left column of graphs represents the pre-identified PFP's, while the right are the ridges. The approximate location of each microform within the site is represented by P (PFP) and R (ridge). Note, the elevation change on each graph representing the change in peat depth, where the top of each graph is the peat surface and the bottom is the mineral substrate surface. Peat depth decreases from north to south and is typically lower in the PFP's than the associated ridges. Dashed lines represent 50 % of C_0 44

Figure 3-7 Sodium concentration in the pore water within the peat profile before (172), during (221) and after (257) experimental loading. Background sodium concentration (2013 and DOY 172) was $< 1 \text{ mg L}^{-1}$. The left column of graphs represents the pre-identified PFP's, while the right are the ridges. The approximate location of each microform within the site is represented by P (PFP) and R (ridge). Note, the elevation change on each graph representing the change in peat depth, where the top of each graph is the peat surface and the bottom is the mineral substrate surface. Peat depth decreases from north to south and is typically lower in the PFP's than the associated ridges. Dashed lines = 50 % of C_0 45

Figure 4-1 A map of the EXP Fen adapted from Chapter 2. Pools are sequentially number from the input pool (north) towards the south. Ribs follow the same sequential numbering starting for the first rib down-gradient (south) from Pool 1. 59

Figure 4-2 Pool and pore water temperatures for the low-lying region of Rib 1 (mbgs), Pool 1 and Pool 2 (from surface (FS) and from bottom (FB)). There was not distinct differences in temperatures between Rib 1, 2, and 10 at a given depth..... 64

Figure 4-3 DOC concentrations at the EXP Fen ribs and pools, and the reference sites. Error bars are max/min. Pool samples represent only 1 replicate..... 65

Figure 4-4 pH at the EXP Fen ribs and pools, and reference sites. Error bars are max/min. Pool samples represent only 1 replicate..... 65

Figure 4-5 Ca^{2+} concentrations at the EXP Fen ribs and pools, and reference sites. Error bars are max/min. Pool samples represent only 1 replicate. 66

Figure 4-6 Manually interpolated NO_3^- and NH_4^+ concentration contour maps at the EXP over the study period. Input concentrations were 7.1 and 9.1 mg L^{-1} for NO_3^- and NH_4^+ , respectively. 67

Figure 4-7 Manually interpolated PO_4^{3-} concentration contour maps at the EXP over the study period. Input concentration 7.4 mg L^{-1} 68

Figure 4-8 Manually interpolated SO_4^{2-} concentration contour maps at the EXP over the study period. Input concentration 27.2 mg L^{-1} 69

Figure 4-9 Treatment efficiency (TE) for NO_3^- , SO_4^{2-} , NH_4^+ , and PO_4^{3-} in Rib 1 and Pool 1. 1st – 3rd nests refer to the position of a nest in proximity to Pool 1 along a given north-to-south transect (i.e., 1st nest are the 4 nests closest to Pool 1 and 3rd nests are furthest from Pool 1). Negative values indicate a net release of a given contaminant..... 70

Figure 4-10 Concentration of THg (black bars), MeHg (grey bars), and %MeHg (black line) in Pools 1 & 2, Rib 1, and the reference sites. Error bars are 1 standard deviation from the mean (n= 4 in the pools, 12 in the rib, and 16 at the reference sites). Note the two different y-axis, where the primary y-axis concentration and the secondary y-axis is the %MeHg. 71

Figure 4-11 The %MeHg overlaid with SO_4^{2-} contours for pre-loading 29 days after the experiment began, and post-loading (14 days after the experiment ceased). Both pre and post-loading SO_4^{2-} concentrations were below background levels..... 72

Figure A - 1 Linear regression between piezometer measured log10 K and the integrated log10 K determined by integrating the transmissivity curve over the piezometer screen opening depth. The lumped regression (dashed black line) accounts for all measurements, while hydraulic

conductivities greater than 1 m day^{-1} (dark grey points and line) and less than 1 m day^{-1} (grey points and line) were separated. 102

Figure A - 2 K' vs screen length for all nine tested wells. 103

Figure A - 3 Hydraulic conductivity distribution at the EXP Fen. Above 0.3 m the hydraulic conductivity was determined through the packer method, while below 0.3 m the values were determined from the piezometer tests. The difference in maximum elevation is due to the differing surface elevations at the EXP Fen. Ribs 1-3 surface elevation is $\sim 87.4 \text{ m asl}$, while the rest of the site is $\sim 87.0 \text{ m asl}$ 104

List of Tables

Table 2-1 Inter-year comparison of hydrological parameters available for 2013 -2015 (DOY 177 - 234). Outputs from the EXP Fen displayed as negatives and inputs as positive. The change in storage was calculated as the total change in water table elevation over the study period multiplied by the measured specific yield. The residual term is a combination of the total error and the groundwater fluxes.....	19
Table 2-2 Runoff ratios for all measured months. Pumping input were not included in these estimates, when included runoff ratios decrease to <0.04 during pumping in both 2014 and 2015.	22
Table 3-1 Average (\pm S.D.) pool residence time for the first 4 pools over the entire study period. Due to limited well installations it was not possible to calculate residence times for other pools; however, pool volumes were <3 m ³	42
Table 3-2 The hydraulic conductivity of the upper 10 cm and 25 cm of the saturated peat profile determined by Chapter 2, maximum transmissivity, average n_e , v , and v_s for the regions within the bulk of the solute plume. No data is available beyond Rib 3 until Rib 8, where the plume was not observed, due to lack of instrumentation. East and West Bog refers to the lateral bogs to the east and west of the site.....	43

1 Introduction

With the discovery and subsequent development of mineral resources in the James Bay Lowland (JBL), the potential for contaminants to enter these ecosystems has increased. Furthermore, the development and operation of mining camps results in the generation of domestic wastewater that must be safely and efficiently treated prior to release into the surrounding ecosystems. Domestic wastewater is usually elevated in nutrients (i.e., nitrate, ammonium, phosphate, etc.) (Kadlec & Wallace, 2009), while many of the ecosystems in the JBL, specifically peatlands, are limited towards these nutrients and many base cations (Campbell & Bergeron, 2012; Ulanowski & Branfireun, 2013). Additionally, peatlands have been used to treat (Yates *et al.*, 2012) and polish domestic wastewater (Kadlec, 2009a; Ronkanen & Klove, 2009) in northern environments, similar to the JBL. However, there is little information on the transport and fate of many of these domestic wastewater contaminants and associated hydrology in peatlands in general.

The JBL is part of the Hudson Bay Lowlands, which is the second largest wetland complex in the world (Gorham, 2008), comprising a mosaic of bog and fen peatlands (~90 % of the land cover) and small areas of mineral uplands along river channels (Riley, 2011). Underlying the peatlands is a marine origin mineral sediment (Price & Woo, 1988; Whittington & Price, 2013) that was deposited ~8000 years ago with the generation of the Tyrell Sea (Lee, 1960). The mineral sediments, which can be several hundreds of metres thick (Dredge & Cowan, 1989), limit the percolation of water from the peatlands to the regional aquifers due to low hydraulic conductivities (Whittington & Price, 2013). As such, the primary loss of water during the ice-free season is through evapotranspiration (Leclair *et al.*, 2015; Reeve *et al.*, 2000), with minimal runoff (Richardson *et al.*, 2012) or groundwater flow to the surrounding aquatic ecosystems (Leclair, 2015; Perras, 2015; Richardson *et al.*, 2012). However, during periods of high or perched water tables, the hydrological connectivity of the landscape is very high, often generating overland flow (Price & Maloney, 1994; Quinton & Roulet, 1998; Richardson *et al.*, 2012) through the ladder fen peatlands that drain the large bog complexes found in the JBL (Leclair, 2015; Perras, 2015; Siegel & Glaser, 1987). However, there remains a dearth of knowledge regarding the mechanisms and

processes that govern the flow and transport of both water and solutes within peatlands, which limits our ability to safely use these systems for wastewater polishing or treatment.

In large peatland complexes, the bogs provide a water storage role within the landscape and fens are the conveyers of water that shuttle water from the bogs to the aquatic ecosystems during periods of high landscape hydrological connectivity (Quinton *et al.*, 2003; Siegel & Glaser, 1987). Both ladder fens and the larger ribbed fens consist of a pool-rib-pool morphology where the peat ribs are orientated perpendicular to the direction of water flow (Leclair, 2015; Perras, 2015; Price & Maloney, 1994; Quinton & Roulet, 1998). The transmission of water through these systems relies on a spill-and-fill mechanism (Spence & Woo, 2003), where a threshold water table elevation is required to generate flow between pools (Price & Maloney, 1994; Quinton & Roulet, 1998). Typically the threshold has been assumed to be the peat surface, where once the water table exceeds the surface, overland flow occurs (Quinton & Roulet, 1998); however, high hydraulic conductivity peat can result in similar hydrological connectivity but this process has only been identified in one study (Price & Maloney, 1994). Thus, it has been assumed that the fill-and-spill mechanism is primarily controlled by rib topography (i.e., topographical microform), either the low-lying preferential flow paths (PFP) that increase connectivity or the topographically higher ridges that impede water flow (Price & Maloney, 1994; Quinton & Roulet, 1998). Although there is a broad understanding of the processes that govern water flow in ladder fens, the specific hydrological mechanisms are still unknown. Furthermore, there is no known information on solute transport within ladder fens that is vital to understand when using these systems for wastewater treatment or polishing.

At the field scale, solute transport in peatlands is at best poorly understood as there are only two published field scale solute transport studies (Baird & Gaffney, 2000; Hoag & Price, 1995). These two studies have resulted in a broad understanding of the processes governing solute transport, where the majority of solute is transported within the near surface high hydraulic conductivity layers (Baird & Gaffney, 2000; Hoag & Price, 1995) and limited vertical advection occurs due to the inherent anisotropy of peat (Beckwith *et al.*, 2003b, 2003a). Furthermore, peat inherently retards solutes, both reactive and conservative, due to the diffusion of solutes into an inactive porosity, which accounts for 40 – 90 % of the total porosity (Hoag & Price, 1997; Ours *et*

al., 1997; Rezanezhad *et al.*, 2012). Thus, advection only occurs within the effective, or active, porosity that represents 10 – 60 % of the total porosity (Hoag & Price, 1997; Ours *et al.*, 1997; Rezanezhad *et al.*, 2012) and typically decreases with depth and, by extension, state of decomposition (Hoag & Price, 1997; Quinton *et al.*, 2000). Long term storage of solutes within the inactive porosity is unlikely unless the concentration of the solute in the active porosity remains constant over time (Hoag & Price, 1997; Ours *et al.*, 1997). Furthermore, peat has a high cation exchange capacity (Gogo *et al.*, 2010; Kyzoil, 2002; Rippey & Nelson, 2007) that can remove some contaminants through geochemical adsorption (Heiberg *et al.*, 2012; Ho & McKay, 1999; Kyzoil, 2002). In addition to adsorption, the sorption of phosphate and other anions (Gerke & Hermann, 1992; Seo *et al.*, 2005) to the organic molecules can further retard reactive solutes. Thus, the geochemistry of peat and peatlands, and by extension ladder fens, creates an environment well suited for contaminant treatment. However, there has yet to be a reactive solute transport study at the field scale and no experimental field scale study of the fate and transport of domestic wastewater within ladder fens in sub-arctic Canada.

The geochemistry of peatlands within the JBL follows the typical patterns observed globally (Boeye & Verheyen, 1994; Fraser *et al.*, 2001; Rydin & Jeglum, 2009; Vitt *et al.*, 2003; Vitt *et al.*, 1993; Wind-Mulder *et al.*, 1996), where *Sphagnum* moss dominated systems are low in base cations, nutrients and pH, while sedge or woody dominated fen peatlands have higher pH and dissolved minerals (Glaser *et al.*, 2004; Ulanowski & Branfireun, 2013). The high water tables of these peatlands create anoxic conditions that limits the decomposition of organic matter, allowing for an abundance of available labile organic matter for biogeochemical processes (Bengtsson *et al.*, 2016; Boelter, 1969; Bonnett *et al.*, 2006; Cabezas *et al.*, 2012; Moore *et al.*, 2005). Yet, many of these peatlands are nutrient limited, particularly towards nitrogen and phosphorus (Campbell & Bergeron, 2012) and would likely provide the rapid removal of nitrate, ammonium and phosphate, due to these limitations, during domestic wastewater treatment or polishing. Furthermore, the anoxic conditions increases the microbial demand for oxidizing chemical species, such as nitrate or sulphate (Blodau *et al.*, 2009; Bottrell *et al.*, 2007; Heiberg *et al.*, 2012; Niedermeier & Robinson, 2007; Rubol *et al.*, 2012). Under these anoxic conditions sulphate undergoes microbial reduction that mediates the production of methylmercury in peatlands (Coleman Wasik *et al.*, 2015; Coleman Wasik *et al.*, 2012; Compeau & Bartha, 1985; Gilmour *et al.*, 1992; Hoggarth *et*

al., 2015; Mitchell *et al.*, 2008). Furthermore, increases in sulphate concentrations have been linked to increases in methylmercury in plot-scale peatland experiments (Branfireun *et al.*, 2001; Branfireun *et al.*, 1999; Coleman Wasik *et al.*, 2015; Coleman Wasik *et al.*, 2012; Mitchell *et al.*, 2008); however, sulphate concentrations are typically low in peatlands (Brown & Macqueen, 1985; Koerselman *et al.*, 1993; Ulanowski & Branfireun, 2013). Although sulphate is usually not found in high concentrations in domestic wastewater (Kadlec & Wallace, 2009), elevated sulphate concentrations of the pore water in the regional aquifers has been observed in the JBL (Boucher, 2012) that may increase the sulphate concentration of the domestic wastewater from mining camps. Consequently, it is unknown if treating domestic wastewater with elevated sulphate concentrations will also produce an increase in methylmercury and what the potential magnitude of this response may be. Furthermore, there is limited information on the fate of many wastewater contaminants in the peatlands of the JBL and represents a critical gap in knowledge to using these systems safely and effectively for domestic wastewater treatment or polishing.

Globally, peatlands have been used for wastewater treatment (Yates *et al.*, 2012) or polishing (Eskelinen *et al.*, 2015; Kadlec, 2009a; Palmer *et al.*, 2015; Postila *et al.*, 2015; Ronkanen & Kløve, 2009; Ronkanen & Kløve, 2007, 2008; Yates *et al.*, 2012) in northern environments, having near complete removal of both biological (i.e., bacteria or parasites) (Eskelinen *et al.*, 2015; Kadlec, 2009) and chemical (i.e., nitrate, ammonium, total nitrogen, phosphate, total phosphorous, sulphate, etc.) contaminants (Eskelinen *et al.*, 2015; Kadlec, 2009a; Palmer *et al.*, 2015; Postila *et al.*, 2015; Ronkanen & Kløve, 2009; Ronkanen & Kløve, 2007, 2008; Yates *et al.*, 2012). Typically, a combination of both open water and subsurface treatment wetland types allows for the effective treatment of a variety of contaminants (Kadlec & Wallace, 2009) but many treatment peatlands lack this combination (Kadlec, 2009a; Ronkanen & Kløve, 2008). However, ladder fens naturally provide both subsurface (peat ribs) and open water (pools) treatment. Although the morphology of ladder fens is conducive to domestic wastewater treatment, the pH (~5 – 6) is lower in natural occurring ladder fen peatlands (Ulanowski & Branfireun, 2013) than typical treatment wetlands (~7 – 8) (Kadlec & Wallace, 2009; Kim *et al.*, 2011; Lee *et al.*, 2012) and may decrease the efficiency of the biogeochemical processes that remove domestic wastewater contaminants. Notwithstanding differences between natural and constructed wetlands, the few natural treatment or polishing peatlands have near complete removal of contaminants.

These natural treatment peatlands take advantage of the high organic content of the peat, which facilitates both biological (Cabezas *et al.*, 2013; Kim *et al.*, 2011; Ronkanen & Klove, 2009; Vymazal, 2007; Xing *et al.*, 2011) and geochemical removal (do Carmo Horta & Torrent, 2007; Gerke & Hermann, 1992; Heiberg *et al.*, 2012; Morris & Hesterberg, 2012; Noe *et al.*, 2003; Palmer *et al.*, 2015; Ronkanen & Klove, 2009; Staunton & Leprince, 1996; Xing *et al.*, 2011; Zak *et al.*, 2010). Although the mechanisms of domestic wastewater treatment in natural peatlands are well understood, it is unknown if ladder fens are suitable for wastewater treatment or polishing in remote northern environments, such as the JBL.

1.1 Objectives

The solute transport, hydrology, mercury dynamics, and biogeochemistry in ladder fens are intricately linked; consequently, it is critical to understand the how these different processes control the fate and transport of domestic and internally produced wastewater contaminants. Therefore the overall objective is to determine the hydrochemical processes and mechanisms governing the fate and transport of domestic wastewater in ladder fens during a wastewater polishing experiment at the field scale. The specific objectives are to:

1. Assess the hydrological processes governing the hydrological connectivity in ladder fens,
2. Determine the processes influencing the transport of conservative (chloride), adsorptive (sodium), and wastewater solutes under increased hydrological loading,
3. Identify the fate of typical domestic wastewater contaminants (nitrate, ammonium, and phosphate) during a wastewater polishing experiment,
4. Ascertain whether the elevated sulphate concentrations, similar to the groundwater of the JBL, could influence mercury dynamics during wastewater polishing, and
5. Comment on the suitability of ladder fens for domestic wastewater treatment in remote sub-arctic regions.

This thesis did not evaluate the transport and fate of elevated organic matter that is often associated with wastewater, pathogens such as bacteria and viruses, or other wastewater constituents that are of emerging concern, such as pharmaceuticals.

1.2 Organization of Thesis

This thesis comprises five chapters following the manuscript option at the University of Waterloo. The introduction, Chapter 1, presents the general concepts, background information and objective of the thesis, where specific concepts are expanded upon within each chapter as required. As such, care has been taken to limit duplication within the introduction and conclusions (Chapter 5) with the rest of the thesis.

Chapters 2 – 4 are the results and analysis of empirical research of a field scale wastewater polishing experiment in a sub-arctic ladder fen. The hydrology of ladder fens under high water tables and the processes governing the hydrological connectivity is presented in Chapter 2 and specifically addressing objective 1. The transport of conservative and adsorptive solutes (objective 2) under wastewater polishing conditions (i.e., elevated water tables and hydrological connectivity) is presented in Chapter 3. Finally, Chapter 4 investigates the transport and fate of domestic wastewater contaminants and sulphate during a domestic wastewater polishing experiment, addressing objectives 3 and 4.

The final chapter (5) are overall conclusions and recommendations for future research and best management practices for the safe and effective use of ladder fens for domestic wastewater treatment and polishing.

An appendix (A), at the end of the thesis, is attached to provide the mathematical development of the transmissivity calculations and comparison to measured piezometer hydraulic conductivity values.

2 Experimental hydrological forcing to illustrate water flow processes of a ladder fen in the James Bay Lowland, Canada

2.1 Summary

Large peatland complexes dominate the landscape of the James Bay Lowland (JBL) in sub-arctic Ontario, Canada. However, there is not an in-depth understanding of the hydrological processes occurring in these important systems, particularly how ladder fens connect large domed bogs to the aquatic ecosystems that drain the peatland complex. To assess the hydrological connectivity, the role of the water table, peat transmissivity, and microtopography of a small ladder fen, dominated by rib and pool microtopography, was studied for 3 summers (2013-2015) in the JBL. The system was manipulated with a sustained hydrological forcing (water addition) to the top of the system during 2014 ($38 \text{ m}^3 \text{ day}^{-1}$) and 2015 ($30 \text{ m}^3 \text{ day}^{-1}$). There was an exponential increase in transmissivity towards the peat surface due to extremely high hydraulic conductivities within the upper few centimeters of the peat deposit. In the upper few centimeters of peat, hydraulic conductivity varied depending on peat microtopography (preferential flow paths = $42 - 598 \text{ m day}^{-1}$ and ridges = $16 - 52 \text{ m day}^{-1}$), resulting in high hydrological connectivity periods. Furthermore, during 2015 there was an abnormally large amount of precipitation (300 mm vs. long-term average $\sim 100 \text{ mm}$) that resulted in complete surface water connectivity of the site, which caused rapid movement of water from the top of system to the outlet ($\sim 15 \text{ hr}$) and runoff ratios >1 , compared to low water table periods (runoff ratio ~ 0.05). Through understanding the periods of high connectivity within ladder fens, and by extension the landscape, this study highlights the importance of ladder fens on water retention and drainage, and potentially on solute transport, within these landscapes.

2.2 Introduction

In large peatland complexes, fen peatlands are considered the conveyers of water, while bog peatlands typically provide a water storage role (Quinton *et al.*, 2003) and release water to fen peatlands (Siegel & Glaser, 1987). Fen peatlands typically receive shallow groundwater from the

larger domed bogs and represent an important interface between the terrestrial peatlands and surrounding aquatic ecosystems (Glaser *et al.*, 1981; Reeve *et al.*, 1996; Siegel & Glaser, 1987). The quantity and timing of runoff generation from these peatlands depends on the proportion of bogs and fens within a catchment, whereas a greater proportion of fens typically results in higher runoff and more rapid responses (Richardson *et al.*, 2012). Many large domed bogs are drained by internal fen water tracks (Glaser *et al.*, 2004); these are classified as “ladder fens” in the Canadian Wetland Classification System (National Wetlands Working Group, 1997). These are within the bog margin and focus bog water discharge, particularly once threshold storage has been exceeded (Leclair, 2015; Quinton *et al.*, 2003; Ulanowski, 2014). Ladder fens are typically geochemically distinct, with elevated base cations and pH (Perras, 2015), compared to the bogs they drain. However, determining the hydrological connectivity of these systems is critical to understanding the movement of water and solutes within large peatland complexes to the down-gradient aquatic ecosystems.

Ladder fens consist of a pool-rib-pool topography similar to the larger scale ribbed fens, where the hydrological connectivity pool-to-pool is inversely related to the size and directly related hydraulic conductivity of the peat rib (Price & Maloney, 1994). Ribbed fens exhibit a fill-and-spill hydrology where a threshold water table is required to generate flow through the peat ribs to the down-gradient pools (Price & Maloney, 1994; Quinton *et al.*, 2003; Quinton *et al.*, 2000; Roulet, 1991). Typically, the fill-and-spill mechanism is a combination of flow through the high hydraulic conductivity layers (Chason & Siegel, 1986; Price & Maloney, 1994; Ulanowski, 2014) of the peat ribs, or as diffuse flow over the peat ribs through vegetation (Price & Maloney, 1994; Roulet, 1991) and the pool-to-pool connectivity will control the maximum flow rate through the fen (Quinton *et al.*, 2003; Quinton & Roulet, 1998). The majority of flow over the ribs occurs as rivulets on or around the ribs during periods of high water table (Quinton & Roulet, 1998). During low water periods, flow through the ribs has been assumed negligible due to low hydraulic gradients (Quinton & Roulet, 1998) and the exponential decrease in transmissivity (T) as water table declines (Leclair, 2015; Perras, 2015). However, Price and Maloney (1994) found hydraulic conductivities several orders of magnitude higher than Quinton and Roulet (1998) that did not decrease substantially with water table decline; thus, the pool-to-pool connectivity could still be relatively high during periods of low water tables depending on local site conditions. Nevertheless,

the upper peat layers typically have very high hydraulic conductivities (Carey *et al.*, 2007; Quinton *et al.*, 2008; Surridge *et al.*, 2005; Ulanowski, 2014) through which most water (and solutes) move (Ulanowski, 2014). Perras (2015) found ~5 fold increase in DOC flux during high water table (i.e., high hydrological connectivity) periods in ladder fens in the James Bay Lowland (JBL). Furthermore, ladder fens have been found to drain the surrounding bogs as a single source area during periods of elevated hydrological connectivity through high hydraulic conductivity layers (Ulanowski, 2014). Thus, during periods with high water tables (i.e., spring freshet and autumn wet-up), a substantial proportion of the nutrients, and potentially contaminants (i.e., methylmercury) (Kirk & St. Louis, 2009; Ulanowski, 2014), could leave the peatland complexes and enter downstream aquatic stream ecosystems.

Ladder fens control the drainage of water, and by extension solutes, from bog peatlands into aquatic ecosystems and the flux of both are governed by the fill-and-spill mechanism. However, there is only a broad understanding of this mechanism in ladder fens, which is typically assumed to be controlled by surface water flow. Given the exponential increase in T with water table height in ladder fens, it is likely that high hydrological connectivity would occur without overland flow, similar to some ribbed fens, but there is not yet an in-depth understanding of these processes in ladder fens. Therefore, the objectives of this study are to:

1. Further explore role of the peat ribs and changes in T in governing the hydrological connectivity of ladder fens,
2. Assess the ability of these systems to export water under periods of intense hydrological loading (e.g., high water tables) through a continuous water table manipulation experiment.

2.3 Study Site

The study site (EXP Fen) (N 5860348.772, E 705883.366) is located in the JBL, ~ 90 km west of Attawapiskat near the De Beers Group of Companies Victor Diamond Mine. Regionally, two long-term (1971 – 2000) meteorological records are available from Moosonee (coastal, 250 km southeast) and Lansdowne House (inland, 300 km southwest) and a nine-year record from the Victor Mine meteorological monitoring station. During July and August, regional average meteorological conditions at Moosonee (14.9 °C and 90 mm) (Environment Canada, 2015a) and

Lansdowne House (16.4 °C and 105 mm) (Environment Canada, 2015b) were similar and agreed well with the local meteorological monitoring station (15.6 °C and 154 mm).

The peatland complex is characterized by 1.5 – 2.5 m of peat overlying fine-grained mineral sediment and a deep Silurian limestone aquifer. Dewatering of the mine pit has depressurized the deep limestone aquifer, enhancing recharge from the peatlands proximal to the mine (Whittington & Price, 2012; Whittington & Price, 2013). The cone of depression did not extend to the EXP Fen in 2011 (Leclair et al. 2015) and at the time of this study (2013-2015) the cone of depression beneath the EXP Fen was ~2 m in the underlying limestone aquifer (Monninger, 2015). The underlying mineral sediments have a relatively low hydraulic conductivity (5.2×10^{-5} m day⁻¹) that helps protect against enhanced percolation losses (Whittington & Price, 2013), so the

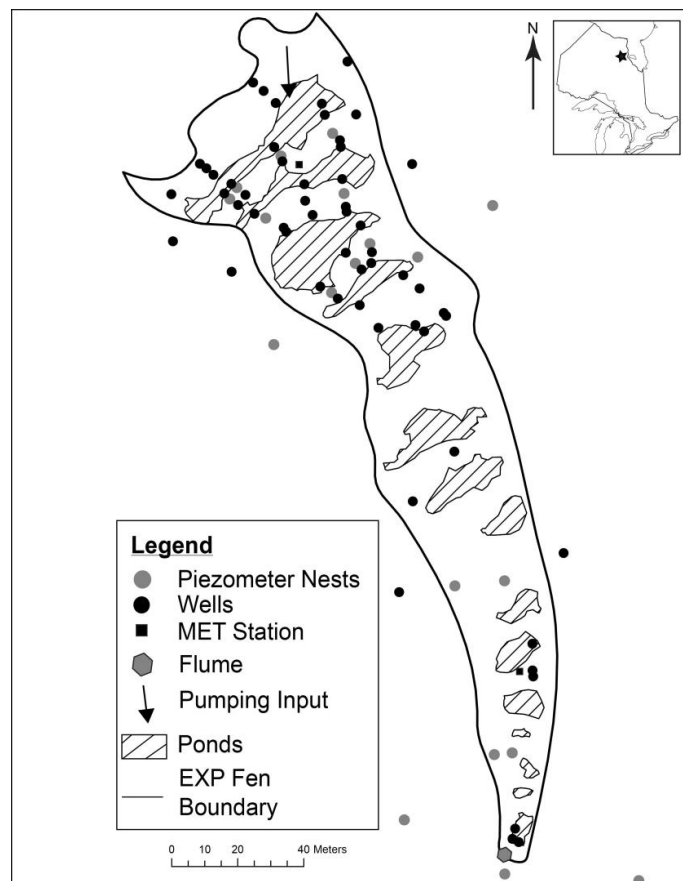


Figure 2-1 A map of the EXP Fen with all relevant measurement points. Pools number increases to the south from Pool 1, where the hydrological loading occurred. Ribs are also numbered sequentially towards the south, where Rib 1 is the rib directly south of Pool 1. Hydraulic and elevation gradients are from north to south.

effect of the drawdown from the mineral sediment was minor compared to the scale of evapotranspiration fluxes experienced at the site (Leclair et al. 2015). The EXP Fen was found to be similar in hydrological function, response to atmospheric conditions (i.e., wetting and drying events) and DOC export to three other nearby ladder fens of similar size and form, all located progressively closer to the mine (Perras, 2015) and is similar to a nearby (~5 km) ladder fen (Ulanowski, 2014), designated Reference Site 3 in this study.

The EXP Fen exhibits a pool-rib-pool morphology (Figure 2-1), similar to other ladder fens in the region. The direction of water flow is perpendicular to the peat ribs, with 0.67 m elevation decline over 250 m. Pools and ribs are numbered

incrementally with the northern-most pool as Pool 1 and immediately downslope (south) is Rib 1. The area of the EXP Fen (9800 m²) and the pools (2240 m²) and peat ribs (7560 m²) was delineated through a combination of air photo interpretation and DGPS surveys. Peat depth was greatest in the north, between 1.85 - 2.45 m (average 2.05 m), decreasing along the flow path towards the south where average peat depth is 1.85 m. Within individual ribs, surface elevation variability is about 0.2 – 0.5 m between the low-lying Preferential Flow Paths (PFP) and ridges. For example, low-lying PFP were typically ~0.3 m lower than the crest of the rib. The site is laterally (west and east) bound by two bogs, a large pool to the north, and the north branch of North Granny Creek to the south. The bogs and up-gradient pool typically contribute groundwater to the EXP Fen (Perras, 2015). There are two distinct vegetation zones within the EXP Fen; the northern half exhibits poor fen vegetation and the south host's moderate rich fen vegetation. Between Pools 7-10 (Figure 2-1) there is a large flat expanse of *Sphagnum rubellum* with minimal pool-rib-pool morphology. There are three nearby reference sites that are well beyond the influence of the mine's aquifer drawdown (Monninger, 2015). These include Reference Site 1 – N 5860348.772, E 705883.366; Reference Site 2 – N 5860472.091, E 705811.312; and Reference Site 3 – N 5860472.091, E 705811.312. They have similar topography, vegetation, and peat depth; their hydrology was monitored to better understand natural variability of these systems.

2.4 Methods

The EXP Fen was intensively studied in 2013 (day of year, DOY, 170 – 287), 2014 (DOY 156 – 287), and 2015 (DOY 177 – 235). The three reference sites were monitored for water table elevation and vertical hydraulic gradients over the same time periods; however, inclement weather and equipment availability prevented regular access to the reference sites in 2015 because they are accessible only by helicopter. Inter-year comparison was performed solely on the overlapping time periods (DOY 177 – 235) but all data collected are presented here. During 2014 and 2015, a point source hydrological load was applied to the EXP Fen at an average rate of 38 m³ day⁻¹ (2014, DOY 192 – 243) and 30 m³ day⁻¹ (2015, DOY 185 – 226) to raise the average water table and monitor the hydrologic response, simulating natural periods of high hydrological connectivity (i.e., high water tables). A short pumping trial occurred in 2013 (50 m³ day⁻¹, DOY 218 – 223). The water supply was provided by a solar powered pump from a nearby (170 m) bog pool complex. Water

was pumped into a 23 L bucket fitted with a v-notch, before discharging into Pool 1. A stage-discharge relationship was determined for the bucket weir, which was equipped with a Slumberger micro-diver to continuously record its water level.

2.4.1 Field Methods

Manual measurements of water table and hydraulic head occurred at least every 4 days at the EXP Fen and every 10 days at reference sites in 2013 and 2014, while bi-weekly measurements were performed at the EXP Fen in 2015. Wells (1.25 m slotted intake, 0.025 m I.D., 0.034 m O.D.) and piezometers (0.25 m slotted intake, 0.025 m I.D., 0.034 m O.D.) were constructed with PVC pipes; piezometer screens were centred at 0.125, 0.375, 0.675, 1.125 m bgs and 0.125 m above the mineral sediment substrate. Both wells and piezometers were screened with a geochemically inert geotextile filter sock (Rice Engineering & Operating LTD., 2" Filter Sock) over the entire open screen length. The wells at each of the 13 piezometer nests at the EXP Fen (Figure 2-1) were fully penetrating (1.85 – 2.45 m slotted intake, 0.052 m I.D., and 0.062 m O.D). Piezometer nests were preferentially installed in a mixture of PFP's and Ridges using visual identification of microforms based on elevation. At the three reference sites, a total of 18 piezometer nests (six nests per site) with accompanying 1.25 m slotted intake wells were installed, along with wells used to measure water level in two pools per reference site. Slumberger micro-divers were used to continuously record water table at the EXP Fen and reference sites and barometrically corrected with a Schlumberger baro-diver recording at the same frequency.

Meteorological conditions were recorded on Campbell Scientific CR1000 data loggers measuring every 5 seconds and averaging over twenty minutes. Net radiation (Q^*) was measured with net radiometers (REBS Q7.1 Net Radiometer) over Rib 1 and Pool 1, and ground heat flux (Q_g) was measured with a heat flux plate (REBS HFT3) installed 0.05 m bgs in Rib 1. Precipitation (P) was measured using a tipping bucket rain gauge (Texas Instruments TE525M-L tipping bucket rain gauge), with values totalled every 20 minutes. Wind speed (METOne 14A Anemometer) was measured at 1 and 3 m above Rib 1. Air temperature and relative humidity were measured with a weather enclosed HOBO UX100-023 Temperature/RH Data Logger.

Daily evapotranspiration (ET) was estimated separately for the peat ribs (ET_r) and pools (E_p) and fractionally weighted based on their aerial coverage and then summed to determine a site estimate of ET for the EXP Fen. The area of the pools was determined by a DGPS bathymetric survey of the pools and adjusted for changes in pools surface area based on water table height. The Priestley and Taylor (1972) combination method was used to determine ET_r , where

$$ET_r = \alpha \left(\frac{s}{s + \gamma} \right) \left(\frac{Q^* - Q_g}{L_v \cdot \rho_w} \right) \quad \text{Equation 2-1}$$

and where α is the coefficient of evaporability, s is the slope of the saturation pressure vs. temperature curve ($\text{Pa } ^\circ\text{C}^{-1}$), γ is the psychrometric constant ($\text{Pa } ^\circ\text{C}^{-1}$), Q^* is the net radiation flux (J day^{-1}), Q_g is the ground heat flux (J day^{-1}), L_v is the latent heat of vaporization (J kg^{-1}), and ρ_w is the density of water (kg m^{-3}). A site-specific α value was determined by the slope of the line relating actual evapotranspiration to equilibrium evapotranspiration, which is determined by Equation 2-1 when $\alpha = 1$. To determine actual evapotranspiration, six weighing lysimeters were placed throughout the EXP Fen. Lysimeters were installed over a gradient of soil moisture and vegetation conditions to ensure a representative site-wide average. Each lysimeter was 0.3 m in diameter and 0.45 m deep and was weighed at least every two days. All periods of precipitation were excluded from the analysis, resulting in a total of 108 actual evapotranspiration measurements used to determine the site α value. Infrequent visits to the reference sites precluded similar measurements there.

Evaporation from the pools (E_p) was determined using the Penman (1948) equation for open water surface with no vegetation,

$$E_p = \frac{sQ^* + \gamma\lambda_v\rho_wK_E\nu_a\{e_a^* - e_a\}}{\lambda_v\rho_w\{s + \gamma\}} \quad \text{Equation 2-2}$$

where, ν_a is the velocity of air (m day^{-1}), e_a^* is the saturation vapour pressure at ambient air temperature (Pa), e_a is the saturation vapour pressure (Pa), and K_E is the mass transfer coefficient (Pa^{-1}) calculated by the Thornthwaite and Holzman (1939) equation,

$$K_E = \frac{0.622\rho_a k^2}{p\rho_w[\ln\{(z_a - z_d)/z_0\}]^2} \quad \text{Equation 2-3}$$

where, k is the von Karmen's constant (0.4), ρ_a is the density of air (kg m^{-3}), p is the atmospheric pressure (Pa), z_a is the height of the velocity and air temperature measurement (m), z_d is the zero plane displacement (~ 0 for water), and z_0 is the surface roughness height (~ 0.0003 m for open water, Oke (1987)).

Surface water discharge of the EXP Fen was determined at a small outlet with a 0.5 m long by 0.15 m wide and 0.3 m high flume (Figure 2-1). The flume was constructed of $\frac{3}{4}$ inch plywood and was installed flush with the peat surface in the small rivulet through which the fen drains. Expanding installation foam was sprayed into gaps between the flume walls and surrounding peat to ensure that flow was directed through the flume. Surface water discharge was determined through instantaneous salt slug (0.1 L of 0.5 molar NaCl solution) injections (Moore, 2005) and the salt spike was measured as specific conductivity (SC) at the end of the flume with an YSI Model 63. Given the short length and minimal roughness within the flume, the discharge velocity was determined by the time between the instantaneous injection and the peak of the measured SC curve at the end of flume. A stage-discharge relationship was determined for the outflow flume, which was equipped with a Slumberger micro-diver to continuously record its water level. Runoff ratios were determined for each month using the sum of the area normalized (EXP Fen boundaries) discharge associated with a precipitation event divided by the total precipitation for a given month.

2.4.2 Hydraulic Conductivity and Transmissivity

Hydraulic conductivity (K) and T of each nest was measured in 2014 and the data applied to all study years. The T measurements were attempted in 2015 but high water tables resulted in recovery rates too rapid to measure, even with the aid of pressure transducers. The K of each piezometer was determined through bail tests where $\sim 40\%$ of the total pipe volume was removed and the rate of refill was measured manually or using a Slumberger micro-divers recording at 1-second intervals. Manual measurements were performed for T measurements. Manual

measurements were made with a 1.5 m long blow stick, measuring at 0.001 m increments. Temperature correction to 15 °C (average well water temperature during the T measurements) was applied to all data (Klute, 1986; Surridge *et al.*, 2005). The hydraulic conductivity was then calculated using Hvorslev (1951) time-lag solution,

$$K = \frac{r^2 \ln(L/R)}{2LT_0} \quad \text{Equation 2-4}$$

where, r (m) is the internal radius of the pipe, R (m) is the external radius of the pipe, L (m) is the length of the intake, and

$$T_0 = \frac{\log 0.37}{s_r} \quad \text{Equation 2-5}$$

where, $\log 0.37$ is an empirical fitting parameter determined by the shape of the piezometer, s_r is the slope of the log-linear head recovery calculated by,

$$s_r = \frac{H_i - h(t)}{H_i - H_0} \quad \text{Equation 2-6}$$

where, H_i (m) is the initial water level in the piezometer, H_0 (m) is the water level in the piezometer immediately following bailing, and $h(t)$ (m) is the water level in the piezometer at time t (hr).

To determine the T of the peat profile, a series of bail tests were performed on the wells associated with the each piezometer nest (i.e., fully penetrating wells) with incrementally smaller screen lengths. The first bail test was performed on the entire fully penetrating well and the response was recorded. Once the first bail test was completed, an inflatable well packer (2" Inflatable Pipe Plug, Perma-Type Rubber) was lowered into the well and inflated 0.3 m above the bottom of the well to isolate that region from the rest of the well (i.e., if the well was 3 m long, 0 to 2.7 m of the well remained unblocked). Once inflated, a bail test was performed on the remaining non-isolated section of the well above the packer and the response recorded. This was repeated in

0.3 m increments until ~0.7 m below the water table when the increments were decreased to 0.1 m to gain higher data resolution in the upper peat profile; where, presumably the head recovery would vary the most. The data were then analysed separately by a modified Hvorslev (1951) variable head solution, where instantaneous differences in head were used to estimate the hydraulic conductivity of each head change (K_i) by considering the recharge a series of steady state conditions (Lagacé, 1986). Each of these individual K_i were solved using Hvorslev (1951) method, accounting for changing L , h , H_i and H_0 parameters, as appropriate.

Given the expected exponential increase in hydraulic conductivity closer to the top of the water table (Leclair, 2015; Perras, 2015), seepage faces are likely to occur and need to be accounted for in estimations of K_i (Chenaf & Chapuis, 2007; Schneebeli, 1956). To account for potential seepage faces during bail tests, Schneebeli (1956) developed an analytical solution to estimate the seepage face height (h_{sf}) without additional monitoring wells (Chenaf & Chapuis, 2007; Schneebeli, 1956), where,

$$h_{sf} = \sqrt{h_w^2 + \left(\frac{Q_t}{\pi K_{est}}\right) \cdot \left[0.4343 \cdot \ln\left(\frac{Q_t}{\pi K_{est} r^2}\right)\right]} - 0.4 - h_w \quad \text{Equation 2-7}$$

and, h_w (m) is the water table at time t (hr) and Q_t ($\text{m}^3 \text{ day}^{-1}$) is the volumetric discharge into the well between time t_t and t_{t-1} . The seepage face estimation is added to the screen length in Equation 2-4 to calculate a hydraulic conductivity for the time period between each head recovery measurement (K_i).

The geometric mean of the measured K_i for a given packer depth was then used to develop an average hydraulic conductivity for a given well screen length (K'). Plotting K' vs screen length results in a power function and the hydraulic conductivity at a given point (K_y) within the peat profile is determined by taking the derivative of the K' -screen length power function (see Appendix A for further detail), then solving for $K_y(d)$

$$K_y(d) = (1 - B)Ad^{-B} \quad \text{Equation 2-8}$$

where, A and B are fitting parameters, d is the depth, and K_y (m day^{-1}) of a given depth range (i.e., 0.25 – 0.50 m bgs) can be determined by

$$K_{y_{d_2-d_1}} = \frac{\int_{d_1}^{d_2} (1-B) A d^{-B}}{\int_{d_1}^{d_2} \partial d} \quad \text{Equation 2-9}$$

where, d_1 and d_2 is the depth range for which the hydraulic conductivity is determined and $\int_{d_1}^{d_2} \partial d$ is the length of the depth range. The T for a given depth range is the numerator of Equation 2-9.

2.5 Results

In the upper 0.1 m of the saturated peat, hydraulic conductivity was between 42 – 598 m day^{-1} and decreased following the power function described above (Equation 2-8) with depth

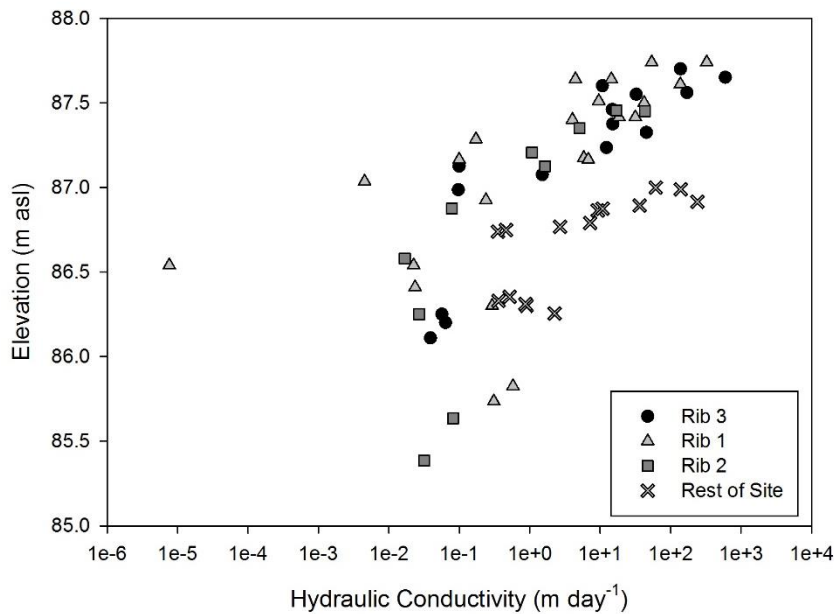


Figure 2-2 Hydraulic conductivity distribution at the EXP Fen using a combination of packer tests (0-0.3 m bgs) and piezometer (>0.3 m bgs) measurements. The difference in maximum elevation is due to the differing surface elevations at the EXP Fen. Ribs 1-3 surface elevation is ~ 87.4 m asl, while the rest of the site is ~87.0 m asl. Hydraulic conductivity as a function of depth below water table is presented in Appendix A, Figure A-3.

below the water table across the EXP Fen (Figure 2-2). In Rib 1 & 2 a minimum hydraulic conductivity (2 – 3 orders of magnitude lower than the above measurements) was observed between 86.5 – 87 m asl; approximately, 0.7 – 1.0 m below the surface (Figure 2-2). A slight increase in hydraulic conductivity (~1 order of magnitude) was observed in the peat below 86.5 m asl (~1.0 – 2.3 m below the water table) in

Ribs 1 & 2 (Figure 2-2). This decrease in hydraulic conductivity between 86.5 – 87.0 m asl was only observed in Ribs 1 & 2 and not found throughout the site (Figure 2-2). The rest of the site follows the exponential decrease (power function) with depth (Figure 2-2).

The T of a given well was controlled by the hydraulic conductivity of the upper 0.1 m of saturated peat and minimal additions from below this region were noted. During the dry 2013 season T varied between $0.1 - 6.1 \text{ m}^2 \text{ day}^{-1}$ depending on location; on average they increased by $1.3 \text{ m}^2 \text{ day}^{-1}$ from low ($0.1 - 3.9 \text{ m}^2 \text{ day}^{-1}$) to high ($0.2 - 6.1 \text{ m}^2 \text{ day}^{-1}$) water tables (a rise of 0.25 m). Conversely, T in 2014 varied between $0.2 - 69.3 \text{ m}^2 \text{ day}^{-1}$ and on average increased by $17.7 \text{ m}^2 \text{ day}^{-1}$ from low ($0.2 - 6.3 \text{ m}^2 \text{ day}^{-1}$) to high ($0.7 - 69.3 \text{ m}^2 \text{ day}^{-1}$) water tables (a rise of 0.19 m). Typically, the lowest 2014 T (average $2.3 \text{ m}^2 \text{ day}^{-1}$) were of a similar magnitude as the highest values in 2013 (average $2.7 \text{ m}^2 \text{ day}^{-1}$). In both years, there was no identifiable pattern in T with microform. High water tables (Figure 2-3) precluded T and hydraulic conductivity measurements in 2015 due to extremely quick head recovery; thus, they would likely be well above the 2014 maximum value.

The three study years represent a range of precipitation conditions from dry (2013), average (2014), and extremely wet (2015) (Table 2-1). Evaporation from the pools was consistently higher than the ribs and averaged 2.6, 4.0, 2.7 mm day⁻¹, while average evapotranspiration from the ribs 1.9, 3.0, 2.1 mm day⁻¹ in 2013, 2014 and 2015, respectively. Aerially weighted evapotranspiration from the EXP Fen was 2.1, 3.2, and 2.2 mm day⁻¹ in 2013, 2014 and 2015, respectively. The pumping resulted in average inputs of 5.6, 3.7 and 3.1 mm day⁻¹ normalized over the EXP Fen area in 2013, 2014, and 2015, respectively (Figure 2-3); however, pumping as a point source influx into Pool 1 was 125, 89 and 69 mm day⁻¹, in 2013, 2014 and 2015, respectively. In 2014, the low water level in the bog pool from which water was pumped resulted in debris clogging the pump intake, which caused sporadic pumping rates. In 2013 and 2014 the pumping resulted in rapid increase in Pool 1 water level, and sharp drops when the water pump failed or was shut off (Figure 2-3). The very wet conditions in 2015 masked the response to pumping. In 2013, water table fluctuations at the EXP Fen were typically less than 0.1 m (not including the short pumping test) and responded rapidly to precipitation events (Figure 2-3). The reference sites responded to evapotranspiration and precipitation events similarly to the 2013 EXP Fen, notwithstanding larger

absolute water table variability ($\sim 0.2 - 0.3$ m, Figure 2-3). In contrast, in 2014 and 2015, an increase of $0.15 - 0.20$ m in water table was observed at the EXP Fen during pumping and water tables were relatively unresponsive to precipitation events (Figure 2-3). In 2014, the water table responded sequentially to pumping in each down gradient pool, typically within 1-3 days after the immediate up-gradient pool responded. The flume responded after 34 days (DOY 226), which coincided with a large precipitation event (Figure 2-3). Contrary to 2014, in 2015 the water table response to pumping across the site was nearly instantaneous, as the flume water table responded ~ 15 hr after Pool 1 (Figure 2-3). Once pumping ceased, rapid water table decline was observed in 2013 and 2014, while absent in 2015 (Figure 2-3). High precipitation following the end of pumping in 2015 was coincident with sustained high water tables (Figure 2-3). Both 2013 and 2015 showed limited change in storage over the study season (Table 2-1), while a positive change in storage (66 mm) was observed in 2014 (based on average S_y , 0.23 determined in Chapter 3, of the ribs and a S_y of the pools of 1).

Table 2-1 Inter-year comparison of hydrological parameters available for 2013 -2015 (DOY 177 - 234). Outputs from the EXP Fen displayed as negatives and inputs as positive. The change in storage was calculated as the total change in water table elevation over the study period multiplied by the measured specific yield. The residual term is a combination of the total error and the groundwater fluxes.

	2013	2014	2015
Precipitation (mm)	87	109	298
Evapotranspiration (mm)	-99	-189	-130
SW _{out}	0	-9	-300
Pumping	34	187	130
Change in Storage (mm)	-1	66	0
Residual (mm)	21	164	-2

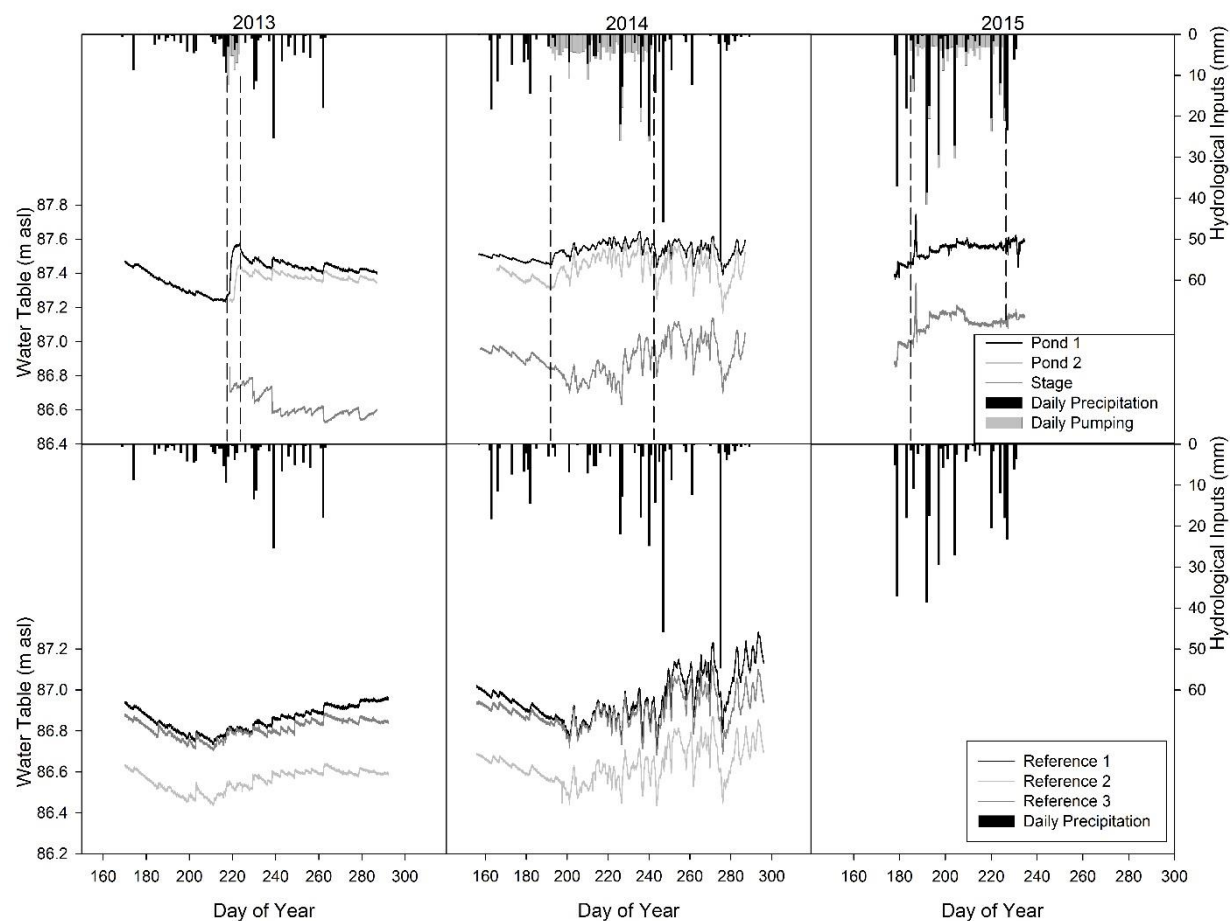


Figure 2-3 Water table elevations for Pool 1 (black), Pool 2 (grey), and at the end of the site (flume measurement point, dark grey) for the EXP Fen (top) and the three average water tables for the reference sites. In-between the vertical dashed lines is the pumping period. Note no data at the reference sites in 2015 due to instrumentation limitations.

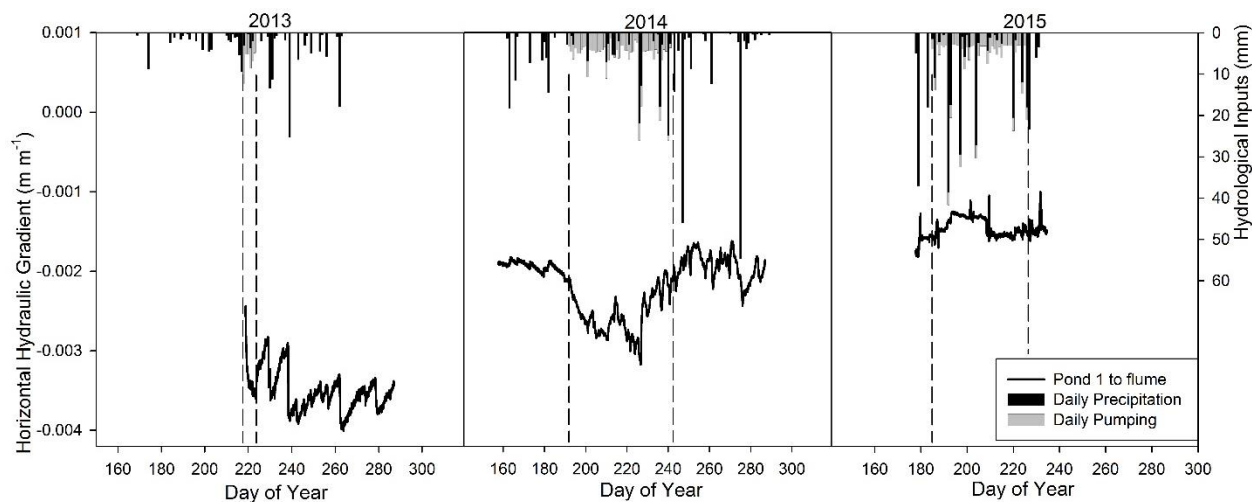


Figure 2-4 Total horizontal hydraulic gradients at the EXP Fen between water tables at Pool 1 and the flume measurement point. More negative indicates an increased hydraulic gradient. In-between the vertical dashed lines is the pumping period.

Horizontal hydraulic gradients between Pool 1 and the flume varied between -0.003 to -0.004 in 2013, while the additional hydrological inputs (both precipitation and pumping) in 2014 and 2015 resulted in weaker horizontal hydraulic gradients (Figure 2-4). The lowest horizontal hydraulic gradients (Pool 1 to flume) observed in 2014 and 2015 were similar to the highest in 2013 (~ -0.003). Once the flume water table responded in both 2014 and 2015, the horizontal hydraulic gradients were similar, typically around -0.0025.

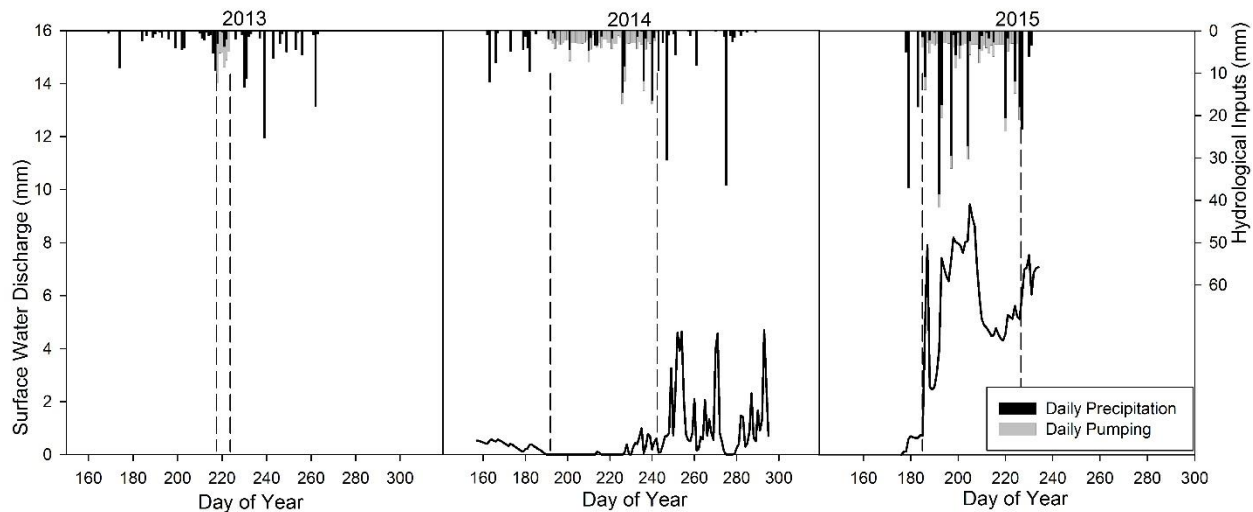


Figure 2-5 Surface water discharge measured at the flume measurement point for all three years at the EXP Fen. In-between the vertical dashed lines is the pumping period.

Unlike 2013 where there was no surface water discharge, 2014 and 2015 had 9 and 300 mm of surface water discharge, respectively. On average in 2014, surface water discharge was $0.2 \pm 0.2 \text{ mm day}^{-1}$ (13 mm total) relative to the EXP Fen area during the spring and summer (Figure 2-5) but increased autumn precipitation resulted in total area normalized discharge rates of $0.6 \pm 1.0 \text{ mm day}^{-1}$ (Figure 2-5). In contrast, surface water discharge was consistently high in 2015 ($5.1 \pm 2.6 \text{ mm day}^{-1}$) (Figure 2-5). Runoff ratios increased due to pumping and precipitation (Table 2-2). Pumping combined with greater than average precipitation resulted in runoff ratios greater than 1 in 2015 when pumping was excluded from the calculation (suggesting an expanding contributing area) and < 0.04 (2014 and 2015) when included. By comparison, in 2014 the pumping increased runoff ratios from ~ 0.05 pre-pumping to 0.47 in conjunction with autumn precipitation events (Figure 2-5, Table 2-2).

Table 2-2 Runoff ratios for all measured months. Pumping input were not included in these estimates, when included runoff ratios decrease to <0.04 during pumping in both 2014 and 2015.

	June	July	August	September	October
2013	0.00	0.00	0.00	0.00	0.00
2014	0.17	0.04	0.05	0.47	0.29
2015	No data	1.01	1.38	No data	No data

2.6 Discussion

Given the exponential increase in hydraulic conductivity with elevation in the peat profile, there is a non-linear increase in T with water table rise. In 2014, as water was pumped into Pool 1 the water level responded immediately, followed by a rise in Rib 1 water table after only ~0.3 days (Figure 2-3). This water passed through Rib 1 via near-surface flow especially in PFPs, and cascaded into Pool 2 (Figure 2-6), increasing its water level by 0.1 m in ~1.4 days. The delayed water table response in the pool-to-pool transfer illustrates the fill-and-spill mechanism (Spence & Woo, 2003) in the ladder fen. Under average climatic conditions (2014) the fill-and-spill mechanism within the pool network was initiated by pumping, which caused a ~20% increase in average Rib 1 T (from 1.97 ± 0.75 to $2.33 \pm 0.97 \text{ m}^2 \text{ day}^{-1}$) associated with the 0.1 m water table rise. Within Rib 1 the constant pumping eventually raised the water table by ~0.15 m from the pre-pumping stage, which thereafter was relatively constant while pumping was maintained. Under this condition Rib 1 average T had increased two-fold (to $5.0 \pm 4.7 \text{ m}^2 \text{ day}^{-1}$) and high hydrological connectivity was achieved in the upper reaches of the EXP Fen. In spite of this, the average conditions typified in 2014 provided sufficient storage and evapotranspiration loss that the increased hydrological loading did not transfer water down to the tail of the system, and there was no system outflow until late August and autumn. In 2013, the water table was well below the high hydraulic conductivity layers (Figure 2-2) and the average T of Rib 1 varied between low ($1.4 \pm 1.1 \text{ m}^2 \text{ day}^{-1}$) and high ($2.7 \pm 2.0 \text{ m}^2 \text{ day}^{-1}$) water tables and limited flow through the rib was

observed. Conversely in 2015, water tables exceeded the peat surface in the low-lying PFPs and induced high pool-to-pool connectivity after less than one day of pumping.

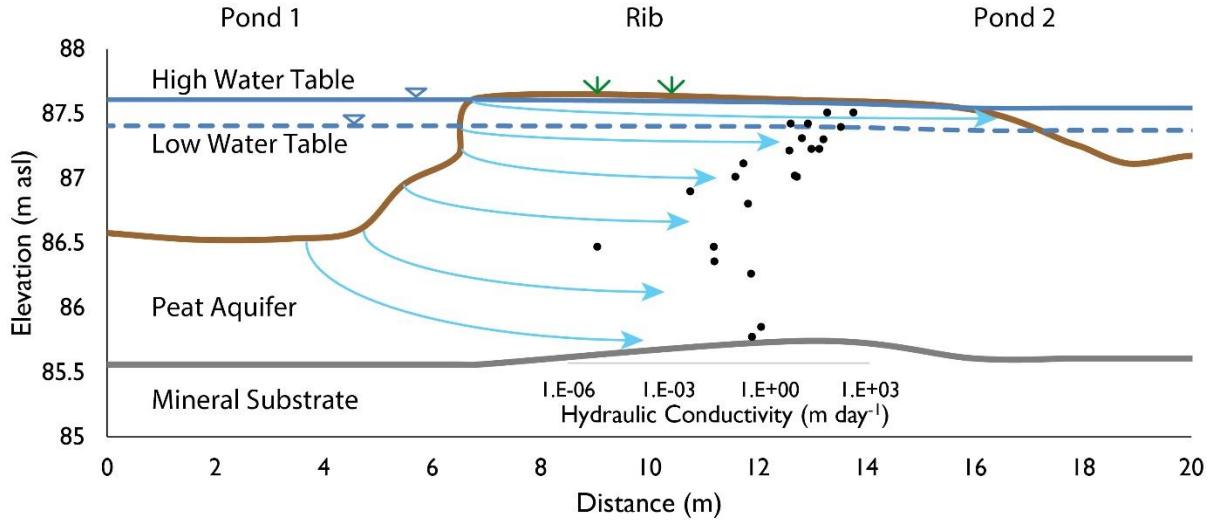


Figure 2-6 A conceptual diagram of flow and connectivity in a typical pool-rib-pool sequence. The solid blue line is the high water table and the dashed blue line the low water table in 2014. The blue arrows represent idealized flow paths, where the longer the arrow the greater proportion of flow occurs in that region. The inset of is the hydraulic conductivity distribution determined for Rib 1 at the EXP Fen. The hydraulic conductivity within the upper few centimeters of peat governs the majority of flow during high water table periods.

Once the condition of high hydrological connectivity was achieved, there was a muted water table response to precipitation events that added more water to the system because: 1) the specific yield of the near-surface peat approached unity, and was unity when the water table was above the surface; and 2) the exponentially increasing T with increasing water table elevation rendered the system highly efficient at moving water downslope (i.e., the precipitation rate was lower than the capacity of the system to shuttle water down gradient). Under this regime the fill-and-spill mechanism becomes almost redundant and connectivity down the system was maximized. At the EXP Fen, this threshold (water table ≈ 87.6 m asl in Rib 1, Figure 2-6) was apparent in 2014 and 2015, but not 2013, where much higher precipitation and pumping (Table 2-1) resulted in relatively constant water tables (Figure 2-3). This threshold corresponds to the water table residing in the upper few centimeters of peat in the PFPs, where the highest hydraulic conductivities were observed ($42 - 598 \text{ m day}^{-1}$), or exceeding the peat surface and generating overland flow (Figure 2-6). Although In addition to the potential for surface flow in PFPs, where the surface elevation was lower, the hydraulic conductivity of peat in PFPs was higher than that in the ridge at the same elevation ($16 - 52 \text{ m day}^{-1}$; data not shown) and decreased more rapidly below

this layer (0.1 – 0.2 m, 4 – 14 m day⁻¹). Thus the movement of water through ladder fens was primarily controlled by the T and the peat surface elevation, which define the threshold water table required to generate significant flow between pools.

When the EXP Fen was not impacted by pumping (2013 and pre-DOY 192 in 2014), the hydrology was similar to that at the reference sites (Figure 2-3) and little or no runoff was generated from the site (Figure 2-5, Table 2-2) because the available storage was not filled. In 2013 and 2014 precipitation was below or at the long-term average (~100 mm) (Table 2-1). In contrast, in 2015 nearly 50 % of the average annual precipitation (700 mm) fell during the study period (58 days), resulting in an abnormally wet July and August (DOY 177 – 235). Evapotranspiration was the dominant water loss during July and August 2013 and 2014 (99 and 189 mm, respectively), while surface water outflow increased substantially in 2015 and was the dominant water loss (Table 2-1). Autumn precipitation events in 2014, along with the high residual water storage associated with hydrological loading (filled the available storage, ~180mm), produced large amounts of surface runoff (56 mm) after pumping ceased (Figure 2-5, post-DOY 243) and was the dominant loss during this period. This resulted in increased hydrological connectivity of the site, as indicated by the runoff ratios increasing from 0.05 (July and early August) to 0.47 (autumn). Conversely, when these systems' storage capacity is full (2015), runoff occurs within hours; given the addition of pumped water the resulting runoff ratio > 1 (Table 2-2) (see Figure 2-5). The hydrological connectivity (i.e., runoff and water table response) of the EXP Fen is inversely related to the hydraulic gradient between Pool 1 and the flume (Figure 2-4 & Figure 2-5) where hydrological connectivity increased, even with lower absolute hydraulic gradients (i.e., smaller difference in water table elevation across the site). When these systems are dry (2013), a larger absolute, hydraulic gradient is observed between Pool 1 and the flume (Figure 2-4) but there is poor hydrological connectivity due to low aquifer T , thus the EXP Fen is not well connected to the down gradient aquatic ecosystem (i.e., the nearby stream).

The large residual in the 2013 and 2014 water budgets (Table 2-1) are a combination of total error and the groundwater fluxes from/to the flanking bogs. Although error can be ~ ±15 % of total inputs when a drainage area is well defined (Price & Maloney, 1994), the groundwater flux out of the EXP Fen to the lateral bogs was potentially high in 2014. For instance in the most

hydrologically impacted area (Pool and Rib 1, ~10 % of the total area) ~83 mm left the EXP Fen towards the lateral bogs during pumping in 2014, which would significantly decrease the residuals. The groundwater discharge from the EXP Fen to the lateral bogs likely decreased away from Pool and Rib 1 due to lower hydraulic gradients and water tables. In 2013 the hydraulic gradients into the bog followed the trend observed in 2014, where groundwater was likely leaving the EXP Fen. Conversely, in 2015 the hydraulic gradients between the EXP Fen and lateral bogs were minimal and no flow was likely to occur. Furthermore, the low runoff ratio when including the pumped water suggests a large proportion was shuttled into the bogs and stored rather than generating runoff. Notwithstanding these lower gradients, water tables, and runoff ratios (when including pumping), the flux into the later bogs may decrease the residuals significantly, resulting closure of the water budgets. However, the highly impacted region (Pool and Rib 1) was the only area where sufficient *T* data was available to perform these calculations; thus, were not included in the water budget (Table 2-1).

These high water table and high connectivity periods generated by adding pumped water mimic key aspects of the spring freshet or autumn high-flows (Perras, 2015) when the hydrological connectivity of the landscape is high (Quinton *et al.*, 2003; Quinton & Roulet, 1998; Quinton *et al.*, 2005). When overland flow is not present, the high hydrological connectivity was due to the increased hydraulic conductivity in the near-surface (Figure 2-6). Thus, the pool-rib-pool connectivity is ultimately controlled by the hydraulic conductivity distribution within the rib, when overland flow is not present (Figure 2-6). Only during extremely wet years (i.e., 2015) or during significant artificial hydrological loading (2014 and 2015) do these high connectivity periods occur outside of the spring freshet or autumn wet-up. Furthermore, given the large storage capacity of these systems, a significant amount of water is needed during the preceding autumn (2013 ~ 146 mm, 2014 ~ 52 mm and 2015 ~ 183 mm) and winter snowpack (2013 ~ 78 mm, 2014 ~ 360 mm and 2015 ~ 276 mm) (note, snowpack data provided by De Beers Group of Companies Victor Mine March Snowpack Survey, Ternes personal communication) to ensure the hydrological storage is full. Once full, the high water tables would maintain strong hydrological connectivity throughout the spring and early summer as observed in both 2014 (large snowpack) and 2015 (autumn precipitation and large snowpack). Even with large precipitation events, such as in 2015, it is unlikely that the system will remain hydrologically connected throughout the summer without

additional hydrological loading, as noted by the sharp decrease in surface water discharge between DOY 250, 275, 287 in 2014 and DOY 230 – 232 in 2015 (Figure 2-5) once precipitation ceased. Similarities in the June 2014 water table to those measured in both the spring and autumn of 2012 by Perras (2015) provide reassurance that the function of the EXP Fen (runoff ratio = 0.17, Table 2-2) has not been measurably affected by mine operations. Furthermore, measured June 2014 water tables (similar to high water table in Figure 2-6) potentially describes the normal spring and autumn runoff regime. These periods have been identified as times where high fluxes of nutrients (Perras, 2015; Ulanowski, 2014) and contaminants (i.e., methylmercury) can enter the aquatic ecosystems (Brigham *et al.*, 2009) due to the increase in landscape hydrological connectivity (Kirk & St. Louis, 2009; Ulanowski, 2014), as noted by an increase in DOC export in the autumn Perras (2015). Furthermore, a greater density of fen peatlands typically results in more rapid stream flow response within a catchment (Richardson *et al.*, 2012), the antecedent conditions within the fen peatlands will ultimately control the magnitude and timing of the response. If under wet conditions, available storage is full, response occurs within hours, while under dry conditions the response is muted as only direct flow from riparian ecosystems enters the stream channel. Thus, the hydrological connectivity (rib T and surface elevation) of ladder fens have a large impact on the quantity, and quality, of water entering the downstream aquatic ecosystems.

2.7 Conclusions

Ladder fens typically act as water and solute conveyers from domed bog peatlands to down-gradient aquatic ecosystems; the flux is controlled by the hydrological connectivity and, by extension the fill-and-spill mechanism when the water table is below the peat surface. The peat T and microform elevation define the critical water table above which connectivity is strong, and contribute to the fill-and-spill mechanisms in ladder fens. The exponential increase in T at higher water tables can greatly increase the hydrological connectivity of ladder fens and is likely active during the spring freshet and autumn wet-up; however, once overland flow occurs, the hydrological connectivity of these systems vastly increases compared to non-overland flow periods. The highly variable hydraulic conductivity distribution within a given rib seems to follow the microtopography but T did not. This study illustrates that T , on average, is similar between microforms and it is the local hydraulic conductivity distribution (primarily the upper 0.1 m of

saturated peat) that controls the flux through the peat. Additionally, this study presents a modified method to determine the hydraulic conductivity at high spatial (vertical) resolution and the T of an unconfined aquifer using a single bail test performed over hours instead of an entire season. The vast majority of water flows through the upper 0.1 m of saturated peat, which is a smaller vertical region than previously assumed (~0.5 m). Without access to the high hydraulic conductivity layers, surface water outflow may be delayed days or indefinitely (if available storage is not yet full), while under intense hydrological loading (2015) ladder fens are able to rapidly shuttle water from the top of the system to the outlet; highlighting efficiency of these system to export excess water within hours under intense hydrological loading (i.e., spring freshet). Furthermore, this study highlights the importance of understanding the high flow periods, as these periods of high connectivity are critical to understanding the transport of water, and by extension nutrients and contaminants, from the surrounding peatlands to the aquatic ecosystems in the JBL but further research on the flow of solutes is still required.

2.8 Acknowledgements

The authors would like to acknowledge funding from the NSERC Canadian Network for Aquatic Ecosystem Services. Furthermore, we would like to thank the De Beer Group of Companies Victor Diamond Mine Environment Staff for their help and hospitality. Lastly, we would like to thank Robin Taves, James Sherwood, Aaron Craig, Nicole Balliston, and Matthew Cartwright for their invaluable help collecting field data.

3 The transport dynamics of chloride and sodium in a ladder fen during a continuous wastewater polishing experiment

3.1 Summary

Ladder fen peatlands have excellent potential for wastewater polishing as they naturally contain both open water (pools) and subsurface (peat) treatment landforms; however, there is a poor understanding of solute transport in ladder fens with and without the increased hydrological load imposed by wastewater discharge. To better understand solute transport in ladder fens under wastewater polishing conditions a continuous solute (NaCl) tracer experiment ($38 \text{ m}^3 \text{ day}^{-1}$ of water, chloride – 47.2 mg L^{-1} , and sodium – 25.3 mg L^{-1}) was conducted during the summer of 2014 (day of year 192 – 243) in a small ladder fen in the James Bay Lowland. The transmissivity distribution and effective porosity (average 0.5) of the peat ribs were determined through repeated bail tests and the drainable porosity of 18 peat cores at -100 mb, respectively. Water samples (Na^+ and Cl^-) were taken at least every 7 days to capture the solute plumes. Both solute plumes never reached the site outflow ($\sim 250 \text{ m}$ downgradient) and displayed complex plume morphology, typically following the patterns of hydraulic conductivity within the upper 0.1 m of the saturated peat and not microtopography. Based on the 50 % breakthrough isotherms, Cl^- and Na^+ were transported at an average solute velocity of 1.9 and 1.1 m day^{-1} , respectively (average linear groundwater velocity = 2.1 m day^{-1}); thus the solutes were retarded by a factor of 1.2 and 2.1 for Cl^- and Na^+ , respectively. Due to the inherent retardation of solutes into inactive pores and relatively high solute residence times, this study demonstrates the potential for wastewater polishing in ladder fens.

3.2 Introduction

The discovery of large mineral deposits, such as diamondiferous kimberlite and chromite, in the James Bay Lowland (JBL) has prompted the building and operation of remote mining operations. This increased development pressure increases the likelihood of unintentional (spill) or intentional (wastewater polishing) contaminant release into the surrounding peatlands. Fen

peatlands have recently been used intentionally for polishing wastewater (Chapter 2; Kadlec, 2009a; Steinback, 2012a; Yates *et al.*, 2012), since they direct flow through the peat substrate, which can remove certain contaminants through biogeochemical processes (Kadlec, 2009a; Palmer *et al.*, 2015). However, intentional or sustained discharges of contaminated water creates a hydrological loading that raises the water table to levels observed in the spring freshet or autumn wet-up (Chapter 2), reducing the system's ability to detain water and contaminants. A better understanding of how fen peatlands transport and transform contaminants is needed. However, to our knowledge there are only two published field scale studies that investigate controlled solute transport experiments in peatlands. Hoag and Price (1995) used sodium chloride (electrical conductivity) in a blanket bog, and Baird and Gaffney (2000) used bromide in a drained basin fen, to determine the geochemical transport of the respective systems. Neither of these examined the implications of an increased hydrological load caused by the release of wastewater, on the hydrological performance of the systems.

Wastewater polishing and treatment wetlands are most effective when the water storage capacity, thus residence time, of the system is high, which allows for increased biogeochemical reactions that remove contaminants from the pore water (Kadlec & Wallace, 2009). Ribbed and ladder fen peatlands (National Wetlands Working Group, 1997) provide both high hydrological residence times (i.e., low hydrological connectivity) and high storage capacity within pools during the summer months (Chapter 2; Price & Maloney, 1994; Quinton *et al.*, 2003; Quinton & Roulet, 1998), thus may be particularly effective as wastewater polishing wetlands (Yates *et al.*, 2012). In ladder and ribbed fens there is an exponential increase in aquifer transmissivity as water tables increase (Chapter 2; Leclair, 2015; Perras, 2015; Price & Maloney, 1994) due to the activation of the extremely high hydraulic conductivity layers near the peat surface (Chapter 2). Under dry conditions typical in summer, there is limited water flow within these systems and the primary loss of water is through evapotranspiration (Chapter 2; Price & Maloney, 1994; Quinton & Roulet, 1998). Consequently, the capacity to transmit solutes laterally is small. Conversely, during periods of high water table (i.e., spring freshet and autumn wet-up) flow is predominantly through the high hydraulic conductivity peat layers or is above the peat surface, and a substantial increase in hydrological connectivity is observed (Chapter 2; Quinton & Roulet, 1998), thus capacity for transport. This is enhanced by microtopography of the peat ribs, where apparent preferential flow

paths (PFPs) occur in low-lying sections of the ribs (Chapter 2; Price & Maloney, 1994; Quinton *et al.*, 2003; Quinton & Roulet, 1998). These apparent PFPs typically experience overland flow and have higher average transmissivities (Chapter 2) than the topographically higher ridge microforms. Furthermore, the numerous pools found within the rib-pool topography of these systems may create windows of relatively unimpeded solute transport; however the function of pools on solute transport and retention has not previously been characterised.

The ability of peat to retard conservative solutes is well known, being caused primarily by the dual porosity structure of the peat matrix (Hoag & Price, 1997; Ours *et al.*, 1997; Price & Woo, 1988; Rezanezhad *et al.*, 2012). The effective, or active, porosity (n_e) is typically 0.1 – 0.6 depending on the degree of decomposition and parent vegetation material that forms the peat (Hoag & Price, 1997; Ours *et al.*, 1997; Quinton *et al.*, 2000), while the inactive porosity is conceptualized as connected to the active pore network but not contributing to flow (Rezanezhad *et al.*, 2012). Solutes can diffuse from the active pore network into the inactive pore network driven by chemical concentration gradients (Hoag & Price, 1997; Ours *et al.*, 1997); this decreases the apparent solute velocity (v_s) compared to average linear groundwater velocity (v). In a blanket bog, Hoag and Price (1995) observed limited transverse horizontal and vertical dispersion of a sodium chloride plume and found that the peat inherently retarded the plume by a factor of 2.2 (v_s/v), which was interpreted as being caused by diffusion of the solute into inactive pores (Hoag & Price, 1997; Ours *et al.*, 1997) or through sodium sorption to the peat and other organic molecules (Caron *et al.*, 2015; Ours *et al.*, 1997). The majority of the plume remained near the spill point and advection occurred near or at the top of the water table within the high hydraulic conductivity layers (Hoag & Price, 1995). Conversely, Baird and Gaffney (2000) found an abundance of macropore flow causing the conservative tracer (bromide) to arrive at the measurement points quicker than calculated by v . Although Baird and Gaffney (2000) attributed this to macropore flow, they do consider potential errors in the calculation of average well hydraulic conductivity, which averages the hydraulic conductivity distribution across the peat aquifer. By using an average peat hydraulic conductivity, variations in hydraulic conductivity within the peat profile were not considered, potentially skewing the calculation of v . Furthermore, they used the total porosity (0.7 – 0.9) for the calculation of v and not n_e , which is typically much lower (0.1 – 0.6) (Hoag & Price, 1997; Rezanezhad *et al.*, 2012) and results in a higher v_s (Bear, 1972). Both of these field scale solute

tracer tests were performed with an instantaneous application of the tracer but there is no known work on continuous application of tracers (or solutes), similar to the process of wastewater treatment and polishing wetlands (Kadlec, 2009a; Kadlec & Wallace, 2009).

The increasing industrial and mining development in subarctic and boreal ecosystems increases the probability of an unintentional release of contaminants in peat-dominated ecosystems, for which better knowledge is required to provide appropriate response. Moreover, these systems have the potential to provide a water polishing function, such as for treated wastewater. Understanding the mechanisms governing transport is key to managing solute releases. Currently there is a dearth of information on transport processes relating to continuous loading of solutes, such those associated with wastewater polishing (continuous loading) or a pipeline leak. Therefore, this study aims to determine the processes governing both conservative (chloride) and adsorptive (sodium) contaminants in a ladder fen under increased hydrological loading at the field scale. Thus, the specific objective are: 1) determine the difference of the two solute plumes between a conservative (chloride) and adsorbing (sodium) tracer in a ladder fen, 2) clarify the role of microtopography and peat hydrophysical properties on solute transport at the field scale, 3) elucidate the influence pools have on the transmission of solutes, and 4) comment on the suitability of ladder fens to retain solute with a specific focus on wastewater polishing processes.

3.3 Study Site

Located in the JBL near the De Beers Group of Companies Victor Diamond Mine (N 5860348.772, E 705883.366), the hydrological function of an experimental ladder fen (EXP Fen) was determined in Chapter 2 for 2013 – 2015. Average July and August (9 years, 2006-2015) temperature and precipitation (15.6 °C and 154 mm) from the local meteorological station agreed well with two regional meteorological stations' 30 year average; Moosonee (14.9 °C and 90 mm) (Environment Canada, 2015a) and Lansdowne House (16.4 °C and 105 mm) (Environment Canada, 2015b). During 2014 (day of year, DOY, 151 – 257) a total of 274 mm of precipitation, 328 mm of evapotranspiration, 40 mm of surface water discharge, and 187 mm of pumping

occurred at the EXP Fen. The majority of surface water discharge occurred in the spring and autumn, notwithstanding the additional hydrological loading during 2014 (Chapter 2).

Elevation and hydrological gradients were from the north to south (Chapter 2) and water flows perpendicular to the peat ribs (Figure 3-1). The rib microtopography can be separated into two apparent microtopographies; low-lying preferential flow paths (PFPs) and topographically higher ridges (0.2-0.5 m higher than the PFPs). Pools account for ~23 % of the EXP Fen surface area, while the remaining 77 % (total area 9800 m²) was peat. Peat depth was greatest at the north end of the site at 1.85-2.5 m (2.1 m average) and decreases to 1.50-1.85 m (1.85 m average) in the

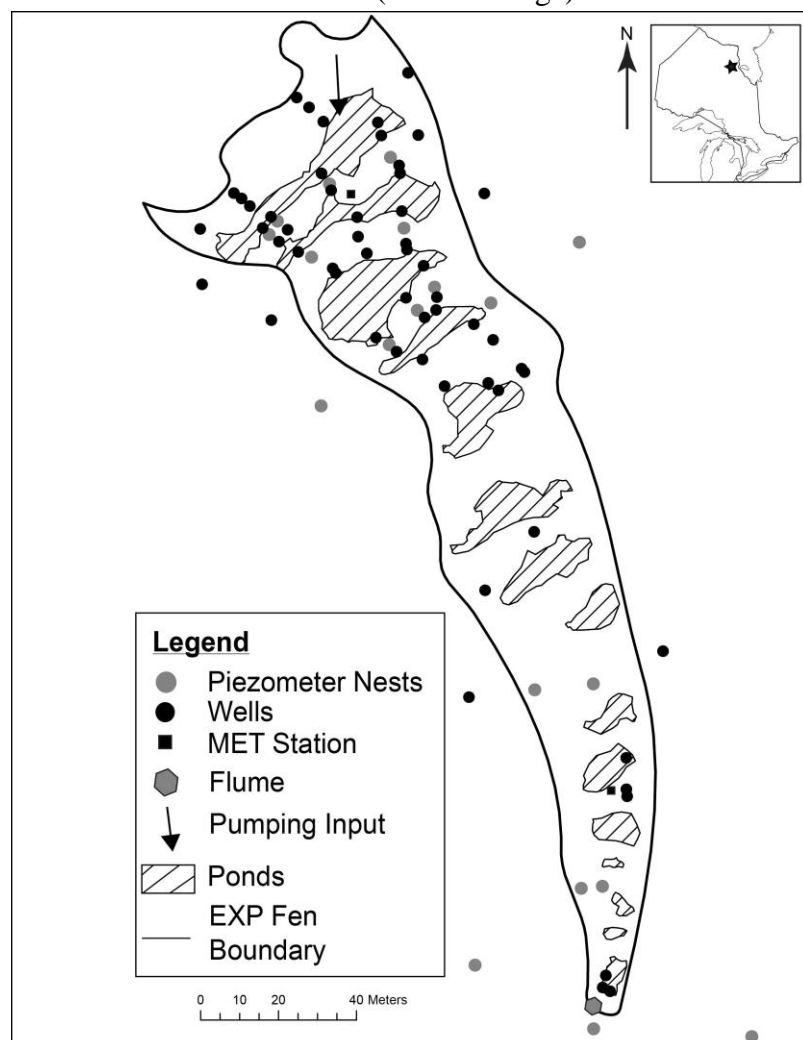


Figure 3-1 Map of the EXP Fen, adapted from Chapter 2.

south. The adjacent bogs and a large pool to the north typically provide groundwater inputs into the EXP Fen and constrain groundwater flows within the fen boundary, while low hydraulic conductivity of the underlying mineral substrate limited vertical hydrological exchanges (Chapter 2).

The hydrological connectivity of the EXP Fen is a function of water table height, where an exponential increase in transmissivity occurs due to increasing water tables within the peat ribs (Chapter 2). This increased transmissivity reflects the several orders of magnitude

higher hydraulic conductivity of peat near the surface as the water table rises into it (Chapter 2). Typically, the hydraulic conductivity of the upper 0.1 m are between 42 – 598 m day⁻¹ in PFPs and

16 – 52 m day⁻¹ in ridges (Chapter 2), decreasing exponentially below this layer to ~0.02 m day⁻¹ within 0.2 m (~86.5 – 87 m asl). In the upper two ribs the hydraulic conductivity followed the site-wide trend of exponentially decreasing hydraulic conductivity until ~86.5 – 87 m asl but a slight increase (0.08 – 0.5 m day⁻¹) in hydraulic conductivity is noted in the lowest layers of peat. This increase is not observed in the remaining ribs and peat deposit at the EXP Fen (Chapter 2). Three nearby reference sites (Reference Site 1 – N 5860348.772, E 705883.366; Reference Site 2 – N 5860472.091, E 705811.312; and Reference Site 3 – N 5860472.091, E 705811.312) were found to be hydraulically similar to the EXP Fen (Chapter 2) and are used as geochemical analogues in this study.

3.4 Methods

The EXP Fen was continuously injected (2014 DOY 192 – 243) with simulated wastewater derived from a custom blend fertilizer and associated hydrological loading (38 m³ day⁻¹). Water for the hydrological loading was pumped using a solar powered submersible water pump (Lorentz PS150-Centric Submersible Pump) from a nearby bog complex (170 m). The injected fertilizer solution contained: SO₄²⁻, NO₃⁻, NH₄⁺, PO₃³⁻, K⁺, Na⁺, and Cl⁻. Only the fate and transport of Na⁺ (25.3 mg L⁻¹), and Cl⁻ (47.2 mg L⁻¹) are considered in this paper. The loading mimicked the wastewater effluent from a nearby mining operation (Steinback, 2012a) and coastal arctic communities (Yates *et al.*, 2012). A concentrated injection of the fertilizer solution was pumped every two hours into a mixing bucket weir, which the pumped water entered, to achieve target wastewater concentrations. The simulated wastewater was continuously discharged into Pool 1 (Figure 3-1) from DOY 192 – 243 in 2014.

Prior to solute injection, the concentrated wastewater source was mixed using a bilge pump (Attwood Tsunami T-500, 500 gph) to circulate the solution within the storage container (250 L plastic food grade barrel), ensuring a well-mixed solution. Solute injection pumps (controlled by a DC switch timer) ran for ~2.5 minutes (~1 L min⁻¹ for 2.5 min, total 2.5 L per injection period) every 2 hours during the experimental loading. Discharge rates of both the water and solute injections were tested every two days. If the discharge rates deviated from the target rates, adjustments were made to pumping rates or pumping time to ensure a near-constant flow rate and

concentration was maintained. In Chapter 2 a stage-discharge relationship of the v-notch bucket weir was determined to ensure continuous measurements of the volume of pumped water and solutes. To ensure Pool 1 was well mixed after pumping and no preferential flow occurred due to proximity to the wastewater loading point, an electric trolling motor (Minn Kota Endura Max 40 lbs 36-inch Trolling Motor) was installed and automatically turned on for 10 minutes after each solute injection period. The trolling motor was anchored in the pool sediment and ran at 40 RPM, this provided enough circulation to ensure Pool 1 was well mixed. The hydrological and geochemical (NaCl) conditions were monitored throughout June-September 2013 and 2014 with the wastewater experiment occurring in July and August 2014 (DOY 192 – 243).

3.4.1 Field Methods

At the EXP Fen, manual measurements of water table and hydraulic head occurred at minimum of every 3 days in wells (1.25 m slotted intake (S.I.), 0.025 m I.D., 0.034 m O.D.) and piezometers (0.25 m S.I., 0.035 m I.D., 0.017 m O.D.) along with specific conductance (SC) and temperature (°C), using a YSI Model 63 calibrated weekly, of the well water. Three pipe volumes were flushed from each pipe prior to taking SC and temperature readings to ensure the measurements were representative of the surrounding pore water. Piezometer screens were centred at 0.125, 0.375, 0.675, 1.125 m bgs and 0.125 m above the mineral substrate. At each piezometer nest (13) and two wells in the lateral bogs the wells were fully penetrating 0.051 m I.D. and 0.031 m O.D (Figure 3-1). These nests were preferentially installed in topographically high (ridges) and low (PFPs) regions to better identify the role of microtopography on solute transport in ladder fens. All piezometers and wells were screened with a geochemically inert geotextile filter sock (Rice Engineering & Operating LTD., 2” Filter Sock). A total of 18 piezometer nests with accompanying 1.25 m S.I. wells were installed at the three reference sites (six nests per site), along with two wells measuring pool water table per reference site. Manual measurements of SC and temperature in the wells were performed at the reference sites every 10 days.

3.4.2 *Water Sampling and Analysis*

Well water sampling for major ions occurred at least weekly at every well location within the solute plume in the EXP Fen and surrounding bogs. Sharp increases in SC were used to determine the terminal extent of the solute plume and sampling occurred at least one rib beyond the terminal extent to ensure the entire plume was sampled. Prior to sampling, three pipe volumes were purged the day prior and only occurred when no precipitation fell for three days prior to the sampling event. Each well at the EXP Fen was sampled in 2013 to provide background Na^+ and Cl^- concentrations. Piezometers were sampled three times over the 2014 season, DOY 178 (pre-pumping), DOY 221 (during pumping), and DOY 254 (post pumping). The reference sites were sampled three times (DOY 197, 212, and 237) in 2014 to assess the representativeness of the geochemistry of the EXP Fen. Samples were taken in 50 mL FlipMate bottles (Delta Scientific Laboratory Products Ltd.) and stored in the field in a cooler with ice packs. Prior to filtering, the sample SC and pH were determined using an Orion Star™ A215 benchtop meter. Samples were filtered within 24 hours using 0.45 μm polyethersulfone filters. Once filtered, samples were then frozen for shipment to the Western University Biotron facility and analysed using EPA 300.0 on a Dionex ICS-1600 with AS-DV Autosampler (precision = 0.01 mg L^{-1}). Both Cl^- and Na^+ iso-concentration maps were manually interpolated and drawn.

3.4.3 *Physical Soil Parameters*

Effective porosity (n_e), specific yield, and bulk density of the peat was determined for peat that was approximately at the elevation of the water table maintained by pumping (equilibrium water table), and also at ~ 1.5 m bgs. A total of 15 sampling locations were selected throughout the EXP Fen, focusing on the upper three ribs (9 samples). The remaining six cores were distributed evenly throughout the southern half of the EXP Fen. At each location two cores (one shallow and one deep) were taken. Cores were extracted in late September 2014, by taking 30 semi-cylindrical cores using a Russian Corer. Each core was placed into a semi-cylindrical PVC container of the same I.D. as the Russian Corer and covered with plastic wrap for transport to the University of Waterloo Wetland Hydrology Laboratory for analysis.

Each core was visually inspected for evidence of compression due to sampling and any portions of the core that were visually compressed were not used in analysis. Each core was subdivided into three 0.1 m high samples for analysis. The cores were saturated with R.O. water for 24 hours and specific yield was determined by allowing the samples to drain upright (height = 0.1 m) under gravity for 24 hours. Once completed, the drainable porosity at -100 mb was determined to estimate n_e . Lastly, the samples were oven dried at 85°C for 48 hours to determine the bulk density.

In mineral soils under saturated conditions n_e is equivalent to the drainable porosity at the field capacity (-100 mb) (Bear, 1972; Klute, 1986); while in peat, Rezanezhad *et al.* (2012) used soil water retention curves and model calibration to determine n_e , and both Quinton *et al.* (2000) and Hoag and Price (1997) used visual estimation of thin cross-sectional areas of peat to estimate n_e . Both of the methods used in peat require extensive laboratory and analytical work to generate an estimate of n_e and are difficult to reproduce or compare between studies. Since the drainable porosity at -100 mb easily encompasses the range of pores sizes in peat that transmit the majority of the flow, it should give a reasonable estimate of n_e . Thus, n_e was determined as the drainable porosity at -100 mb pressure (Bear, 1972; Klute, 1986) using a pressure cell with a 1 bar pressure plate (Soil Moisture Equipment Corp. 5 Bar Pressure Plate Extractor). Once completed, the samples were dried at 80°C for 48 hours and bulk density was determined. A Shapiro-Wilk normality test was performed on the data and an ANOVA with Tukey's HSD test to determine if microform, site location (north or south) and sample depth had a significant influence on n_e . All statistical analysis were performed in R Statistical Software (R Development Core Team, 2010).

3.4.4 Pool Residence Times

Pool bathymetry was determined by a DGPS survey with “bog plate” attachment by resting the weight of the unit on the pool bottom. The bog plate, ~ 175 cm², allowed for more consistent measurement in the soft pool bottoms. Once the bathymetric survey was completed the data were imported into ARC GIS 10.2 and a TIN was generated for the calculation of the pool surface area and volume at each water table elevation recorded throughout the study. The average stable water table during pumping was used in the final calculation of residence times (rt) as pool volumes and

saturated peat thickness were not changing, an assumption of Equation 3-1. Thus, the rt for Pools 1-4 was estimated by

$$rt = \frac{V}{Q_p + Q_{sw} + P} \quad \text{Equation 3-1}$$

where, Q_p ($\text{m}^3 \text{ day}^{-1}$) is the volumetric discharge through the peat, Q_{sw} is the volumetric discharge from the water input pipe (only pertains to Pool 1) based on the bucket weir discharge determined in Chapter 2, P is the precipitation, and V is the pool volume at the average stable water table. The limited groundwater monitoring network past Pool 4 precluded the calculation of residence time for these pools but typically they were shallow and small ($<1 \text{ m}^3$). Discharge through the peat was determined by a form of Darcy's law such that

$$Q_p = \sum_{i=1}^n (-b_i K_i i) \quad \text{Equation 3-2}$$

where, b_i is the thickness of a given layer, K_i is the hydraulic conductivity of a given layer, and i is the total hydraulic gradient.

3.4.5 Retardation Factors

Average linear groundwater velocity, v , was determined at the EXP Fen as,

$$v = \frac{Ki}{n_e} \quad \text{Equation 3-3}$$

where, n_e is determined for a given transect using the shallow sample, i is the total hydraulic gradient between pools and K (m day^{-1}) is the hydraulic conductivity of the upper 0.10 m of the water table ($K_{0-10 \text{ cm}}$) determined in Chapter 2. The hydraulic conductivity from 0 – 0.10 m was determined for a given well (see Appendix A) by averaging the hydraulic conductivity along the transmissivity curve within the upper 0.1 m of the top of the saturated peat.

Chloride and sodium breakthrough (measured concentration 50 % of the input concentration, $C/C_0 = 0.50$, were determined for individual transects, as well as a site averaged value (maximum extent). Two calculations of the retardation factor (R) were performed: 1) the entire site including pools and 2) only the peat to better compare these results to past studies that did not have any open water pools.

The residence times and distance across pools were removed from the calculations to provide an estimate of v and v_s , the average solute velocity, for the peat substrate and the R were determined by

$$R = \frac{v}{v_s} \quad \text{Equation 3-4}$$

where, v_s is determined as

$$v_s = \frac{l_s}{t_{c/c_0=0.5} - \sum t_{res}} \quad \text{Equation 3-5}$$

where, l_s is the length along a well transect, or maximum extent of the plume when $C/C_0 = 0.50$, $t_{c/c_0=0.5}$ is the time of solute breakthrough ($C/C_0 = 0.50$) that is linearly interpolated between sampling periods and t_{res} is the sum of all pool residence times up-gradient from the measured point. To determine R_{site} , the site average retardation (including pools), v was determined by the average v of each individual transect (9) and v_s was estimated by the maximum observed solute breakthrough distance (l_s) and associated time ($\sum t_{res} = 0$). To determine the R within only peat (R_{peat}), the same calculations were completed but the average distance across the pools were removed from l_s and the sum of the residence times of Pools 1-4 ($\sum t_{res}$) was subtracted from $t_{c/c_0=0.5}$.

3.5 Results

Average (\pm standard deviation) solute concentrations at the reference sites (chloride $0.8 \pm 1.1 \text{ mg L}^{-1}$ and sodium $0.5 \pm 6.0 \text{ mg L}^{-1}$) were similar to those found at the EXP Fen in 2013 (1.2

$\pm 0.5 \text{ mg L}^{-1}$ and $3.9 \pm 1.3 \text{ mg L}^{-1}$, respectively). No seasonal trends were observed in chloride or sodium at the reference sites. SC increased with depth from $39.9 \pm 28.4 \text{ }\mu\text{S cm}^{-1}$ at the water table to $88.0 \pm 48.7 \text{ }\mu\text{S cm}^{-1}$ at 1.25 m bgs at the reference sites, similar to that at the EXP Fen prior to loading, at $19.0 \pm 2.5 \text{ }\mu\text{S cm}^{-1}$ and $65.0 \pm 36.2 \text{ }\mu\text{S cm}^{-1}$, respectively.

Hydrological loading of $37.7 \text{ m}^3 \text{ day}^{-1}$ began on DOY 192 (July 11th). This resulted in an average daily input of 3.7 mm of water normalized over the EXP Fen area, or a point source influx into Pool 1 of $\sim 89 \text{ mm day}^{-1}$ (Chapter 2). The discharge resulted in rapid increase in Pool 1 water table (Figure 3-2); the periodic sharp decreases in Pool 1 water table resulted from the water pump failure. During hydrological loading the water table close to the pumping source (Pool 1) increased immediately and responded rapidly (within a few days) in the upper 3 ribs but was not evident further down-gradient in the EXP Fen. Typically, sodium and chloride concentrations increased following the rise in water table, although the relative concentration of sodium was lower compared to chloride (Figure 3-2). In the lower part of the EXP Fen sodium and chloride concentrations remained at background levels.

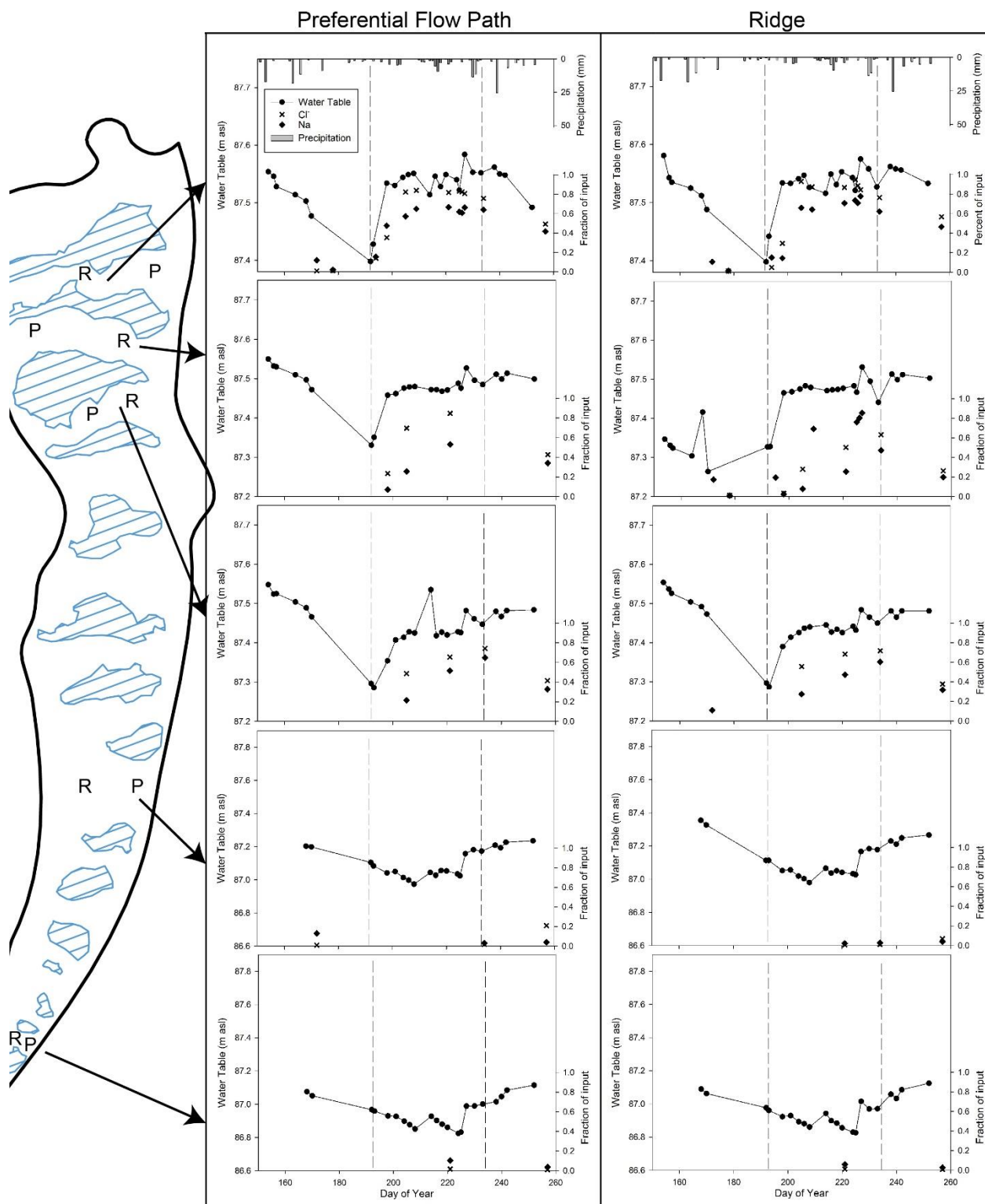


Figure 3-2 Water table, precipitation (secondary y-axis) and C/C_0 for chloride and sodium during the study period. Experimental loading occurred between the dashed lines (DOY 192 – 243). In-between the vertical dashed lines is the pumping period. The left column of graphs represents the pre-identified PFP's, while the right are the ridges. The approximate location of each microform within the site is represented by P (PFP) and R (ridge).

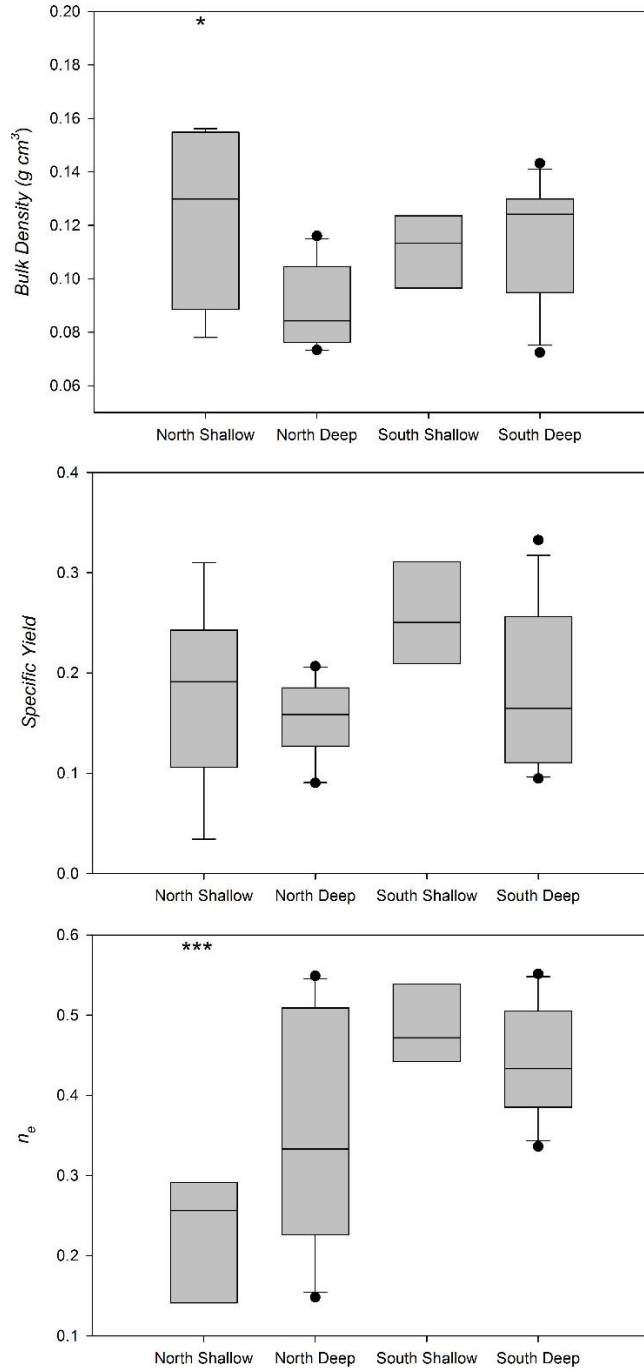


Figure 3-3 Bulk density, specific yield and effective porosity the EXP Fen divided into the northern half (north) and southern half (south). Shallow and deep refer to the depth of each sample: shallow = at the top of the water table and deep = ~ 1.5 m below the top of the water table. *** and * indicates significantly different at $p < 0.001$ and $P < 0.05$, respectively. Specific yield data presented by McCarter and Price (in review).

Specific yield was not statistically different across the site or between microtopography (Figure 3-3). However, bulk density was statistically higher ($p < 0.05$) in the shallow north region of the site (Figure 3-3). Furthermore, no statistical difference in n_e was observed between different microtopographies ($p > 0.1$) but the north (Ribs 1 & 2) had significantly lower n_e (0.29 ± 0.14) than the south (0.47 ± 0.09 , $p < 0.001$) (Figure 3-3). In the north, n_e increased with depth (0.21 ± 0.11 vs. 0.35 ± 0.15 , $p = 0.047$, while in the south there was little variation with depth (0.50 ± 0.10 vs. 0.45 ± 0.07 , $p > 0.1$) (Figure 3-3). Upon visual inspection of the cores, slight compression due to the sampling technique was observed at the top and bottom (< 5 cm) of the samples, thus were not used for analysis; the rest of the cores did not display pronounced smearing or deformation.

3.5.1 Solute Transport

Chloride was transported at an average rate (v_s) of 2.2 m day^{-1} (Figure 3-4) when excluding pool residence times and distances (Table 3-1), slightly lower than that of water (v), which was 2.5 m day^{-1} ; thus, chloride was retarded ($R_{peat \text{ Cl}}$) by a factor of 1.1 in the peat. However, v ranged from $0.3 - 13.3 \text{ m day}^{-1}$

¹ and v_s for chloride ranged between 0.34 – 2.11 m day⁻¹ depending on local gradients, hydraulic conductivity and n_e (Table 3-2) of a given peat transect; this resulted in a range of $R_{peat\ Cl}$ of 0.4 – 31.2. Sodium (Figure 3-5) was transported more slowly relative to chloride (Figure 3-4) at an average rate of 1.2 m day⁻¹ ($R_{peat\ Na} = 2.0$). However like chloride, sodium displayed local variation in peat v_s (0.26 – 0.97 m day⁻¹) and thus a range of $R_{peat\ Na}$ (1.0 – 42.2) depending on local hydrophysical conditions (Figure 3-3), which microtopography did not influence. When including the pools (R_{site}) in the calculation of R , both solutes had higher R ($Cl^- = 1.2$ and $Na^+ = 2.1$), as v_s decrease to 1.9 and 1.1 m day⁻¹ for chloride and sodium, respectively. Both solutes displayed complex plume behaviour (Figure 3-4 & Figure 3-5) and travelled ~107 m in 42 days.

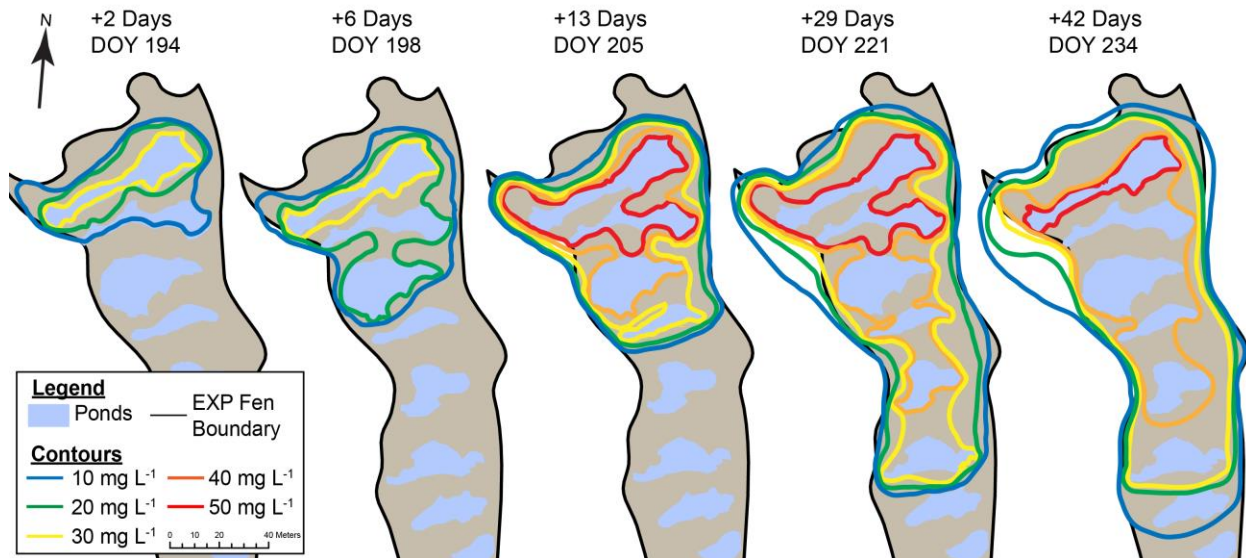


Figure 3-4 Chloride concentration iso-concentration map of the EXP Fen generated from the well water sample data during the experimental loading. Note the highly irregular plume development.

Table 3-1 Average (\pm S.D.) pool residence time for the first 4 pools over the entire study period. Due to limited well installations it was not possible to calculate residence times for other pools; however, pool volumes were $<3\text{ m}^3$.

	rt (day)
Pool 1	2.9 ± 0.4
Pool 2	1.4 ± 0.7
Pool 3	3.2 ± 1.0
Pool 4	1.5 ± 0.7

The majority of solute (sodium and chloride) was transported within 0.25 m of the top of the saturated peat (Figure 3-6 & Figure 3-7, DOY 221) as indicated by the strong relationship and

near 1:1 slope (1.06) between C_{Cl} measured in the wells and that in the 0.25 m piezometers ($p < 0.001$, df 10, $adj. R^2$ 0.995). By comparison, C_{Cl} is lower in the 0.5 and 0.75 m piezometers than in the wells ($p < 0.001$, slope 0.35, df 11, $adj. R^2$ 0.700 and $p < 0.001$, slope 0.05, df 11, $adj. R^2$ 0.614, respectively). The shallowest piezometers (that have similar C_{Cl} to that in the wells) have the highest hydraulic conductivity (Table 3-2), corresponding to the saturated hydraulic conductivity that increases exponentially towards the surface.

Table 3-2 The hydraulic conductivity of the upper 10 cm and 25 cm of the saturated peat profile determined in Chapter 2, maximum transmissivity, average n_e , v , and v_s for the regions within the bulk of the solute plume. No data is available beyond Rib 3 until Rib 8, where the plume was not observed, due to lack of instrumentation. East and West Bog refers to the lateral bogs to the east and west of the site.

	$K_{0-10\text{ cm}}$ (m day^{-1})	$K_{0-25\text{ cm}}$ (m day^{-1})	T_{max} ($\text{m}^2 \text{ day}^{-1}$)	Avg. n_e	v (m day^{-1})	v_s (m day^{-1})
Rib 1 Nest 1	42	19	6	0.29	1.2	0.8
Rib 1 Nest 2	54	24	7	0.29	2.6	0.4
Rib 1 Nest 3	137	60	17	0.29	5.2	0.4
Rib 1 Nest 4	324	138	37	0.29	13.3	0.4
Rib 2 Nest 1	5	2	1	0.12	0.3	0.3
Rib 2 Nest 2	43	20	4	0.12	3.0	2.3
Rib 3 Nest 1	138	61	22	0.50	0.8	2.1
Rib 3 Nest 2	598	256	18	0.50	4.8	1.4
Rib 3 Nest 3	170	76	69	0.50	1.9	1.3
East Bog	2	1	50	N/A	N/A	N/A
West Bog	4	1	34	N/A	N/A	N/A

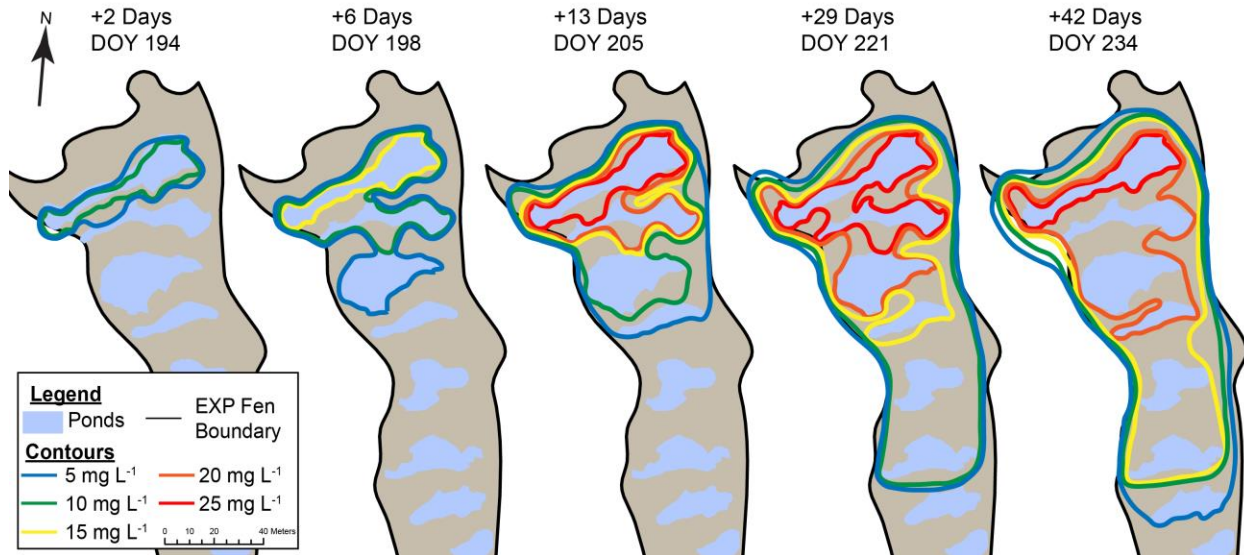


Figure 3-5 Sodium concentration iso-concentration map of the EXP Fen generated from the well water sample data during the experimental loading. Note the highly irregular plume development.

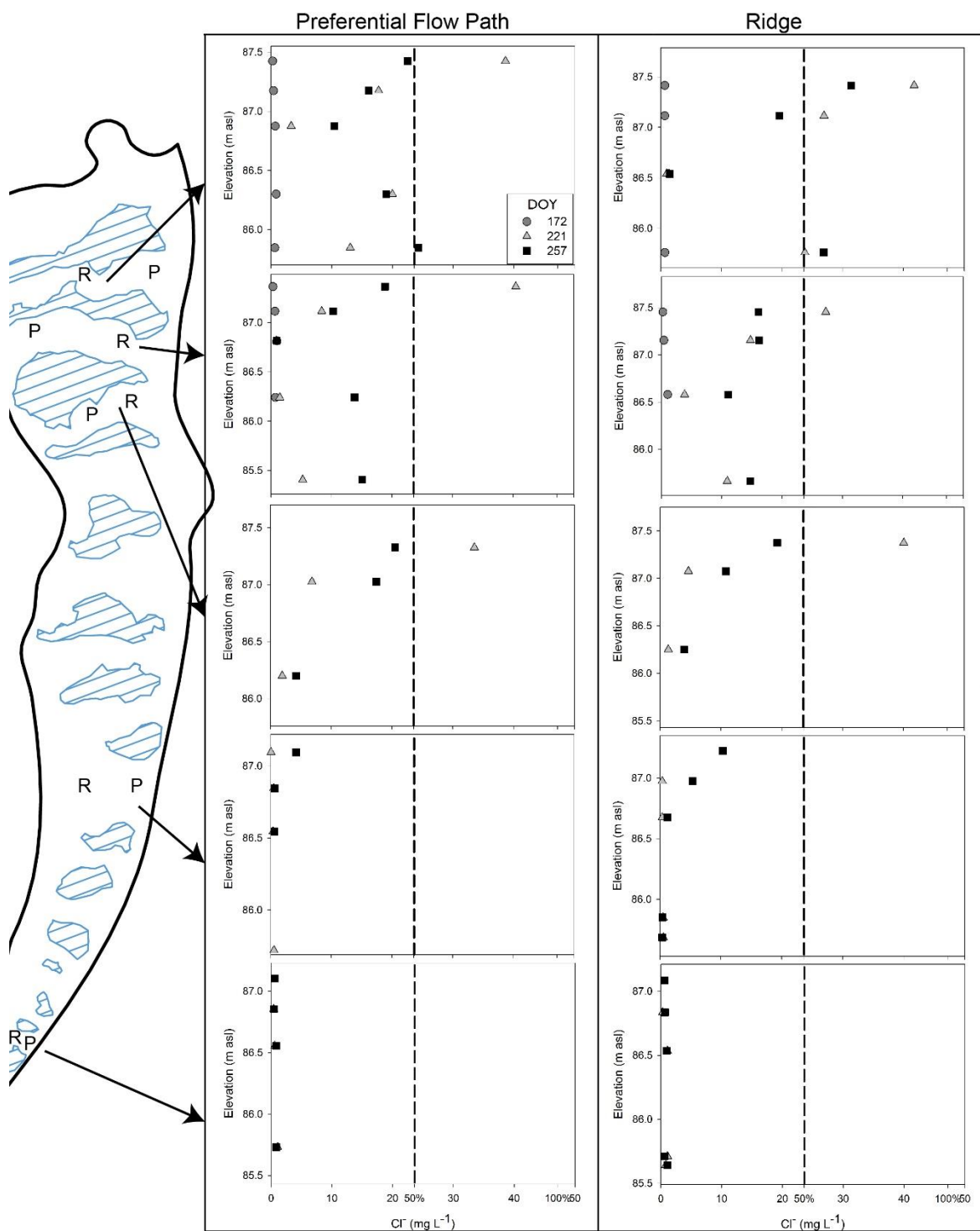


Figure 3-6 Chloride concentration in the pore water within the peat profile before (172), during (221) and after (257) experimental loading. Background chloride concentration (2013 and DOY 172) was $< 1 \text{ mg L}^{-1}$. The left column of graphs represents the pre-identified PFP's, while the right are the ridges. The approximate location of each microform within the site is represented by P (PFP) and R (ridge). Note, the elevation change on each graph representing the change in peat depth, where the top of each graph is the peat surface and the bottom is the mineral substrate surface. Peat depth decreases from north to south and is typically lower in the PFP's than the associated ridges. Dashed lines represent 50 % of C_0

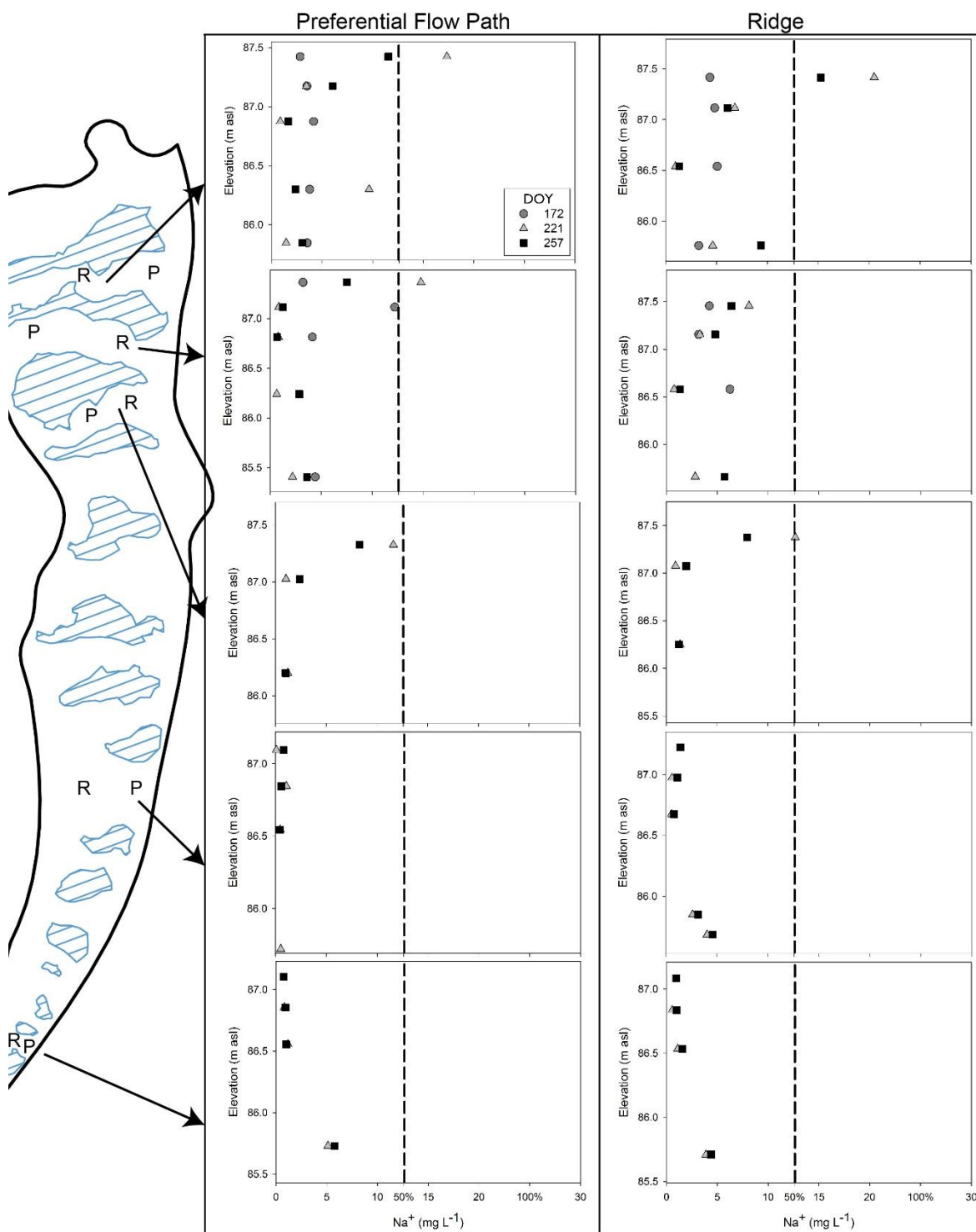


Figure 3-7 Sodium concentration in the pore water within the peat profile before (172), during (221) and after (257) experimental loading. Background sodium concentration (2013 and DOY 172) was $< 1 \text{ mg L}^{-1}$. The left column of graphs represents the pre-identified PFP's, while the right are the ridges. The approximate location of each microform within the site is represented by P (PFP) and R (ridge). Note, the elevation change on each graph representing the change in peat depth, where the top of each graph is the peat surface and the bottom is the mineral substrate surface. Peat depth decreases from north to south and is typically lower in the PFP's than the associated ridges. Dashed lines = 50 % of C_0

Background sodium concentrations (Figure 3-7) were typically elevated compared to chloride (Figure 3-6). Towards the southern portion of the site, sodium concentrations are $\sim 5 \text{ mg L}^{-1}$ directly above the mineral (Figure 3-7), while chloride concentrations remain at or below detection limits (Figure 3-6). Little downward transport of the solutes occurred (Figure 3-6 & Figure 3-7). In the upper two ribs the lowest chloride and sodium concentrations were found between 0.7 and 1.0 m below the surface (Figure 3-6 & Figure 3-7). Solute concentrations increased slightly past this depth (Figure 3-6 & Figure 3-7). This trend was exaggerated after pumping (DOY 257), as the solute below this layer concentration increased or remained constant during this measurement period, while chloride, and typically not sodium (Figure 3-7), was flushed from the upper peat layers (Figure 3-7). In the rest of the site, there was a continuous exponential decrease in solute concentration with depth (Figure 3-6 & Figure 3-7). Due to low temporal sampling resolution, estimates of vertical transport rates were not available. Reference sites and 2013 (pre-solute release) showed low sodium ($< 1 \text{ mg L}^{-1}$) and chloride ($< 1 \text{ mg L}^{-1}$) pore water concentrations.

3.6 Discussion

At the EXP Fen n_e typically decreased with decreasing bulk density ($R^2 = 0.22$, $p = 0.002$) and increased with specific yield ($R^2 = 0.36$, $p < 0.001$) based on linear regression, following the broad trend observed in the literature (Hoag & Price, 1997; Quinton *et al.*, 2005). However, there was no observable trend between the hydraulic conductivity and the measured physical parameters, likely due to differing sampling intervals, locations, and scales. It was expected that the *Sphagnum* dominated peat (shallow samples) in the northern portion of the site would have a higher n_e than the deep or southern samples because lower n_e is typically associated with sedge or woody peat and greater levels of decomposition (Hoag & Price, 1997; Quinton *et al.*, 2005); however, this was not observed and the surficial northern peat had a lower n_e ($p < 0.001$) than the rest of the site (Figure 3-3). The lower n_e coincided with a higher bulk density ($p < 0.05$), suggesting that the surficial peat in the north of the site was physically different than that of the rest of the site. Furthermore, there was a greater range and lower minimum specific yield observed in these samples (Figure 3-3), yet were not statistically different ($p > 0.1$). The higher bulk density of the shallow northern samples agrees well with the conceptual model of peat where increased bulk

density has a lower n_e (Hoag & Price, 1997; Quinton *et al.*, 2005). The southern region of the site follows the trends observed in the literature (Hoag & Price, 1997; Quinton *et al.*, 2005) where the surficial poorly decomposed *Sphagnum* dominated peat had, on average, lower bulk density and higher specific yield and n_e . At depth bulk density increased and both specific yield and n_e decreased (Figure 3-3) but not significantly ($p > 0.1$). The significantly lower n_e (Figure 3-3) in the upper section of the EXP Fen may be due to enhanced decomposition of the peat during the experiment caused by the additional nitrate and sulphate load (Bayley & Thormann, 2005; Cabezas *et al.*, 2012). These compounds have a higher redox potential, thus are energetically favourable for microbial decomposition, than is typical in these peatlands (Niedermeier & Robinson, 2007). However, there is a dearth of knowledge on how decomposition affects the hydrophysical properties of peat and further study is required to better understand the evolution of peat under enhanced decomposition.

The raised elevation and lower transmissivity (Table 3-2) within the adjacent bogs limited the solute plume to the confines of the EXP Fen, as no solute breakthrough (50% breakthrough, $C/C_{0\text{ Cl}} = 0.50$) was observed at any bog monitoring well ($C/C_{0\text{ Cl}} = 0.33$, 8.3 m, 42 days, Figure 3-4). Furthermore, microtopography within the EXP Fen contributed to the complex plume morphology through the variation in near surface hydraulic conductivity distribution and n_e (Table 3-2); however, variations in n_e were not clearly related to microtopography. For instance, on Rib 2 apparent PFPs were identified on the western third of the rib (Figure 3-2), yet the primary solute breakthrough was typically through the centre of Rib 2 (Figure 3-4 & Figure 3-5). Complex solute plumes have been observed in a basin fen by Baird and Gaffney (2000), where tracer (bromide) peaks were observed intermittently along transects due to macropores generating preferential flow paths for solutes. In the EXP Fen, no macropore flow was observed (i.e., no increases in solutes outside of the plume) and the complex plume development was due to variations in hydrophysical parameters within a rib.

The largest control on solute transport was the hydraulic conductivity within the upper 0.1 m of the saturated peat. The hydraulic conductivity of the upper 0.25 m of saturated peat ($K_{0-25\text{ cm}}$) was much lower than that of the upper 0.1 m ($K_{0-10\text{ cm}}$) (Table 3-2) and when used to calculate $R_{\text{peat Cl}}$ it produces values lower than 1. The $R_{\text{peat Cl}}$ lower than 1 potentially indicates macropore

flow (Baird, 1997; Baird & Gaffney, 2000) or, more likely, incorrect determination of the hydrophysical parameters. Using the hydraulic conductivity of the upper 0.1 m of the saturated peat to calculate R produces the values as reported (Table 3-2); thus, it is likely that the majority of solutes are transported in the upper 0.1 m of the saturated peat and the sampled solute concentration within the piezometer was dominated by preferential flow through this layer. Although inferences can be made on projected plume development based on microtopography, it is critical to understand the near surface hydraulic conductivity distribution as the majority of contaminants are transported within this layer, which has the strongest control on solute transport.

The observed maximum plume distance of sodium and chloride were similar but high concentrations of sodium (Figure 3-5, $\sim 20 \text{ mg L}^{-1}$, $C/C_{0 \text{ Na}} = 0.80$) were limited to the upper reaches of the EXP Fen. Conversely, high concentrations of chloride (Figure 3-4, $\sim 40 \text{ mg L}^{-1}$, $C/C_{0 \text{ Cl}} = 0.80$) were observed much further down-gradient as fewer processes retard chloride transport (Ours *et al.*, 1997; Rezanezhad *et al.*, 2012). As chloride and sodium were transported down-gradient in the EXP Fen, both were subject to physical diffusion into inactive pores (Hoag and Price, 1997), as evidenced by the retardation factor for chloride being greater than unity ($R_{\text{peat Cl}} = 1.1$). Additionally, sodium was also influenced by geochemical (sorption) retardation in addition to diffusion into inactive pores (Rezanezhad *et al.*, 2012), so a higher retardation factor ($R_{\text{peat Na}} = 2.0$) was observed. It is noteworthy that the observed range of R for the peat within the EXP Fen ($R_{\text{peat Cl}} = 0.4 - 31.2$, $R_{\text{peat Na}} = 1.0 - 42.2$) includes values below 1 indicating the likelihood for preferential or macropore flow (Baird & Gaffney, 2000; Rezanezhad *et al.*, 2012), surface water flow (not observed) (Chapter 2; Price & Maloney, 1994; Quinton & Roulet, 1998) or local variations in the hydrophysical properties (i.e., n_e , K , and anisotropy) (Chapter 2; Hoag & Price, 1995; Quinton *et al.*, 2008; Quinton *et al.*, 2005), which can cause the solute to arrive at the measurement point before the calculated average pore-water velocity, v . Retardation factors for chloride and sodium are similar to those reported in the literature for peat: chloride: 2.7 – 7.3 (Hoag & Price, 1997), sodium: 1.73 (Rezanezhad *et al.*, 2012), and EC (NaCl): 2.2 (Hoag & Price, 1995). The observed average $R_{\text{peat Na}}$ was similar to the R_{EC} observed by Hoag and Price (1995). In the only other published field study we could find, Baird and Gaffney (2000) were unable to calculate R because of macropore flow and/or because they did not account for the

effective porosity; this resulted in $R < 1$. Notwithstanding differences in K and n_e between Hoag and Price (1995) and the values determined in this study, in simple two chemical component (i.e., Na^+ and Cl^- , NaCl) tracer experiments the electrical conductivity is an expression of both solutes when calculating R (Mastrocicco *et al.*, 2011). While the sodium values agree with those reported in the literature, the role of competitive adsorption in peat (Ho & McKay, 1999; Ho *et al.*, 2002) between sodium and the other wastewater cations (i.e., potassium and ammonium) is unknown. However, given the large cation exchange capacity observed in peat (Gogo *et al.*, 2010), it is unlikely that the cation exchange capacity was exceeded during this experiment.

The pools in the EXP Fen were typically shallow (<0.3 m deep, except for Pool 1 with a maximum depth of 1.5 m) and elongated, typically reaching a stable SC within 2-6 days after initial detection (data not shown) indicating a pool was at the input concentration of solute. Thus, depending on the volume and morphology of the pool, transmission of solutes was delayed by 2-6 days due to dilution. Pools are unable to efficiently store solutes in hydraulically dead-zones once the input concentration is achieved; these dead-zones are a function of the shape of the pools (Figure 3-1) (Persson *et al.*, 1999; Polprasert & Bhattarai, 1985; Postila *et al.*, 2015; Thackston *et al.*, 1987). However, the near equal influent and effluent zone lengths (north and south pool edge, respectively), approximately parallel edges, and large length to width ratios results in minimal dead-zones (Persson *et al.*, 1999; Persson & Wittgren, 2003; Thackston *et al.*, 1987) and high pool hydraulic efficiency in the small, shallow pools, such as those found in the EXP Fen (Thackston *et al.*, 1987). Given that the length to width ratios are above 10 (data not shown) and the pools are typically <0.6 m deep, the hydraulic efficiencies are high (>0.75) (Persson, 2000; Persson *et al.*, 1999; Persson & Wittgren, 2003; Polprasert & Bhattarai, 1985; Thackston *et al.*, 1987). This suggests the natural morphology of ladder fens may be ideal for open water wastewater treatment and polishing as the majority of the pool volume is active (Persson *et al.*, 1999; Persson & Wittgren, 2003). However, once at the input solute concentration the pools transported the solute slower than the input v_s , as n_e increases to unity (Bear, 1972). Thus, the pools create regions of lower solute transport due to the decreased v_s (assuming conservation of mass) within the pools, lowering the site wide v_s ($\text{Cl}^- = 1.9 \text{ m day}^{-1}$ and $\text{Na}^+ = 2.1 \text{ m day}^{-1}$). Furthermore, the pools, regions of lower v_s , occupy $\sim 26\%$ of the linear distance the chloride plume during the experiment and consequently slightly increased $R_{\text{site Cl}}$ to 1.2 (1.1). Sodium displays similar behaviour as chloride,

where $R_{site Na}$ increases 2.1 (2.0). However, these values assumes plug-flow through the pools and does not account for the effect of wind mixing of both water and solutes, where solute transport can be accelerated or decreased depending on the prevailing wind direction (Shaw *et al.*, 1997). Shallow pools, such as those found at the EXP Fen, will have a greater proportion of the pool volume influenced by wind, further limiting the storage of contaminants (Persson, 2000; Persson *et al.*, 1999; Shaw *et al.*, 1997). However, these are speculative findings and a more robust study on solute transport in peatland pools is required. Although pools seem to reduce solute transport in this ladder fen, the effect was minimal and unlikely to alter the release of contaminants to down-gradient aquatic ecosystems.

Prior to loading chloride was negligible ($<1 \text{ mg L}^{-1}$) and sodium was $<5 \text{ mg L}^{-1}$ within the peat pore water at the EXP Fen, except for directly above the mineral substrate (Figure 3-6 & Figure 3-7 DOY 172) where upward diffusion of solutes likely occurred over long time periods (Price, 1991; Reeve *et al.*, 2000, 2001; Siegel *et al.*, 1994). The strong vertical layering in sodium and chloride concentration at the EXP Fen during and after loading typically followed the same pattern as K (Chapter 2). Notwithstanding average downward vertical hydraulic gradients (0.08) observed in Chapter 2, the exponential decrease in K restricted vertical advection of both sodium and chloride during and after the experimental loading (Figure 3-6 & Figure 3-7). A bimodal distribution of chloride and sodium was observed in Ribs 1 & 2 and an exponential decrease in chloride concentration with depth below water table was observed at the rest of the site (Figure 3-6 & Figure 3-7). The lower sodium and chloride concentrations at mid-depth in Ribs 1 & 2 corresponds to a relatively abrupt decrease in K in a layer at that depth, which can cause a flow deflection (Bear, 1972). The bisecting flow resulted in solute advection directly to the deep peat layers from the pools, yet at a much lower v_s than in the upper peat layers (Figure 3-6 & Figure 3-7, DOY 257) and may store contaminants at depth over longer time periods. This unintentional contaminant storage is potentially beneficial under wastewater treatment scenarios as it removes a portion of the contaminant from the upper, high permeability, peat layers. However, it is the local site conditions that are driving this storage and, although interesting, may not apply to other ladder fens.

Contaminants within the upper peat layers and pools readily flush from the EXP Fen, as noted by the rapid decrease in chloride concentration between the end of loading and the final sampling date, 14 days post-loading (Figure 3-2 & Figure 3-6, DOY 257). There was an ~50 % decrease in chloride concentration in Ribs 1-3 within the upper peat layers, likely due to a combination of dilution from precipitation and advection (Figure 3-6), and a slight increase in chloride concentration in Rib 8, 140 m down gradient, due to advection. Sodium decreased similarly to chloride in the upper 3 ribs but there was no observed increase at Rib 8 (Figure 3-7), likely due to sorption of the sodium to the peat, which removed it from the aqueous phase (Ho & McKay, 2000; Rezanezhad *et al.*, 2012). SC, an indication of all wastewater solutes injected, of Rib 1 decreased by 75 % by DOY 297 2014 (54 days post loading), while the rest of the site was near or at pre-loading levels (data not shown). This indicates that most of the solutes were; 1) flushed from the site within 54 days post-loading; 2) subject to dilution from precipitation; 3) retained by adsorption in the case of sodium; or 4) a combination of the different processes. Preliminary data from June 2015 (not shown) suggests that some of the wastewater solutes were stored above the water table due to decreasing water tables in the autumn (SC was ~2 to 3 times higher in the vadose zone compared to pre-loading levels as well as that on DOY 297, 2014). Once the EXP Fen water table rose during the spring freshet (2015), the stored wastewater solute was free to be flushed from the vadose zone and redistributed from the upper few ribs to the rest of the site. Notwithstanding the role of ground frost on the hydrology of the system (Quinton *et al.*, 2005; Woo *et al.*, 2000), the high water tables associated within the spring freshet result in rapid transmission of solutes to the down-gradient aquatic ecosystems due to the extremely high hydrological connectivity observed during these periods (Chapter 2; Leclair, 2015; Perras, 2015; Quinton *et al.*, 2003; Quinton & Roulet, 1998). Furthermore, as the ground frost recedes (Woo *et al.*, 2000), the hydrological connectivity remains high with a perched water table located within the high *K* layers, resulting in further contaminant flushing. However, low water tables during the growing season and frozen ground during the winter limits flushing to the shoulder seasons. Thus, it may take several years to completely flush relatively mobile contaminants (i.e., sodium and chloride) from these systems.

3.7 Conclusions

This study illustrates the complex plume morphology of both sodium and chloride due to spatial variations in n_e , K , anisotropy, and sorption, as well as the morphology of the pools. Although this study illustrates the mechanisms controlling the plume complexity, further studies are required to better understand the role of degree of decomposition and compression (i.e., pore structure, anisotropy, etc.) and parent material (i.e., *Sphagnum*, sedges, wood, etc.) on peat hydrophysical properties and solute transport in peatlands. The high spatial variability of peat hydrophysical properties can result in calculated $R < 1$. These low values may be an artefact of the inability to measure hydrophysical properties at a sufficiently dense spatial resolution. Because the determination of n_e is not standard in the peat literature, it is difficult to compare between studies. We propose to adopt the -100 mb drainable porosity standard for saturated peat, as it agrees well with the conceptual model of the dual porosity structure of peat and soil water retention (Hoag & Price, 1997; Ours *et al.*, 1997; Rezanezhad *et al.*, 2012) and would allow for easy comparison between studies.

Both chloride (conservative) and sodium (reactive) were not transported out of the EXP Fen during the 42 day study period, resulting in system residence times much higher than 42 days during a climatically average summer. The majority of solute transport occurring the highly conductive upper 0.1 m of the saturated peat. Other wastewater contaminants likely have higher residence times than either of these solutes as they are bioavailable (Kadlec, 2009a; Kim *et al.*, 2011; Lens *et al.*, 1995; Ronkanen & Klove, 2009), in addition to physical and geochemical removal processes. Thus, treatment efficiencies are likely greatly enhanced compared to sodium and chloride. However, there needs to be careful manipulation and control of the water table to avoid surface water flow within low-lying apparent PFPs, which can greatly increase the hydrological connectivity. Furthermore, maintaining hydrological loading so that the water table remains 0.05 – 0.10 m below the highest hydraulic conductivity layers, where the majority of solutes were transported, will exponentially decrease the solute transport rate (exponential decrease in hydraulic conductivity) and increase the solute residence time, thus treatment efficiency. To further enhance transport predictability, stable water tables need to be maintained

limit solute storage within the vadose zone, which may be remobilized during high water table periods.

The high hydrological connectivity with the aquatic ecosystems in ladder fens during these high water table periods (Chapter 2) questions the suitability of fen peatlands, which convey water to aquatic ecosystems, for domestic wastewater treatment or polishing. Bog peatlands, which play a water storage role in many northern landscapes (Quinton *et al.*, 2003), may be better suited to retaining solutes for longer time periods as the residence time of these systems is typically much longer than fens (Price & Maloney, 1994; Quinton *et al.*, 2003; Quinton & Roulet, 1998). Unlike fen peatlands, which typically have a linear flow regime pool to pool, bogs have an unorganized flow regime where the flow between pools can be sporadic depending on the local hydraulic conductivity and elevation of the intersecting peat between pools (Price & Maloney, 1994). Like ladder fens, the flow pool to pool relies on a threshold water table being exceeded where the hydraulic conductivity increases exponentially towards the surface (Price & Maloney, 1994). Thus, similar hydrological mechanisms to ladder fens may control solute movement within bogs but the unorganized flow path of water and likely solutes would require a larger area to be contaminated and difficult to predict the flow paths. The combination of these features suggest that large bog complexes may be more suitable for domestic wastewater treatment or polishing but further research is required to better understand the movement of solutes within these ecosystems.

This study did not investigate the role of the spring freshet and ground ice on solute transport in peatland and remains an important gap in the literature for these northern environments. Furthermore, a broad understanding of the role of pools was elucidated within this study but the mechanisms governing solute transport within ladder fen pools has not yet been identified and requires further investigation prior to using these systems for wastewater treatment or polishing. This study demonstrates the potential for ladder fens to be used for wastewater treatment and polishing due to the inherent retardation of solutes into inactive pores and relatively high solute residence time during a climatically average summer (~100 mm of precipitation). However, unintentional contaminant releases or wastewater treatment and polishing during high water table periods will result in rapid transport. Unintentional release during low water table periods may result in storage of some contaminants within the vadose zone where they will be

accessible during periods of high water table (i.e., spring freshet) or leached during precipitation events. The differences in transport and storage between these hydrological conditions likely necessitates different remediation techniques and strategies. In either case, careful observation and management of the water table is required to ensure minimal release of wastewater or other contaminants to the surrounding aquatic ecosystems.

3.8 Acknowledgements

The authors would like to acknowledge funding from the NSERC Canadian Network for Aquatic Ecosystem Services. Furthermore, we would like to thank the De Beer Group of Companies Victor Diamond Mine Environment Staff for their help and hospitality. Lastly, we would like to thank Robin Taves, James Sherwood, Aaron Craig, Nicole Balliston, and Matthew Cartwright for their irreplaceable help with data collection.

4 The transport and treatment of domestic wastewater contaminants enhances net methylmercury production in an undisturbed sub-arctic ladder fen peatland

4.1 Summary

Safely treating domestic wastewater in remote communities and mining operations in sub-arctic Canada is critical to protecting the surrounding aquatic ecosystems. Undisturbed fen peatlands have been used to effectively minimize the release of contaminants to the aquatic ecosystems; however, there is a limited understanding of wastewater transport or treatment in undisturbed fen peatlands. To elucidate these processes, a small (9800 m², ~250 m long) ladder fen was continuously injected with a wastewater surrogate derived from a custom fertilizer blend and 38 m³ day⁻¹ of water for 51 days. The simulated wastewater was: sulphate (27.2 mg L⁻¹), nitrate (7.6 mg L⁻¹), ammonium (9.1 mg L⁻¹), phosphate (7.4 mg L⁻¹), and chloride (47.2 mg L⁻¹). Major ion, total mercury (THg) and methylmercury (MeHg) pore water concentrations were measured throughout the study period. No wastewater contaminants were detected in the site outlet (~250 m downgradient) and most wastewater contaminants, except for SO₄²⁻ and Cl⁻, remained relatively immobile. Within the SO₄²⁻ plume, MeHg concentrations became highly elevated relative to background (up to 10 ng L⁻¹) and comprised 80 – 100 % of dissolved THg in the pore water. No MeHg was exported at the outflow. Since the added contaminants were effectively transformed, sequestered or otherwise removed from pore waters in this experimental system, it appears that that fen peatlands have a large capacity to safely treat residential wastewater contaminants; however, the inadvertent generation of THg and MeHg maybe a cause for concern.

4.2 Introduction

In high latitude regions, the treatment of domestic wastewater from communities and commercial operations, such as semi-permanent mine camps, have infrastructural complications that are not faced in the south. Common technical solutions used elsewhere are often challenging to implement logistically and financially because electricity is often generated by costly diesel

generators. In many northern regions peatlands dominate the landscape (Glaser *et al.*, 2004) and have been shown that they can be used for primary wastewater treatment (Yates *et al.*, 2012) or tertiary wastewater polishing (Eskelinen *et al.*, 2015; Kadlec, 2009a; Postila *et al.*, 2015; Ronkanen & Klove, 2009; Ronkanen & Kløve, 2008). Typically, natural treatment or polishing peatlands are dominated by subsurface flow regimes (Ronkanen & Kløve, 2007, 2008) with one or two settling ponds at the influent point (Kadlec, 2009a). However, different contaminants are sometimes better treated by different wetland designs that are not necessarily features of natural peatlands (Ronkanen & Kløve, 2007, 2008). A mixture of both subsurface flow and open water treatment cells often produce the best results for treating a variety of contaminants (Kadlec & Wallace, 2009; Kim *et al.*, 2011). Ladder fens, and the larger ribbed fens, are found throughout the JBL and consist of a series of pools and peat ribs where the water flow is perpendicular to the orientation of the peat ribs (Chapter 2; Chapter 3; Glaser *et al.*, 1981; Leclair, 2015; National Wetlands Working Group, 1997; Perras, 2015; Ulanowski, 2014). The peat ribs bisect pools and are elevated above the pool bottoms by ~1 – 2 m; furthermore, the peat ribs have two distinct microforms that vary in surface elevation by ~0.5 m from the lowest elevation of the rib during low water tables (National Wetlands Working Group, 1997). These low regions are considered preferential flow paths and function as surface water conduits during periods of high water table (Price & Maloney, 1994; Quinton & Roulet, 1998). Topographically higher regions are classified as ridges and act to impede the transmission of water through ladder fens (Price & Maloney, 1994; Quinton & Roulet, 1998). This pool-rib-pool morphology may be ideal for treating a wide range of contaminants as both surface and subsurface features are expressed naturally in these systems. However, there is a dearth of information on the transport and fate of domestic wastewater contaminants in these peatlands and the subsequent the risk of their release to down-gradient aquatic ecosystems.

The peat ribs in ladder and ribbed fens control the movement of water (Chapter 2; Price & Maloney, 1994; Quinton *et al.*, 2003; Quinton & Roulet, 1998) and solutes (Chapter 3) through the non-linear transmissivity-water table relationship common in peatlands (Chapter 2; Leclair, 2015) and the absolute elevation of the low-lying preferential flow paths. During periods of high water table, greater hydrological connectivity with the down-gradient aquatic ecosystems is observed in these systems (Chapter 2; Price & Maloney, 1994; Quinton *et al.*, 2003; Quinton & Roulet, 1998), increasing the likelihood of contaminant release (Chapter 3). The additional

hydrological load associated with wastewater treatment and polishing (Chapter 2; Postila *et al.*, 2015; Ronkanen & Kløve, 2008) increases the water table, resulting in more rapid transport of contaminants (Chapter 3). Although the transport of chloride (Cl^-) and sodium (Na^+) has been identified in these systems (Chapter 3), there is a limited understanding of how more reactive contaminants are transported in peatlands, as published peatland transport studies have focused on sodium chloride (Hoag & Price, 1995) or bromide (Baird & Gaffney, 2000).

Typically, domestic wastewater has elevated phosphate (PO_4^{3-}), ammonium (NH_4^+), and nitrate (NO_3^-) and other contaminants that are above background levels (Eskelinen *et al.*, 2015; Kadlec, 2009a; Postila *et al.*, 2015; Ronkanen & Klove, 2009) and all of these wastewater components are typically not present in measurable amounts in waters of in sub-arctic peatlands (Campbell & Bergeron, 2012). Additionally, peatlands are efficient at removing many of these contaminants through a variety of biogeochemical (Beltman *et al.*, 2000; Boeye *et al.*, 1999; Gerke & Hermann, 1992; Kadlec, 2009a, 2009b; Palmer *et al.*, 2015; Richardson, 1985; Seo *et al.*, 2005) and physical processes (Hoag & Price, 1995; Hoag & Price, 1997; Kadlec, 2009b; Postila *et al.*, 2015). For instance, the diffusion of contaminants into inactive pores will affect both reactive and conservative solutes based on their concentration in the mobile pore water (Hoag & Price, 1997; Rezanezhad *et al.*, 2012) and diffusion coefficient (Appelo & Postma, 2005); this process likely provides relatively minor removal (Rezanezhad *et al.*, 2012) under stable geochemical conditions. In many wastewater treatment wetlands and peatlands, PO_4^{3-} is primarily removed through sorption to metal-humic complexes (i.e., Al^{3+} , Fe^{3+} , or Ca^{2+}) (Richardson, 1985; Ronkanen & Klove, 2009) or precipitation (i.e., calcium phosphate) out of the aqueous phase (Kadlec & Wallace, 2009; Richardson, 1985); however, some removal of PO_4^{3-} may occur as uptake by terrestrial (Kirkham *et al.*, 1996) or aquatic vegetation (Noe *et al.*, 2003; Pietro *et al.*, 2006). Typically open water treatment wetlands are preferred for PO_4^{3-} treatment (Kadlec & Wallace, 2009). Nitrogen, both NH_4^+ and NO_3^- , can be treated in both surface water or subsurface wetlands but subsurface treatment wetlands are typically more effective because of the availability of labile organic matter, sorption sites, anoxic conditions, microbial and vegetation communities (Kadlec & Wallace, 2009). There are two primary removal pathways for NH_4^+ : 1) sorption to colloids or soil material and 2) nitrification to NO_3^- (Eskelinen *et al.*, 2015; Ronkanen & Klove, 2009). Sorption to soil or colloids results in a labile NH_4^+ pool since any change in geochemical conditions

may release the bound NH_4^+ , yet provides a significant proportion of NH_4^+ removal (Kadlec & Wallace, 2009). Alternatively, nitrification to NO_3^- results in either vegetation uptake, which stores nitrogen until senescence, or denitrification, which removes the nitrogen from the system (Ronkanen & Klove, 2009). Given the necessity to treat PO_4^{3-} , NH_4^+ , and NO_3^- , ladder fens, with their pool-rib-pool morphology, may provide an effective natural treatment system in these remote regions.

Domestic wastewater is typically not elevated in sulphate (SO_4^{2-}), but this compound is typically targeted in agricultural treatment wetlands (Kadlec & Wallace, 2009). However, in regions with SO_4^{2-} rich groundwater, for instance the JBL (Steinback, 2012b), domestic water that may be derived from groundwater wells may have elevated SO_4^{2-} concentrations, which eventually appear in the domestic wastewater or other process waters associated with industrial activities. The addition of SO_4^{2-} to waterlogged anoxic peat soil has been shown to increase methylmercury (MeHg) concentrations in peat pore waters (Branfireun *et al.*, 2001; Branfireun *et al.*, 1999; Coleman Wasik *et al.*, 2015; Coleman Wasik *et al.*, 2012; Hoggarth *et al.*, 2015; Mitchell *et al.*, 2008). Although MeHg is formed naturally, and is found in very low concentrations in major rivers in the Hudson Bay region (Kirk & St. Louis, 2009), the treatment of SO_4^{2-} through microbial reduction may increase MeHg production within the peatland pore water because the methylation of mercury is facilitated by SO_4^{2-} reducing bacteria in these environments (Branfireun *et al.*, 1999; Coleman Wasik *et al.*, 2015; Compeau & Bartha, 1985; Gilmour *et al.*, 1992; Hoggarth *et al.*, 2015; Mitchell *et al.*, 2008; Olson & Cooper, 1974); thus, potentially increasing the MeHg load in the down-gradient aquatic ecosystems. However, it is unknown if additional SO_4^{2-} in the wastewater will result in elevated MeHg in these systems while treating other wastewater contaminants.

With increasing development in peatland-dominated northern regions (i.e., the Canadian sub-arctic, JBL) there will be an increased need for domestic wastewater treatment and polishing. Given the limited information on the treatment and transport of wastewater contaminants and mercury dynamics when using ladder fens as wastewater polishing wetlands, this study used an experimental approach to better understand the ability of ladder fens to polish domestic wastewater

in remote peatland dominated landscapes and identify contaminants of concern due to their mobility. Specifically this study sought to:

1. Determine the transport of typical wastewater nutrients (NO_3^- , NH_4^+ , and PO_4^{3-} , SO_4^{2-}) and assess their potential export to down-gradient aquatic ecosystems;
2. Identify the impact of elevated SO_4^{2-} concentrations on the production of MeHg during wastewater treatment;
3. Provide the first assessment on the suitability of ladder fens for domestic wastewater treatment in remote sub-arctic regions.

This study did not evaluate the transport and fate of elevated organic matter that is often associated with wastewater, pathogens such as bacteria and viruses, or other wastewater constituents that are of emerging concern, such as pharmaceuticals.

4.3 Study Site

A continuous wastewater polishing experiment was conducted in a small ladder fen (9800 m²) in the JBL (N 5860348.772, E 705883.366) near the De Beers Group of Companies Victor Diamond Mine, during the 2014 growing season. Average precipitation and temperature during the study period (July and August 2014) were 14.9 °C and 90 mm, respectively, based on a nine year record from a local meteorological monitoring station which agreed well with long-term Environment Canada records at a station ~100 km away (Chapter 2). The experimental fen (EXP Fen) consisted of a series of peat ribs and pools (Figure 4-1), where the peat ribs were perpendicular to the

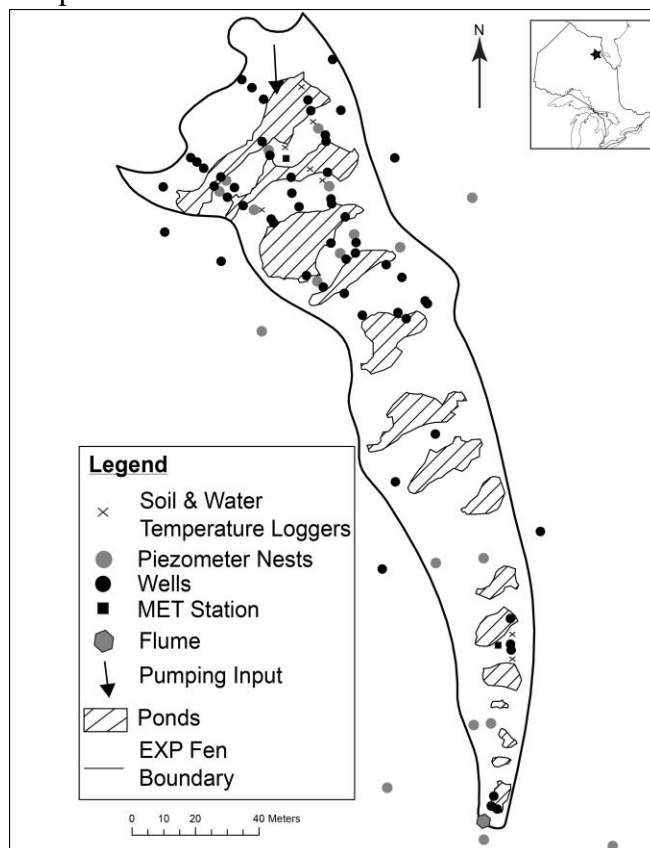


Figure 4-1 A map of the EXP Fen adapted from Chapter 2. Pools are sequentially number from the input pool (north) towards the south. Ribs follow the same sequential numbering starting for the first rib down-gradient (south) from Pool 1.

direction of water flow (Chapter 2) and solute transport (Chapter 3). The ribs were on average ~10 m wide with some areas much narrower (>3 m, Figure 4-1) and consisted of low-lying sections that increased hydrological connectivity during periods of high water tables, and topographically higher ridges that reduce water flow, but typically not solute transport (Chapter 2). Pools account for 2240 m² and are typically < 1 m deep (Chapter 2). In the absence of excess hydrological loading caused by wastewater pumping, the water table generally remains below the elevation of the high hydraulic conductivity peat in the near-surface layer for most of the year. Consequently, the site remains poorly hydrologically connected, except for spring freshet and autumn wet-up (Chapter 2). At this site the addition of water associated with wastewater polishing raised the water table into the high hydraulic conductivity layers (Chapter 2), resulting in most solutes being transported within the upper 0.1 m of saturated peat. Pools lowered the transport rates due to solute dilution and lower solute velocities (Chapter 3). For more detail on the hydrology or solute transport see Chapter 2 and Chapter 3, respectively. The hydrology of the EXP Fen was similar to 3 other nearby ladder fens studied by Leclair (2015) and Perras (2015), as well as 3 other more remote ladder fens that were used as reference sites for this study (Reference Site 1 – N 5860348.772, E 705883.366; Reference Site 2 – N 5860472.091, E 705811.312; and Reference Site 3 – N 5860472.091, E 705811.312). Furthermore, Cl⁻, Na⁺, and specific conductance in the EXP Fen was not distinct from the 3 reference sites (Chapter 3).

4.4 Methods

A concentrated solution of wastewater was created using a custom blend fertilizer to mimic wastewater from the De Beers Group of Companies Victor Diamond Mine domestic wastewater (Steinback, 2012a) and be similar to that reported for other northern Canadian communities (Yates *et al.*, 2012). The concentrated solution was injected (every 2 hours for 2.5 min) into a continuous water input (38 m³ day⁻¹ from a nearby bog pond, ~170 m away) to achieve target average concentrations of SO₄²⁻ (27.2 mg L⁻¹), NO₃⁻ (7.6 mg L⁻¹), NH₄⁺ (9.1 mg L⁻¹), PO₃³⁻ (7.4 mg L⁻¹), K⁺ (24.5 mg L⁻¹), Na⁺ (25.3 mg L⁻¹), and Cl⁻ (47.2 mg L⁻¹) between day of year (DOY) 192 – 243 in 2014. Prior to entering the EXP Fen, the water input and wastewater solution were mixed in a bucket weir that drained into Pond 1 (Figure 4-1). To ensure Pond 1 remained well mixed and preferential flow did not occur due to proximity to the injection point (Chapter 3), a mixing

motor anchored in the sediment of Pond 1 ran for 10 minutes after the solution was injected. Unexpected variations in the volume of water or concentrated wastewater solution pumped into the EXP Fen occurred due to mechanical pumping issues and resulted in large short-term changes in the final concentration of wastewater entering the EXP Fen; between 50 – 180 % of average target concentrations. The hydrological response (Chapter 2) and transport of Cl^- and Na^+ (Chapter 3) are reported elsewhere; thus, only the transport (mobility) and fate of the wastewater contaminants NO_3^- , NH_4^+ , PO_4^{3-} , and SO_4^{2-} are presented in this study, along with THg and MeHg.

4.4.1 Water and Soil Temperature

Water and soil temperature were measured in both the low-lying preferential flow paths and ridge microforms of Ribs 1, 2 & 10 at 0.05 m below the water table, which is the approximate layer in which the majority of solute was transported (Chapter 3), and in Pools 1 & 2 (1 and 5 cm below water surface, 20 cm above the pool bottom and at the pool bottom). Temperatures were measured using copper-constantan thermocouples (Figure 4-1), and were recorded on a Hobo UX120 4-channel Data Loggers at 1-second intervals, averaged every 20 minutes. The variable nature of the pool water level required the upper two thermocouples to be installed on a floating thermopile to ensure constant measurement depths relative to the pool surface.

4.4.2 Water Sampling and Analysis

During the polishing experiment, well water samples (Figure 4-1) for major ions and DOC were taken at least every 7 days between DOY 192 – 243, along with pre- and post-loading samples taken on DOY 172 and 254, respectively. Total mercury (THg) and MeHg were sampled every 7 days for the first 4 weeks of the experiment and every 2 weeks thereafter. Pre-loading mercury samples were taken on DOY 172 and 179 and post-loading mercury sampling occurred on DOY 254. All sampling occurred when no significant precipitation fell for the preceding three days and all wells were purged the day prior to sampling to ensure a representative pore water sample. All piezometers and wells were screened with a geochemically inert geotextile filter sock (Rice Engineering & Operating LTD., 2" Filter Sock). Specific conductance was measured in each well every three days to determine the maximum extent of the wastewater plume and sampling occurred

at least 1 rib beyond the observed maximum extent to ensure sampling captured the entire wastewater plume. The three reference sites were sampled three times over the study period (DOY 192, 212, and 237) for major ions, DOC, THg and MeHg. All water sampling was performed using a low-flow peristaltic pump with PTFE lines. After each sample was collected the lines were flushed with DI water and environmentalized (rinsing the bottle with well water 3 times) prior to taking the next sample. Field, line, DI, filter and preservation blanks were taken during each sampling event to monitor for any potential contamination. Duplicates were taken every 10 samples for major ions, DOC, and THg and MeHg.

Major ions and DOC samples were taken in sterile 50 mL FlipMate bottles (Delta Scientific Laboratory Products Ltd.), which were environmentalized prior to taking the sample. Samples were then stored in a chilled cooler for storage and transport until filtering. Samples were filtered using 0.45 μm polyethersulfone filters within 48 hours (typically < 24 hr) and frozen for transport to the Western University Biotron Institute for Experimental Climate Change Research for analysis. Analysis followed EPA 300.0 methodology using a Dionex ICS-1600 with AS-DV Autosampler. Dissolved organic carbon was analyzed by OI Analytical with persulphate wet oxidation after removing inorganic carbon with H_3PO_4 and purging volatiles on an Aurora 1030W TOC analyzer (limit of detection, LOD = 0.2 mg L^{-1}). Iso-concentration maps were manually interpolated.

Mercury (THg and MeHg) were sampled following the “clean-hands dirty-hands” EPA method 1669 in 250 mL sterile PETG bottles. Each sample was double-bagged and environmentalized prior to taking the sample and stored in a dark chilled cooler in the field. Prior to filtering and preservation, the samples were stored in a dark refrigerator at 4 °C for a maximum of 48 hours (typically < 24 hr). Samples were vacuum filtered (0.45 μm nitrocellulose membrane filters) using an acid-washed PTFE apparatus. Once filtered, samples were acidified to 1 % v/v with OmniTrace Ultra™ hydrochloric acid and rebagged in two clean plastic bags for storage (dark refrigerator at 4 °C) and transport to the Western University Biotron Institute for Experimental Climate Change Research. Total mercury analysis was performed on a Tekran 2600 mercury analyzer following EPA method 1631 (LOD = 0.05 ng L^{-1}) and MeHg analysis performed on Tekran 2700 analyzer following EPA method 1630 (LOD = 0.0054 ng L^{-1}).

4.4.3 Treatment Efficiency (TE)

Dilution and dispersion during transport of the wastewater contaminants mask the geochemical or biological processes polishing the wastewater in the EXP Fen. To separate the hydrological processes from the biogeochemical processes, the injection concentration of a given wastewater contaminant (C_{0s}) was adjusted to the ratio between the observed concentration of Cl^- (C_{Cl^-}) and the injected concentration of Cl^- ($C_{0\text{Cl}^-}$) at a given sampling point, assuming Cl^- is conservative in peatlands (Hoag & Price, 1997; Ours *et al.*, 1997; Rezanezhad *et al.*, 2012). This allows for the calculation of treatment efficiency (TE) solely due to biogeochemical processes, where

$$TE = \left(1 - \frac{C_s}{C_{0s} \cdot (C_{\text{Cl}^-} / C_{0\text{Cl}^-})} \right) \cdot 100\% \quad \text{Equation 4-1}$$

where C_s is the observed wastewater contaminant concentration (mg L^{-1}).

4.5 Results

Pool and rib water temperatures slightly decreased over the study period and on average ribs (average 14.3°C) were 4.3°C cooler than the pools (average 18.6°C) (Figure 4-2). The temperature at the water table within the ribs (low-lying = 0.05 m bgs and ridge = 0.20 m bgs) were not distinct from each other and typically the highest temperatures in the ridges were at the water table (data not shown). Pool 1 showed little stratification in temperature with depth, while Pool 2 had stronger stratification (Figure 4-2).

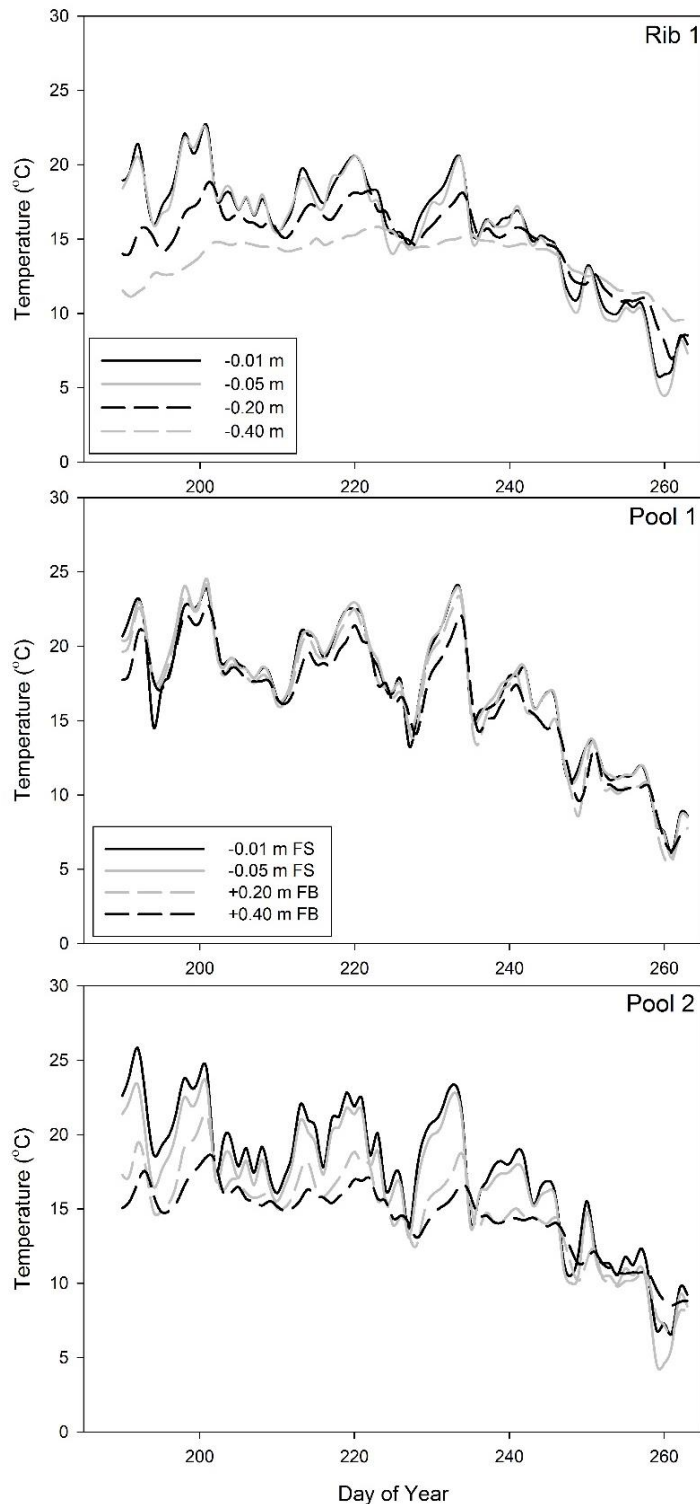


Figure 4-2 Pool and pore water temperatures for the low-lying region of Rib 1 (mbgs), Pool 1 and Pool 2 (from surface (FS) and from bottom (FB)). There was not distinct differences in temperatures between Rib 1, 2, and 10 at a given depth.

The continuous wastewater loading resulted in a shift in DOC, pH, and calcium (Ca^{2+}) concentrations at the EXP Fen, particularly in the uppermost ribs. Dissolved Organic Carbon decreased until DOY 205 after which it followed the same trend as the pumping source water in the uppermost ribs and pools (Figure 4-3). Beyond the uppermost ribs and pool, DOC followed the same trend as the reference sites, slightly increasing over the study period (Figure 4-3). A decrease in pH was observed in the uppermost ribs (highly impacted), while little systematic fluctuation occurred outside of the impacted region and the reference sites (Figure 4-4). Furthermore, the decreased pH in peat rib (1-4) was lower than the pH observed at the reference sites (Figure 4-4). Pool 1 pH (~4.4) did not change throughout the study period, while down-gradient pools followed the same trend in pH as Rib 1 (Figure 4-4), which decreased after ~DOY 198 (+4 days after pumping began). The decrease in pH coincides with an increase in Ca^{2+} concentration within rib pore water and Pool 2 (Figure 4-5). Similar to pH, the Pool 1 Ca^{2+} concentration did not fluctuate throughout the study and

remained low, similar to that at the reference sites (Figure 4-5). In the non-impacted regions Ca^{2+} (Figure 4-5) and pH (Figure 4-4) remained similar to or higher than that at the reference sites depending on the peat thickness, where thinning peat displayed higher Ca^{2+} concentrations due to better connectivity with mineral rich groundwater.

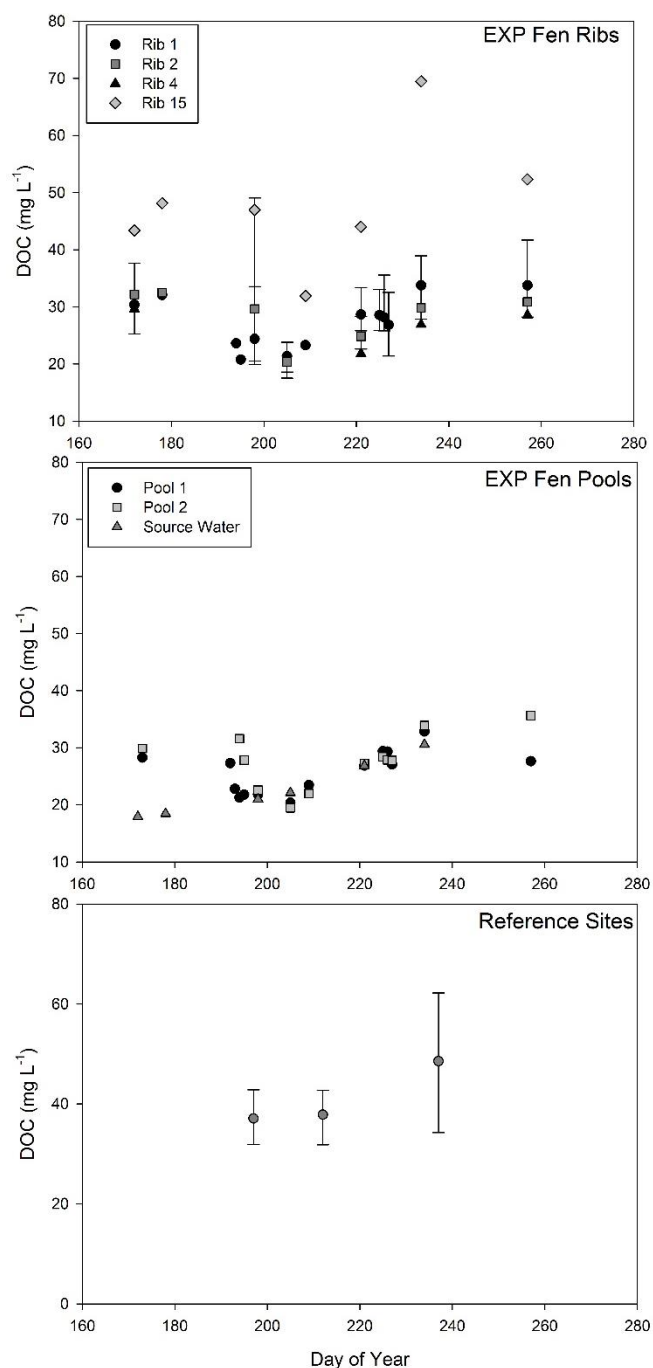


Figure 4-3 DOC concentrations at the EXP Fen ribs and pools, and the reference sites. Error bars are max/min. Pool samples represent only 1 replicate.

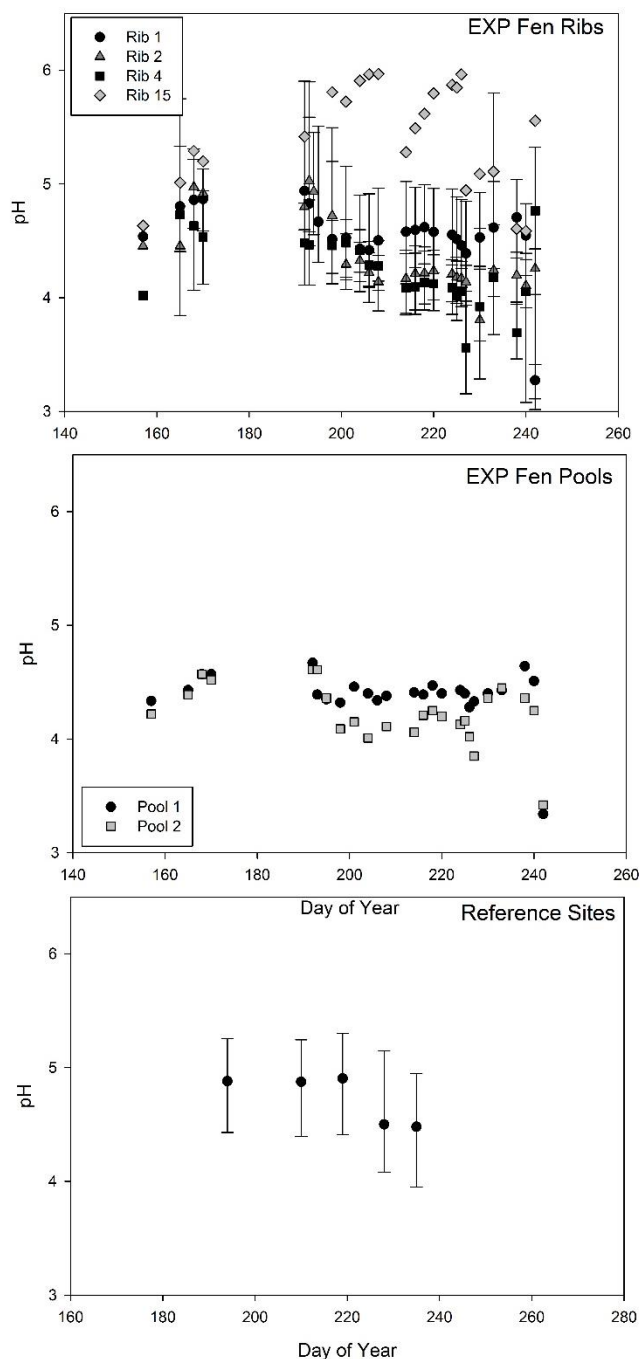


Figure 4-4 pH at the EXP Fen ribs and pools, and reference sites. Error bars are max/min. Pool samples represent only 1 replicate.

4.5.1 Contaminant Transport

Nitrate was not transported beyond Rib 1 and concentrations were low within the peat (Figure 4-6), while concentrations remained near or at the input concentration within Pool 1 (Figure 4-6). During the initial 6 days of the experiment elevated NO_3^- concentrations were detected at a maximum of 6 m from Pool 1; however, elevated NO_3^- concentrations within Rib 1 were not detected past 0.5 m of Pool 1 by the end of the experiment. The calculation of NO_3^- solute velocity was not possible due to the limited transport (i.e., 50 % of its input concentration was not observed outside of Pool 1).

Over the study period NH_4^+ was transported ~69 m, albeit reaching <50 % of its input concentration (29 % of the total distance), with the highest concentrations observed in Pool and Rib 1 (Figure 4-6). Within the peat ribs, NH_4^+ was mobile where NO_3^- concentrations were elevated (Figure 4-6, +2 Days to +13 Days), travelling several meters over 13 days. However,

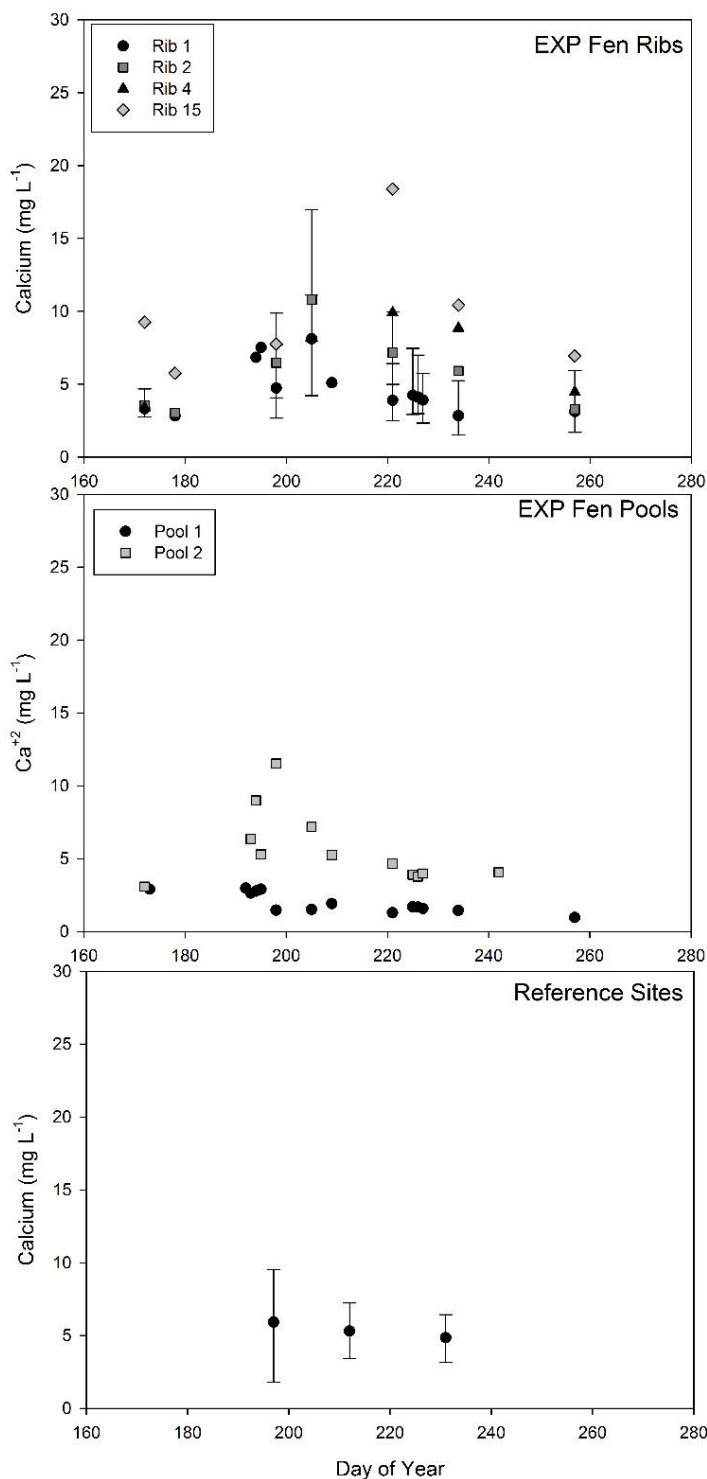


Figure 4-5 Ca^{2+} concentrations at the EXP Fen ribs and pools, and reference sites. Error bars are max/min. Pool samples represent only 1 replicate.

beyond the extent of the NO_3^- plume, NH_4^+ was even more mobile and travelled ~20 m over 13 days (Figure 4-6, +29 Days and +42 Days). Over the entire study period, the velocity of NH_4^+ (calculated as the rate required to observe 50 % of the input concentration at a point) was ~0.3 m day⁻¹.

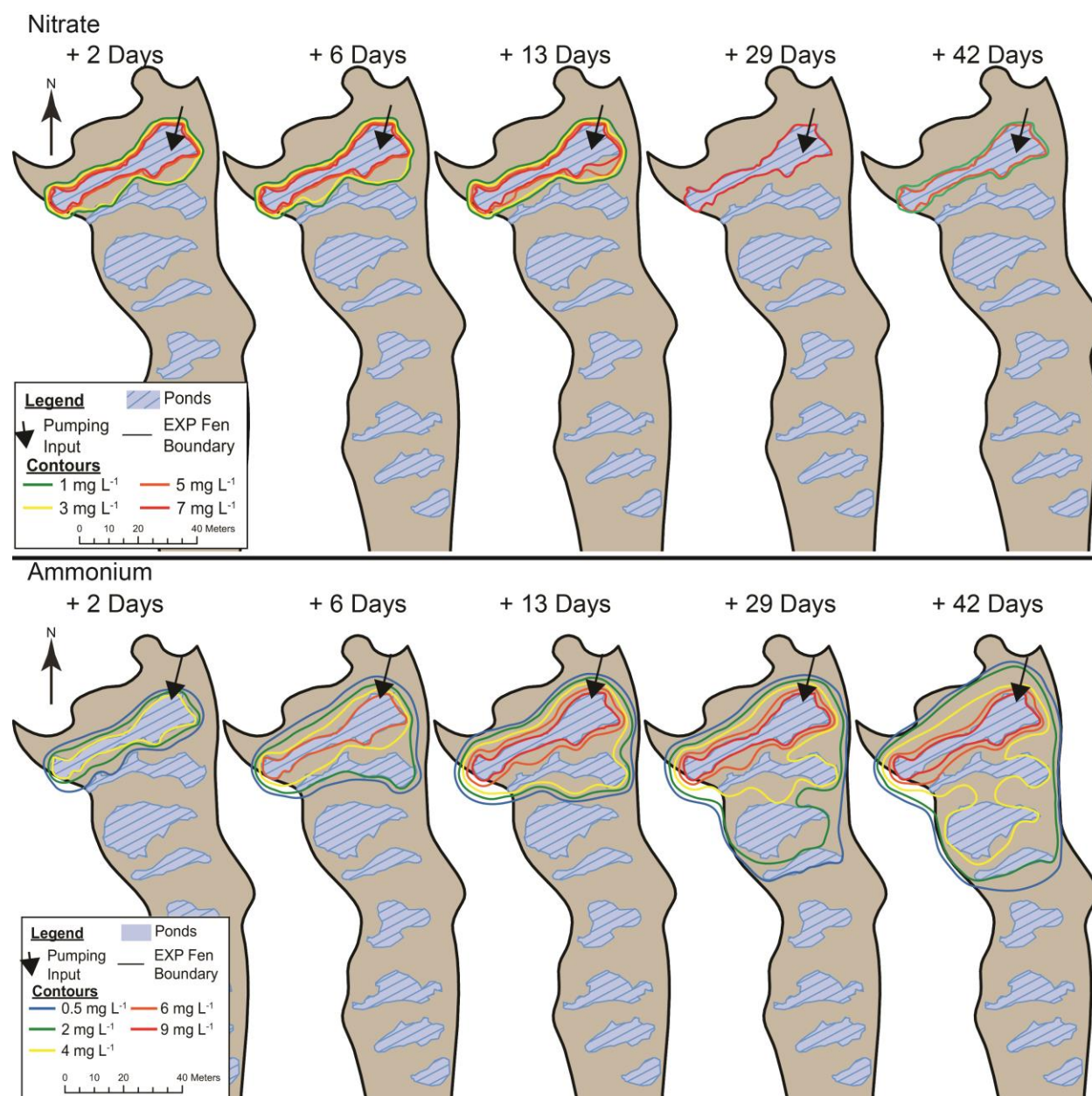


Figure 4-6 Manually interpolated NO_3^- and NH_4^+ concentration contour maps at the EXP over the study period. Input concentrations were 7.1 and 9.1 mg L⁻¹ for NO_3^- and NH_4^+ , respectively.

Phosphate was relatively immobile within the EXP Fen over the study period, travelling only ~32 m or ~13 % of the EXP Fen (Figure 4-7). Although the maximum extent of PO_4^{3-} was ~32 m, it displayed more complex transport behaviour than the other contaminants. During the first 13 days of the experiment PO_4^{3-} was not readily transported within Rib 1 yet became more mobile after this period (Figure 4-7). This mobile phase increased the solute velocity from ~0 m day^{-1} to ~0.3 m day^{-1} by the end of the experiment, resulting a rate of 0.2 m day^{-1} .

Unlike the other wastewater contaminants, SO_4^{2-} was highly mobile within the EXP Fen travelling a total distance of 117 m (~47 % of the EXP Fen) and had a highly irregular plume (Figure 4-8); similar to both Cl^- and Na^+ (Chapter 3). The highest concentrations remained near the source (Pool 1) and rapidly decreased past Pool 3 (Figure 4-8). However, the maximum extent was much farther than the 50% input concentration threshold and the average solute velocity was 1.3 m day^{-1} .

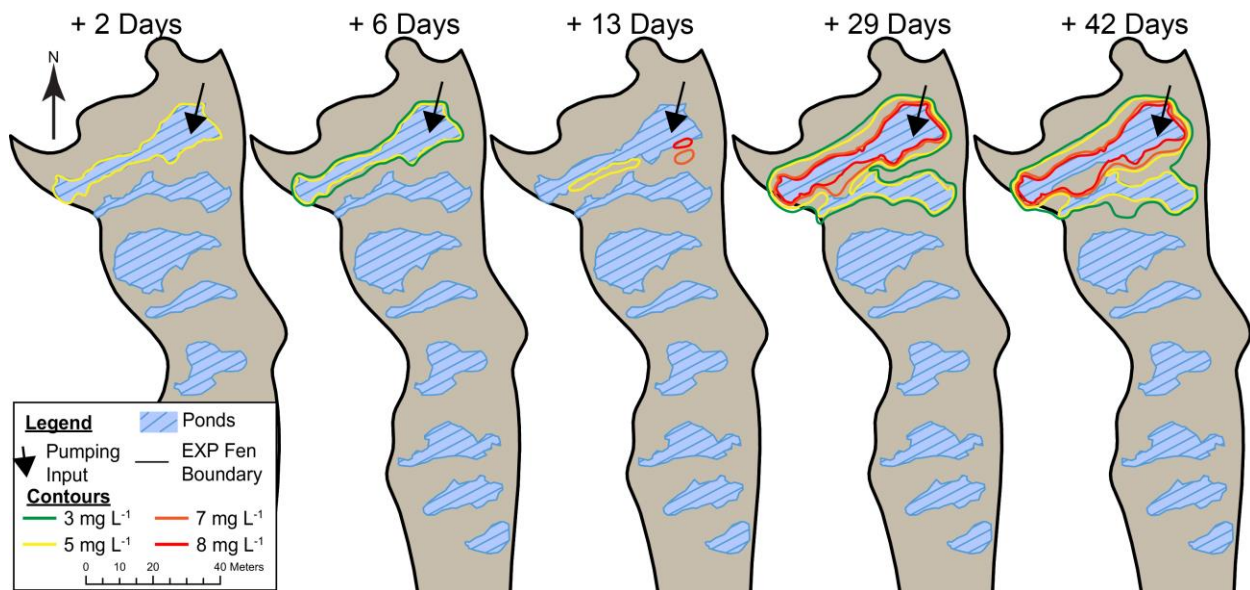


Figure 4-7 Manually interpolated PO_4^{3-} concentration contour maps at the EXP over the study period. Input

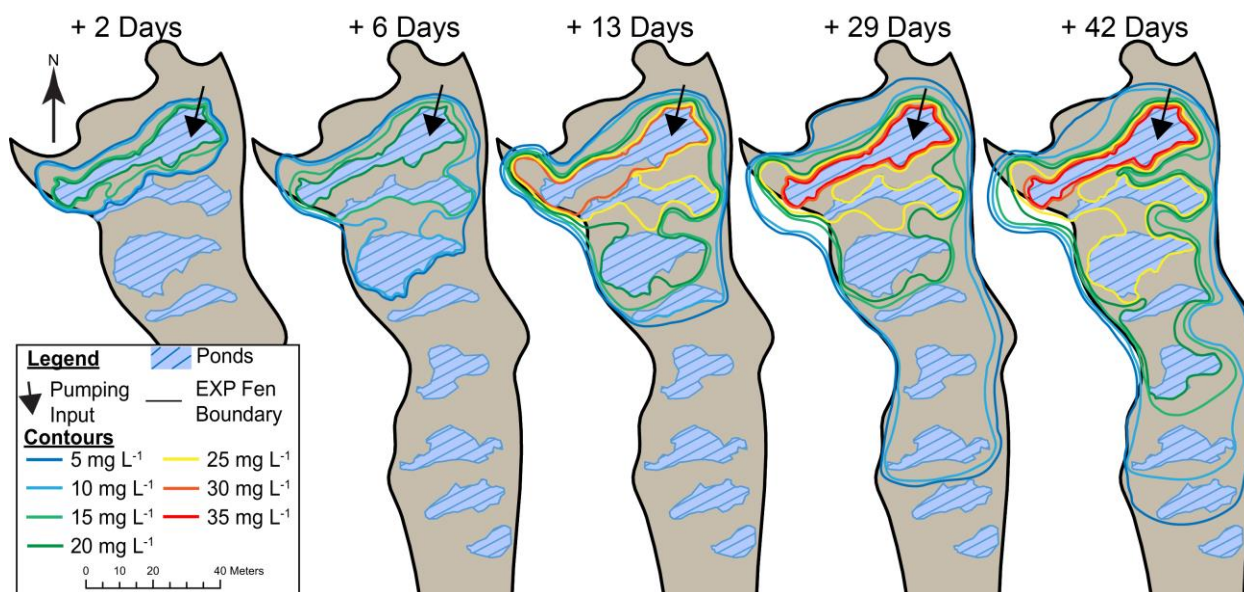


Figure 4-8 Manually interpolated SO_4^{2-} concentration contour maps at the EXP over the study period. Input

4.5.2 Treatment Efficiency

Within Pool 1 NO_3^- TE continuously increased over the experiment (Figure 4-9), plateauing at ~20 – 30 %. During the initial few days after pumping began, NO_3^- TE rapidly increased until DOY 205 – 209 in Rib 1, where it remained relatively constant (80 – 100 %) thereafter in all Rib 1 nests (Figure 4-9). A strong increase in TE was observed with distance through Rib 1; for instance, on DOY 198 the 1st nest's TE was 40 % while the 3rd nest's was 85 % (Figure 4-9). The NO_3^- TE followed this trend until DOY 220 when TE of all nests was ~100 % (Figure 4-9).

Minimal removal of NH_4^+ was observed within the pools (Figure 4-9), with the bulk being removed within the peat ribs (Figure 4-9). Initially there were high TE (40 – 80 %) within the peat of Rib 1; however, this decreased rapidly until DOY 205 when the TE began to plateau between 20 – 50 % depending on location within the rib; typically increasing with distance from Pool 1 (Figure 4-9).

Initially PO_4^{3-} was rapidly removed from both the peat pore water and pools (Figure 4-7) but after DOY 198 a steady, linear, decrease in TE was observed in both Pool and Rib 1 (Figure

4-9). The slope of the decrease is approximately the same between each nest group and only the timing of increase differs based on distance from Pool 1 (Figure 4-9). By DOY 220 PO_4^{3-} in both Pool 1 and the 1st nest was near or below 0 TE, while in the 2nd and 3rd nests was well above 0 but decreasing (Figure 4-9).

There was little to no removal of SO_4^{2-} within the pools, as observed by the near zero slope of the TE in Pool 1 (Figure 4-9) and no relationship in Pool 2 (data not shown). There was a slight increase in TE with distance through Rib 1 (Figure 4-9); however, TE remained low compared to the domestic wastewater contaminants, reaching a maximum TE of ~50 % by the end of the experiment (Figure 4-9). Unlike the other contaminants, SO_4^{2-} TE did not plateau by the end of the experiment and more temporal variability, yet less spatial variability, was observed.

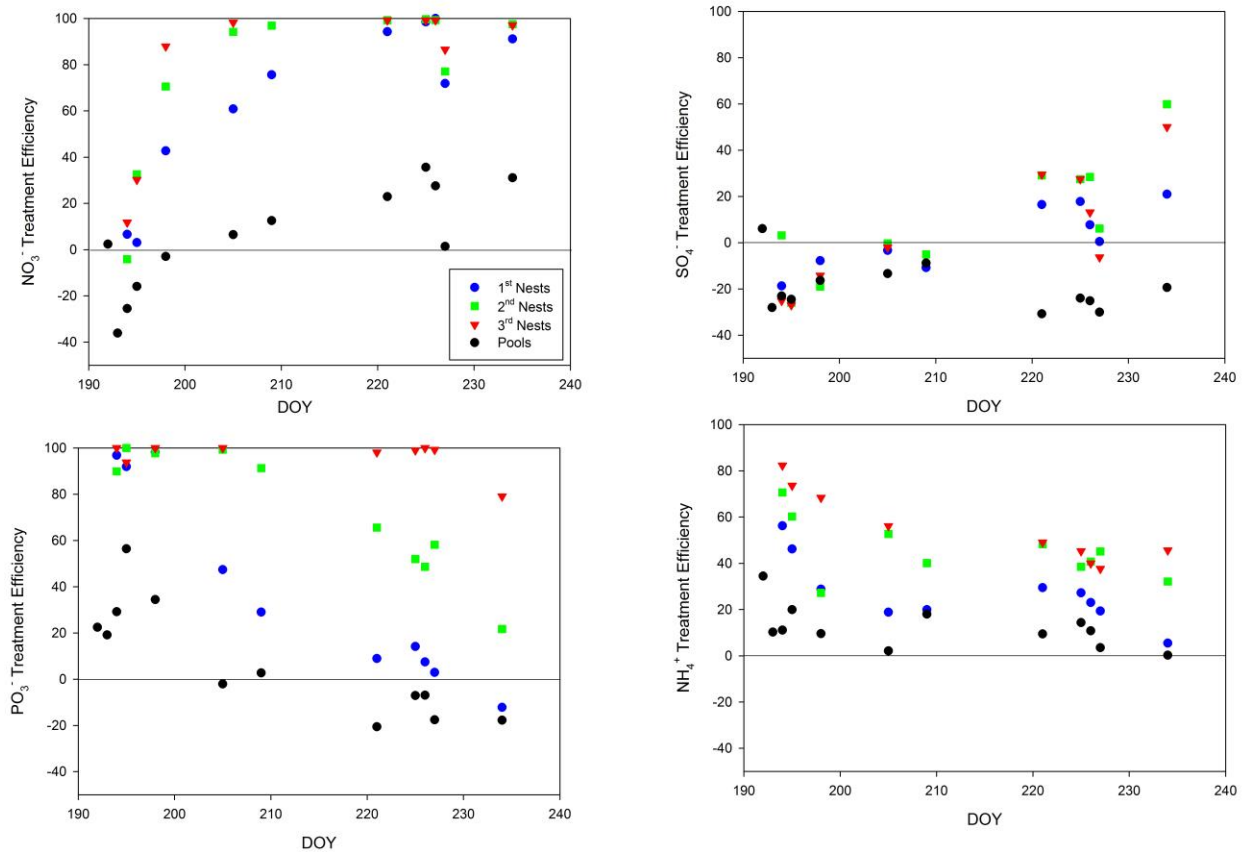


Figure 4-9 Treatment efficiency (TE) for NO_3^- , SO_4^{2-} , NH_4^+ , and PO_4^{3-} in Rib 1 and Pool 1. 1st – 3rd nests refer to the position of a nest in proximity to Pool 1 along a given north-to-south transect (i.e., 1st nest are the 4 nests closest to Pool 1 and 3rd nests are furthest from Pool 1). Negative values indicate a net release of a given contaminant.

4.5.3 Mercury

Prior to wastewater loading, concentrations of THg and MeHg in the pore water (Figure 4-10) and pools were similar to the reference sites across the EXP Fen (Figure 4-10). Once loading began an increase in both THg and MeHg occurred in the peat ribs (Figure 4-10). THg concentrations increased ~5-fold in Rib 1 and the percentage of methylmercury (%MeHg) was nearly 80-100 % by the end of the wastewater loading (DOY 234). The highest MeHg concentrations occurred within Rib 1 in conjunction with high SO_4^{2-} and THg concentrations. Both THg and MeHg concentrations remained low in the pools, showing only slight increases in %MeHg over the experiment (Figure 4-10 & Figure 4-11). Increases in pool THg and MeHg were observed down-gradient from peat ribs (Figure 4-10). Fourteen days post-wastewater loading, absolute concentrations of THg and MeHg decreased (Figure 4-10), while %MeHg within the pore water remained high across the site in the absence of elevated SO_4^{2-} concentrations (Figure 4-11).

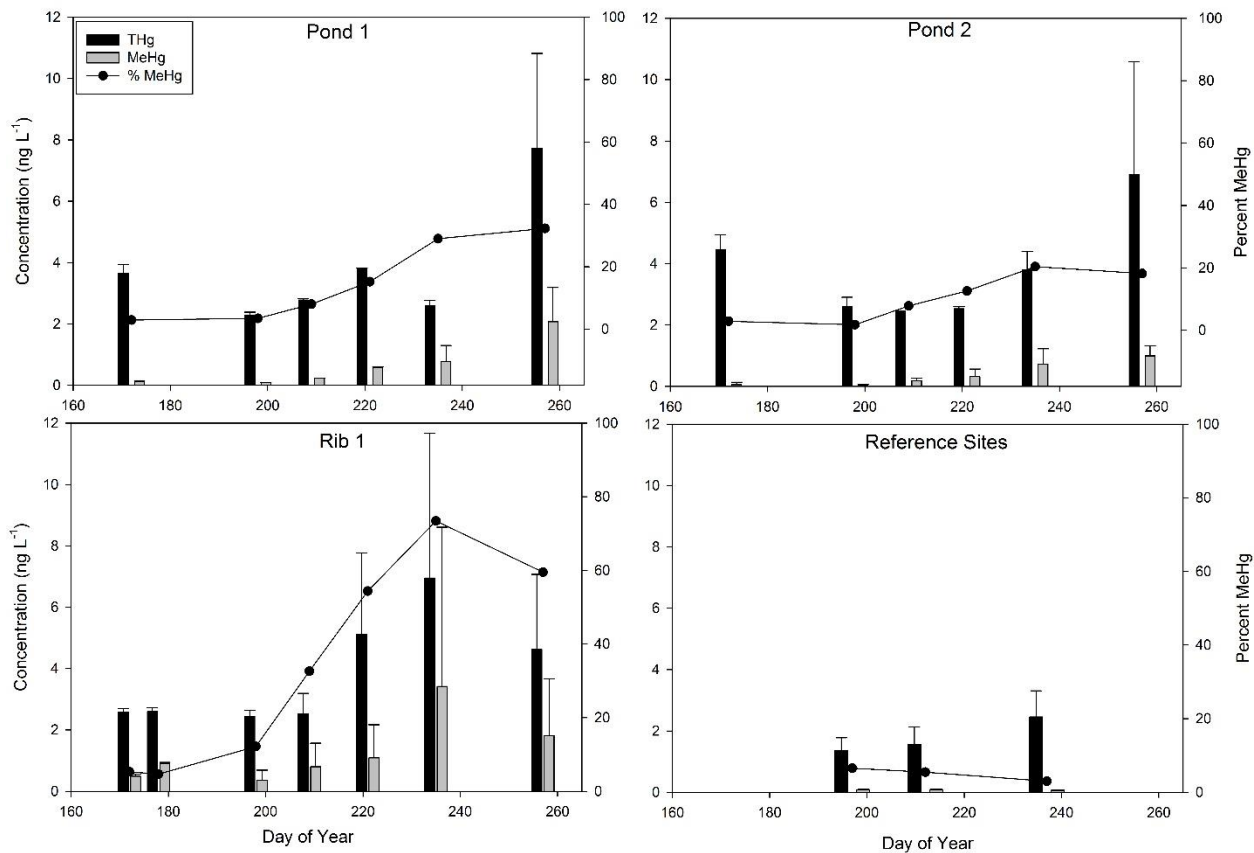


Figure 4-10 Concentration of THg (black bars), MeHg (grey bars), and %MeHg (black line) in Pools 1 & 2, Rib 1, and the reference sites. Error bars are 1 standard deviation from the mean ($n = 4$ in the pools, 12 in the rib, and 16 at the reference sites). Note the two different y-axis, where the primary y-axis concentration and the secondary y-axis is the %MeHg.

4.6 Discussion

There was high variability in wastewater contaminant mobility during the experiment, with NO_3^- being the least mobile and SO_4^{2-} the most mobile (Figure 4-6 & Figure 4-8). The pattern of transport was similar between the wastewater contaminants (Figure 4-6, Figure 4-7 & Figure 4-8) and Cl^- and Na^+ reported in

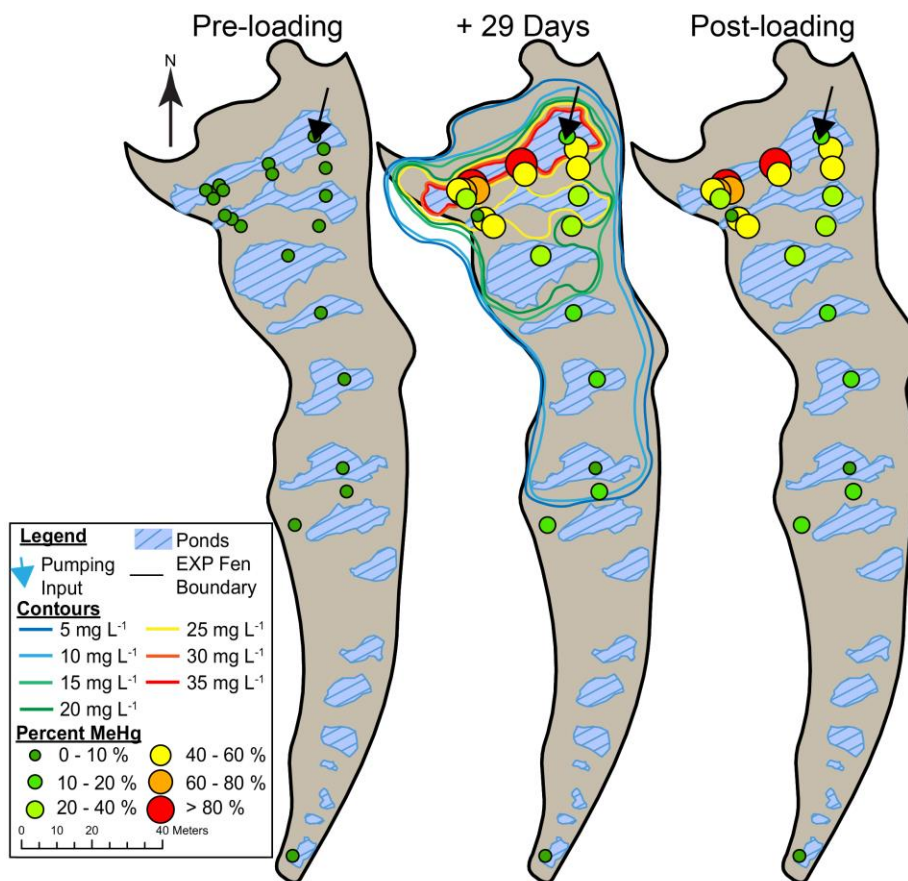


Figure 4-11 The %MeHg overlaid with SO_4^{2-} contours for pre-loading 29 days after the experiment began, and post-loading (14 days after the experiment ceased). Both pre and post-loading SO_4^{2-} concentrations were below background levels.

Chapter 3, typically responding to patterns of high solute velocities, small rib widths and high hydraulic conductivities (Chapter 3). The consistent temperature within the peat ribs at the water table indicates that transport was likely not influenced by temperature.

The minimal temperature stratification of Pool 1 compared to Pool 2 demonstrates that Pool 1 was well mixed, unlike Pool 2 (Figure 4-2), because of the mixing motor. Due to the stratification observed in Pool 2 (Figure 4-2), the active transport portion of the pools could be restricted to the upper few centimeters, which may reduce the storage of contaminants in the pools, and explain the rapid transport across them (Figure 4-6 & Figure 4-8). Furthermore, the pools influenced the transport of the wastewater contaminants similarly to Cl^- and Na^+ , where dilution was initially observed but offered little storage once achieving a given contaminant concentration. Conversely, in Chapter 3 slightly lower solute velocities within the pools (Chapter 3), suggesting

that a the high hydraulic efficiency (Thackston *et al.*, 1987) primarily controlled the accelerated transport of solutes within pools. Both NH_4^+ and SO_4^{2-} followed this trend closely where little removal occurred in the pools (Figure 4-9) and were transported the furthest down-gradient (Figure 4-6 & Figure 4-8), while both the relatively immobile contaminants (NO_3^- and PO_4^{3-}) were removed (slightly) within the pools (Figure 4-9). The relatively rapid transport of NH_4^+ and SO_4^{2-} was potentially assisted by wind induced short-circuiting across the pools (Shaw *et al.*, 1997) that would increase the solute velocity. Furthermore, these two mobile contaminants were typically transported into the pools once an equilibrium water table was reached (Chapter 3), potentially resulting in higher solute velocities than observed with both Cl^- and Na^+ (Chapter 3). However, more in-depth research on the in-pool hydrodynamics and biogeochemical interactions is required to better understand their role and function for both transport and wastewater polishing. When no removal within the pools occurred (SO_4^{2-}), the contaminant plume had similar maximum extent to Cl^- and Na^+ during the study period (Chapter 3). However, the plumes differed in location of the highly elevated concentrations ($< 70\%$ of input concentration) depending on the removal pathways. Although the hydrophysical properties of the EXP Fen governs contaminant plume's shape and extent, the development of these plumes were dependent on the biogeochemical processes influencing each of the wastewater contaminants.

Nitrogen, NO_3^- and NH_4^+ , were both removed from the aqueous phase in both pools and ribs and likely followed separate yet linked removal pathways. Both contaminants were primarily removed within the peat ribs as indicated by their greater TE than that in the pools (Figure 4-9). Within the pools, volatilization of NH_4^+ was likely through nitrification and subsequent denitrification in addition to sorption to colloids or the pool sediments (Kadlec & Wallace, 2009). This variation in NH_4^+ transport, indicates that both of the potential treatment pathways for NH_4^+ occurred in the EXP Fen: 1) geochemical sorption to the peat substrate (Richardson, 1985) and 2) uptake or transformation by biological processes (Noe *et al.*, 2003; Xing *et al.*, 2011). Within the NO_3^- plume, it is likely that geochemical sorption to particles/peat was the dominant treatment pathway for NH_4^+ because NO_3^- is more bioavailable to peatland vegetation (Bubier *et al.*, 2007; Xing *et al.*, 2011) and NH_4^+ requires oxidation to NO_3^- for efficient vegetation uptake (Kadlec & Wallace, 2009; Xing *et al.*, 2011). Oxidation to NO_3^- was limited in the ribs and is likely confined to the capillary fringe because of slow oxygen diffusion (Armstrong, 1967). Outside the NO_3^-

plume, TE increased (Figure 4-9, 2nd & 3rd nests) and remained between 30 – 40 % in the peat ribs beyond Rib 1 (data not shown). It is within these regions of the EXP Fen that both NH_4^+ removal pathways are operating, increasing the TE and limiting transport. Although NH_4^+ was eventually completely removed from the pore water, it remained a relatively mobile contaminant in surface water during periods of enhanced hydrological connectivity, such as those observed in 2015 (Chapter 2). Under these conditions the release of NH_4^+ to the surrounding aquatic ecosystems is likely.

In Rib 1, ~ 80 – 100 % NO_3^- removal occurred, followed by ~20 % removal within Pool 1 (Figure 4-9); this effectively prevented further down-gradient transport of NO_3^- . By DOY 209, near complete removal of NO_3^- had occurred within 0.5 m of the pool edge and no transport was observed past this point (Figure 4-6). The complete removal of NO_3^- from the pore water within the first meter of the peat rib illustrates the nutrient limited status of these anoxic systems (Xing *et al.*, 2011). Due to the high water tables, anoxic and reducing conditions likely dominated the saturated peat, resulting in two pathways for NO_3^- removal: microbial reduction and vegetation uptake (Ronkanen & Klove, 2009; Xing *et al.*, 2011). Microbial reduction of NO_3^- was likely active within this system due to the available carbon (i.e., peat) and anoxic conditions (Basiliko *et al.*, 2006; Lamers *et al.*, 2012); thus, complete removal of nitrogen occurs as N_2O or N_2 gas (Lamers *et al.*, 2012; Xing *et al.*, 2011). The second pathway may have been through terrestrial and aquatic vegetation uptake (Ronkanen & Klove, 2009), which store N- NO_3^- within the vegetation, but potentially release the nitrogen during the fall senescence (Bubier *et al.*, 2007; Ronkanen & Klove, 2009) and subsequent period of high hydrological connectivity (Chapter 2). This pathway could result in significant release of nitrogen to down-gradient aquatic ecosystems; however, internal nutrient cycling can help mediate this release through conversion of organic nitrogen to biogeochemically available forms (Bubier *et al.*, 2007). Both of these pathways occur in aquatic and terrestrial wastewater treatment wetlands (Kadlec & Wallace, 2009). However, unlike many constructed wetlands where the majority of nitrogen is removed within open water treatment systems, in the EXP Fen nitrogen was primarily removed within the peat ribs. Thus, the size and shape of the peat ribs, in addition to the other hydrophysical properties, will likely control the treatment of NO_3^- , and subsequently NH_4^+ , and its potential release to down-gradient aquatic ecosystems.

During the experiment PO_4^{3-} was initially immobilized but was remobilized over the course of the experiment as indicated by the decreasing TE over time and net gain of PO_4^{3-} within Pool 1 by the end of the experiment (Figure 4-7). During the initial few days of the experiment, treatment of PO_4^{3-} likely comes from multiple sources ranging from aquatic vegetation and algae uptake (Pietro *et al.*, 2006), particulate precipitation (Kastelan-Macan & Petrovic, 1996; Morris & Hesterberg, 2012; Noe *et al.*, 2003; Richardson, 1985), terrestrial vegetation uptake (Kirkham *et al.*, 1996), and sorption to metal-humic complexes on the peat or colloids (Nieminen & Jarva, 1996). The absence of PO_4^{3-} within the EXP Fen after 13 days of loading illustrates the large capacity for the biogeochemical processes in peatlands to remove PO_4^{3-} (Figure 4-7). Furthermore, the rapid removal of PO_4^{3-} suggests particulate production or sorption to peat or colloids were the primary mechanisms for PO_4^{3-} removal (Nieminen & Jarva, 1996; Noe *et al.*, 2003; Richardson, 1985). However, this may leave the removed PO_4^{3-} in readily accessible forms if different geochemical conditions occur. For example, after DOY 205 a shift in geochemical conditions occurred, indicated by the decreased pH (Figure 4-4), which corresponded with the observed decrease in PO_4^{3-} TE (Figure 4-9) and increased Ca^{2+} concentrations (~ 5 to 10 mg L^{-1} , Figure 4-5). It is likely that the decrease in pH resulted in the dissolution of calcium phosphate precipitates (Ferguson *et al.*, 1973), releasing bound PO_4^{3-} into the aqueous phase. Additional removal of PO_4^{3-} occurred within the ribs by biological processes as illustrated by the increasing TE between Nests 1-3 for a given time (Figure 4-9), yet became saturated to PO_4^{3-} over time (as noted by the increase in TE at all nests, Figure 4-9). Once the peat is saturated with respect to PO_4^{3-} , no more can be removed through biological or geochemical processes under the prevailing biogeochemical conditions, this further additions of PO_4^{3-} are mobile.

Initially, complete treatment of PO_4^{3-} occurred in Rib 1 over the first 6 days (DOY 192 – 198) but a decrease was observed after this period, which cascaded through Rib 1 to Pool 2 (Figure 4-9). This cascade created PO_4^{3-} fronts, which have been observed in many treatment wetlands (Kadlec & Wallace, 2009) and typically indicate saturation of the system towards PO_4^{3-} (Pietro *et al.*, 2006; Ronkanen & Klove, 2009; Seo *et al.*, 2005). These fronts are exemplified in the EXP Fen where PO_4^{3-} was initially immobile (Figure 4-7) but then broke through to Pool 2 in ~ 13 days and the front was then halted at Rib 2, showing limited movement within this rib for the remainder

of the experiment (Figure 4-7). However, this transport behaviour raises the question of the suitability of ladder fens, and other peatlands, for treating PO_4^{3-} due to the potential for release to aquatic ecosystems over time. Other northern treatment peatlands have observed >90 % phosphorous removal over several years due to humic-aluminum complexes binding most of the PO_4^{3-} entering the wetland (Ronkanen & Klove, 2009); however, it is unknown if there is a large presence of metal-humic complexes in the EXP Fen peat or if calcium phosphate precipitation controls PO_4^{3-} removal. However, given the observed low pH and reducing conditions (generation of MeHg) it was unlikely that metal-humic binding was dominant within the EXP Fen. Raising the pH of the wastewater influent may allow for greater PO_4^{3-} removal through metal-humic complexes and calcium phosphate precipitation because they are more efficient at circumneutral or slightly basic pH (Ferguson *et al.*, 1973; Heiberg *et al.*, 2012; Morris & Hesterberg, 2012; Noe *et al.*, 2003; Staunton & Leprince, 1996). Raising the pH may decrease the likelihood of PO_4^{3-} release to downstream aquatic ecosystems, increasing TE and the longevity of a ladder fen for wastewater polishing. Furthermore, addition of aluminum or iron flocculants prior to release into the polishing peatland may also increase the treatment of PO_4^{3-} (Kadlec & Wallace, 2009) but the implications of these additions in peatlands are unknown and require further study.

4.6.1 Sulphate and Mercury

The lack of removal of SO_4^{2-} in pools (Figure 4-9) coupled with low TE (Figure 4-9) resulted in an extensive plume. Although TE continuously increased over the study period in Rib 1 (Figure 4-9), there was no treatment, or potentially release, ($\text{TE} < 0$) in Pool 1 (Figure 4-9) or other pools (data not shown), indicating that the peat ribs were the primary zone of SO_4^{2-} removal in the EXP Fen (Figure 4-7). The deeply anoxic conditions in peatlands (Bottrell *et al.*, 2007; Koretsky *et al.*, 2006; Rubol *et al.*, 2012) and typically nutrient limited conditions in peatlands (Campbell & Bergeron, 2012; Chapin *et al.*, 2003; Juutinen *et al.*, 2010) promote the accumulation of carbon as peat (Gorham, 1991; Kuhry & Vitt, 1996). Thus, terminal electron acceptors (i.e., NO_3^- or SO_4^{2-}) are an important biogeochemical process in the accumulation of peat and peatlands (Achnich *et al.*, 1995; Keller & Bridgham, 2007; Limpens *et al.*, 2008). Given that production of MeHg is mediated by SO_4^{2-} reduction (Compeau & Bartha, 1985; Gilmour & Henry, 1991) and has been identified as a primary mechanism in peatlands (Branfireun *et al.*, 2001;

Branfireun *et al.*, 1999), it is likely that this process governed the elevated MeHg concentrations in the EXP Fen. Additionally, the higher redox potential within the NO_3^- plume potentially limited SO_4^{2-} reduction (i.e., treatment), resulting in no observed treatment within Pool 1; further suggesting the microbial mediated reduction pathway. Furthermore, there was no observed plateau in TE over the study period; thus, the EXP Fen did not saturate towards SO_4^{2-} and will likely continue to produce MeHg provided temperature does not become limiting. Although under the current geochemical conditions the EXP Fen was not saturated with respect to SO_4^{2-} , suggesting a large storage capacity, the observed high mobility suggests ladder fens have limited capacity for treating this contaminant.

The increase in THg and MeHg in the pore water coincided with the observed decrease pH (Figure 4-4) and elevated SO_4^{2-} concentrations. The decrease in pH increases the solubility of both MeHg and Hg(II) (Melamed *et al.*, 2000), which explains the increase in THg in the pore water (Figure 4-10). Within the peat, the microbial SO_4^{2-} reducing community likely utilized the elevated SO_4^{2-} and Hg(II) concentrations (Compeau & Bartha, 1985; Gilmour *et al.*, 1992), similar to Branfireun *et al.* (1999), and produced the elevated MeHg concentrations. However, the extremely high, MeHg concentrations and %MeHg in the pore water was unexpected and far higher than normally observed in the reference sites (Figure 4-10). Outside of the SO_4^{2-} plume, MeHg concentrations remained at similar concentrations as the background and reference site (Figure 4-10 & Figure 4-11). These data indicate that any increase in SO_4^{2-} concentrations in the peat pore water of this peatland will increase the MeHg concentration in pore waters. Furthermore, the persistence of elevated MeHg concentrations 14 days after the experiment indicates the potential for long-term contamination after wastewater polishing has ceased. These peatlands appear to be conducive to MeHg production particularly under elevated SO_4^{2-} loading, however increased export of MeHg was not observed over the course of this experiment, so the degree of potential impairment of downstream aquatic ecosystems is not known.

4.6.2 Ladder Fens as Wastewater Treatment Wetlands

Peatlands have been shown to effectively treat or polish wastewater in northern environments (Eskelinen *et al.*, 2015; Kadlec, 2009a; Ronkanen & Klove, 2009; Yates *et al.*,

2012). For instance, Kadlec (2009a) observed a three order of magnitude ($\sim 10 - 0.01 \text{ mg L}^{-1}$) decrease in NO_3^- (complete), PO_4^{3-} , and NH_4^+ within 1400 m of in the influent point in a domestic wastewater polishing peatland. However, under continual operation the removal rate coefficient slightly decreased but this was minor as the peatland still effectively removed the contaminants from the pore water (Kadlec, 2009a). Additionally, Ronkanen and Klove (2009) found similar rapid removal of both NO_3^- and phosphorus in two polishing peatlands in Northern Finland. In the EXP Fen, a plateau in TE was observed for both NO_3^- and NH_4^+ (Figure 4-9), indicating a potential sustained removal rate. The rapid and complete removal of NO_3^- resulted in highly efficient TE ($\sim 100 \%$), which agrees well with both Ronkanen and Klove (2009) and Kadlec (2009a). Conversely, NH_4^+ TE was much lower ($\sim 20 - 50 \%$), resulting accelerated transport, similar to Ronkanen and Klove (2009). The observed plateau in TE indicates that Rib 1 saturated towards NH_4^+ by the end of the experiment. Given the observed transport rate, NH_4^+ would potentially be detected at the outflow in ~ 800 days (~ 2.2 years) of sustained use. Once detected at the outlet the system could be considered saturated towards NH_4^+ and once saturated the TE of the EXP Fen would likely be similar to the observed TE plateau. Additionally, PO_4^{3-} did not plateau during the experiment and TE continually decreased (Figure 4-9) indicating that once the system is saturated towards PO_4^{3-} minimal removal may occur; however, this has not been observed in other polishing peatlands (Kadlec, 2009a; Ronkanen & Klove, 2009) and longer-term studies of ladder fens' ability to remove and store PO_4^{3-} are required. Only SO_4^{2-} was mobile ($\sim 1.3 \text{ m day}^{-1}$) and could potentially be released in ~ 200 days, sooner than the domestic wastewater contaminants. However, this is speculative and given the effective polishing observed at other peatlands over much longer time spans, further research is needed to determine the true treatment potential of ladder fens. Notwithstanding the potential for release from the EXP Fen, precautions can be taken to increase the TE or residence time of solutes in ladder fens, thus increasing the time until release.

To increase TE and limit the potential release of contaminants to aquatic ecosystems it may be prudent to alter the geochemical properties of the influent prior to wastewater treatment. Typically, treatment wetlands have a circumneutral or slightly basic pH (Kadlec, 2009a; Lens *et al.*, 1995; Palmer *et al.*, 2015; Vymazal, 2014) that was not observed in the EXP Fen. Increasing the pH of the influent may help increase TE of PO_4^{3-} and decrease the solubility of mercury. By increasing the pH it is possible that the highly elevated methyl and THg concentrations will not

occur, increasing the suitability of ladder fens as treatment or polishing wetlands. The transport and residence time of any contaminant is directly related to the hydrological connectivity of a ladder fen (Chapter 3). Decreasing the hydraulic load associated with wastewater treatment (Chapter 2) will lower the water table and decrease the hydrological connectivity of the system (Chapter 2). This will increase the residence time of the system, allowing for greater contaminant polishing or treatment. Furthermore, by decreasing the hydrological connectivity, mobile contaminants, such as SO_4^{2-} , will be limited spatially; thus, the production of MeHg will be confined to the limited SO_4^{2-} plume. Additionally, the longer residence times within the pools will increase the likelihood of photodegradation of the MeHg (Fleck *et al.*, 2014), further decreasing the potential for contaminant release to the surrounding aquatic ecosystems. Other, less mobile contaminants, will be further spatially limited under a decreased hydrological load but care must be taken to ensure saturation towards a given contaminants (i.e., PO_4^{3-}) does not occur. Seasonal manipulation of the water table may be required to prevent flushing of contaminants during the autumn senescence, which coincides with a period of high hydrological connectivity (Chapter 2). Lowering the inputs during the autumn and spring can prevent the rapid transport of stored contaminants to the aquatic ecosystems as the system residence time during these periods can be hours instead of days (Chapter 2). During extreme hydrological events, such as those experienced in 2015 (Chapter 2), wastewater release should be paused to prevent the rapid transport of contaminants to aquatic ecosystems. Although this study represents a single growing season of wastewater polishing, the 100 % treatment (no observed increase at the outflow) of all contaminants, either added or generated, highlights the ability of ladder fens to polish wastewater contaminants safely in sub-arctic environments.

4.7 Conclusions

There was complete treatment of all contaminants within 50 % of the total EXP Fen length and minimal transport of MeHg after the loading experiment during a climatically average summer. However, the unexpected magnitude of the mercury and MeHg response due to the SO_4^{2-} loading will require careful control of the water table to ensure rapid transport of contaminants does not occur. Given the risks of MeHg contamination, further research is required to determine the biogeochemical dynamics and transport of mercury in wastewater polishing peatlands to ensure

their use minimizes the potential risks. In any case, careful control of the water table by varying the input rate in treatment or polishing ladder fens can help mitigate these risks. Furthermore, creating peat dams (mounds of peat) in the low-lying regions of ribs could help avoid periods of surface water connection from the input to the outflow, significantly decreasing the hydrological (Chapter 2), thus chemical, connectivity of ladder fens. Although the broad function of the pools to treat wastewater was determined in this study, there remains a gap in knowledge of the specific hydrochemical processes occurring within the pools and further study of these processes could lead towards more efficient use of ladder fens as treatment or polishing wetlands. Although this study does indicate the potential for ladder fens to be used for domestic wastewater polishing, there remains a number of questions that should be addressed; chiefly, what is the longevity of these systems and how might the efficiency of these systems change within the context of a changing climate? Furthermore, the effects of biological contaminants or pharmaceuticals were not assessed; thus, pose an unknown risk when using these systems for domestic wastewater treatment or polishing. This study demonstrated that the pool-rib-pool morphology of ladder fens can provide both surficial (pools) and subsurface (peat ribs) treatment wetlands in remote northern regions that can effectively treat various wastewater contaminants provided that the effluent stream discharge rate be managed.

4.8 Acknowledgements

The authors would like to acknowledge funding from the NSERC Canadian Network for Aquatic Ecosystem Services. Furthermore, we would like to thank the De Beer Group of Companies Victor Diamond Mine Environment Staff for their help and hospitality. Lastly, we would like to thank Robin Taves, James Sherwood, Aaron Craig, Nicole Balliston, and Matthew Cartwright for their invaluable help collecting field data.

5 Conclusions and Recommendations

This study demonstrated that the pool-rib-pool morphology of ladder fens provides both surficial (pools) and subsurface (peat ribs) treatment wetlands in remote northern regions that can effectively treat various domestic wastewater contaminants. Nevertheless, this study represents the initial contaminant plume development, a transient state, and does not necessarily represent the transport and fate of domestic wastewater contaminants during sustained use or under changing climatic conditions. Understanding the hydrochemical processes governing the transport and fate of domestic wastewater contaminants is critical to safely and effectively using ladder fens for wastewater treatment or polishing. Ladder fens act as water and solute conveyers from bog peatlands to the aquatic ecosystems and have an immense ability to retard domestic wastewater contaminants; especially during the initial transient phase. However, the ability to treat these contaminants is directly related to the hydrology of ladder fens, which can be split into three distinct phases: 1) low subsurface hydrological connectivity, 2) high subsurface hydrological connectivity, and 3) high subsurface and surface hydrological connectivity. The hydrological connectivity depends on the water table elevation (depth below or above peat surface) and the hydraulic conductivity distribution of the peat profile, where an exponential decrease in hydraulic conductivity and transmissivity below the surface of the peat ribs creates a highly anisotropic aquifer. Consequently, during low hydrological connectivity periods the water table elevation is below the high hydraulic layers and minimal water flow or contaminant transport occurs. Conversely, during periods of high water tables, yet no overland flow, the hydraulic conductivity of the upper few centimeters of peat is exponentially higher than directly below and significantly increased connectivity; however, there can still be a substantial residence time due to a large storage capacity (~34 days), leading to no observed contaminant release. However, the highest connectivity periods occur during overland flow events (i.e., 2015) where the low-lying preferential flow paths are inundated and connect the pools via surface water. This substantially decreases the residence time to mere hours rather than weeks. It is during these high connectivity events (i.e., spring freshet and autumn wet-up) that the majority of solutes are likely transported out of ladder fens and into the surrounding aquatic ecosystems.

Like water, the transport of solutes was primarily governed by the peat ribs, with the pools initially diluting contaminants, delaying their transmission, but having little influence on the transport thereafter as the hydraulic efficiency was near unity and no additional storage was available. The majority of solutes are transported within the upper few centimeters of saturated peat, which corresponds with the high hydraulic conductivity peat layers. The peat hydrophysical properties primarily governed the transport of solutes when no overland flow was observed. The highly heterogeneous distribution of hydrophysical properties within a given rib and the influence of pool morphology results in complex contaminant plumes that would be extremely difficult to predict based on microtopography alone; thus, knowledge of the peat hydraulic conductivity distribution and other hydrophysical properties are required to accurately predict both conservative and reactive contaminant plume development. Furthermore, a more thorough understanding of the influence wind on solute transport within pools is required to better understand the retention processes within ladder fens and other similar peatlands. Additionally, in northern regions, winter, with its associated snowpack and ground ice, influences the hydrology of many ecosystems; these influences were not studied here so require further investigation. The influence of the spring freshet and ground ice on solute transport and domestic wastewater treatment or polishing is poorly understood and may represent a period when enhanced solute transport and decreased treatment or polishing potentially occurs due to perched water tables within the high hydraulic conductivity peat and overland flow; thus, domestic wastewater treatment or polishing wetlands may not be suitable during the spring freshet.

During this transient experiment, nitrate, ammonium and phosphate posed little risk to the surrounding aquatic ecosystems, as the transport was limited to the upper reaches of the EXP Fen; however, sulphate was highly mobile. Within the sulphate plume both MeHg and THg were elevated and 80 – 100 % of the THg was MeHg where the sulphate concentrations were highest. Limiting the mobility of sulphate would decrease the area of elevated MeHg production. As with all the contaminants studied, the effective removal greatly depends on hydrological conditions, chiefly water table elevation.

Although this study has highlighted many mechanisms and processes governing the transport and fate of domestic wastewater contaminants in ladder fens, there remains a large gap in our understanding of many of the processes and mechanisms that control a number of important processes. The mechanisms governing the removal and storage of these contaminants, the biological and hydrophysical evolution of a treatment or polishing peatland, the role of ground ice and spring freshet, and influence of a changing climate are all unknown. It is these gaps that are critical to fill and represent the next steps for contaminant treatment and transport research in ladder fens peatlands, and peatlands in general. Understanding if the change in magnitude of nutrient export during the fall senescence due to the additional phosphorous and nitrogen load is critical in assessing the long-term viability of these systems to treat domestic wastewater. During the fall senescence a proportion of the nutrient load would be flushed from the system, decreasing the treatment efficiency. Additionally, there is still a lack of knowledge of the magnitude of geochemical storage (sorption) of contaminants in ladder fens and potentially represents a large sink within these systems. However, without more knowledge on these processes and the total available geochemical storage, it is difficult to predict the longevity of these systems. Both of these research gaps can be filled using a combination of isotope tracers, mass balances, laboratory experiments, and numerical modelling. Isotope tracers would enable the tracking of some contaminants through the peatland as they enter and exit various storage compartments. Mass balances, for instance N:P, will further identify the primary storage or removal mechanisms when isotopes are unsuitable, and highlight any shifts in biogeochemical processes. Thus, if these two broad methods are combined, a better understanding of the flow of nutrients in these systems could be identified. However, the longevity of these systems is also dependent on the evolution of the peat and vegetation because the presence of both nitrate and sulphate in the domestic wastewater would increase the redox potential of the system, potentially enhancing peat decomposition. However, the evolution of these systems while under a domestic wastewater load remains unknown, as this study only identified the initial non-equilibrium fate and transport during a climatically average summer.

Understanding the relationship between peat decomposition and changes in hydrophysical properties (i.e., effective porosity, pore throat size distribution, bulk density, etc.) will be critical to predicting longevity of these systems. Using solute breakthrough experiments under various

degrees of decomposition and in different parent materials, a better understanding of the relationship between peat decomposition and change in hydrophysical properties can be achieved. Additionally, there is uncertainty about the hydrological effects of a changing climate, which propagates uncertainty regarding the ability of these systems to safely and effectively treat or polish wastewater in the future. Using data from the current literature on degree of decomposition on hydrophysical properties and the above experiments, coupled with region specific climate change scenarios, these processes could be numerically modelled at the field scale. This would allow for a better understanding of the long-term evolution of treatment or polishing peatlands in a changing climate. However, more needs to be known about the evolution of the hydrophysical properties as the vegetation and microbial community compositions evolve. Although there remains a large amount of research needed, this study illustrates that domestic wastewater polishing in ladder fens may be viable under the current hydroclimatic regimes, if certain precautions are taken.

Based on the results of this study there are several practices that can be followed to minimize the risk of contaminant release while using ladder fens for wastewater treatment or polishing. Managing the water table so it, on average, is below the high hydraulic conductivity layers will greatly increase the residence time of the system, increasing treatment efficiency. This practice would further limit the solute advection rate, limiting plume extent, and subsequently decreasing the area of enhanced MeHg and THg production. Controlling the water table could be achieved through two management practices. First, using multiple ladder fens for treatment or polishing, instead of one ladder fen, would decrease the volume of water delivered to a given wetland, thus decreasing the rise in water table compared to that with a single wetland option. The second option is to control the influent load so that high water tables are not produced. This option would involve the most active management as precipitation events or evaporation periods would alter the discharge rate required to maintain a target water table (i.e., below the high hydraulic conductivity layers). Additionally, limiting overland flow by blocking the preferential flow paths with peat dams would decrease the pool-to-pool connectivity and enhance the removal of all contaminants through increased residence time within the organic substrate and pools. In addition to hydrological controls, chemical manipulations may provide additional treatment pathways;

however, there has yet to be enough study of these processes to recommend using them without further research on their effect on the ladder fens.

Notwithstanding the intensive study of this one particular ladder fen, the similar topographical, hydrological, and geochemical conditions between the EXP Fen and the reference sites, as well as previously studied nearby ladder fens, suggests the process identified can likely be applied to other ladder fens. Furthermore, the pool-rib-pool morphology of ladder fens is similar to other peatlands, specifically the larger ribbed fens, in which the hydrological connectivity is controlled by the peat ribs. A combination of surface water flow through low-lying regions and the high hydraulic conductivity layers govern the water flow in ribbed fens, making ladder fens suitable analogs for the hydrology and potentially solute transport but at a smaller scale and more manageable to study. Notwithstanding the limited information on solute transport in ribbed fens, it is likely that the processes governing the transport in these systems is similar to ladder fens due to the similar hydrological controls on these systems. Given their typically larger size, ribbed fens may be ideal for domestic wastewater treatment or polishing in remote northern regions, as a larger volume of water can be introduced before increasing the water table into the high hydraulic conductivity layers or above the peat surface. However, pool morphology may differ between these two peatland types, which will influence the transport and storage of the solutes. It is likely that domestic wastewater contaminants would have similar initial treatment efficiencies for a given flow rate in different peatlands, as removal primarily occurred within the peat ribs and not the pools, further confirming the broader applicability of this study to other peatland types. Additionally, the solute transport in the peat seems to be consistent between different peatland types (i.e., blanket bogs or basin fens) and diffusion into inactive pores retards conservative solutes, indicating this process is common in most peat soils. However, given that fen peatlands convey water in these landscapes rather than store water, and presumably solutes, large domed bog peatlands may be more suitable for domestic wastewater treatment or polishing. Large domed bog peatlands have numerous ponds separated by peat ridges, somewhat analogous to the peat ribs observed in the EXP Fen, and may operate under similar hydrological processes (i.e., threshold spill-and-fill mechanisms). Using domed bogs would likely increase the solute residence time as the drainage pattern is typically unorganized until it reaches the downgradient fen peatlands. This inherent unorganized hydraulic pond-ridge structure could provide suitable storage and treatment

or polishing, notwithstanding the differing geochemical conditions within bogs. However, due to the unorganized structure it would be difficult to predict the solute flow paths and it could impact a much larger area than it would in a ladder fen. Furthermore, the lower pH associated with bog peatlands may influence the treatment efficiency of phosphate and the solubility of THg and MeHg. Further research is needed on the hydrobiogeochemical suitability of bog peatlands for domestic wastewater treatment or polishing. Thus, there remains an interesting question about which peatland type is most suitable for wastewater treatment or polishing in remote northern environments. The similarity of hydrological processes between peatland types suggests that many different types of peatlands with the suitable hydrological conditions (i.e., observable hydrological gradients, both open water and subsurface regions, etc.,) could safely and effectively treat or polish domestic wastewater but more research is required into the longevity of these systems, suitability of various peatland types, the role of winter and ground ice, and the influence of climate change before full-scale adoption of peatland based wastewater treatment or polishing can be adopted.

References

- Achtnich, C., Bak, F., & Conrad, R. (1995). Competition for electron donors among nitrate reducers, ferric iron reducers, sulfate reducers, and methanogens in anoxic paddy soil. *Biology and Fertility of Soils*, 19(1), 65-72. doi:10.1007/bf00336349
- Appelo, C. A. J., & Postma, D. (2005). *Geochemistry, Groundwater and pollution* (2nd ed.). Leiden, The Netherlands: A.A. Balkema Publishers.
- Armstrong, W. (1967). The relationship between oxidation-reduction potentials and oxygen-diffusion levels in some waterlogged organic soils. *Journal of Soil Science*, 18(1), 27-34. doi:10.1111/j.1365-2389.1967.tb01483.x
- Baird, A. J. (1997). Field estimation of macropore functioning and surface hydraulic conductivity in a fen peat. *Hydrological Processes*, 3, 301-295.
- Baird, A. J., & Gaffney, S. W. (1994). Cylindrical piezometer responses in a humified fen peat. *Hydrology Research*, 25(3), 167-182.
- Baird, A. J., & Gaffney, S. W. (2000). Solute movement in drained fen peat: a field tracer study in a Somerset (UK) wetland. *Hydrological Processes*, 14(14), 2489-2503. doi:10.1002/1099-1085(20001015)14:14<2489::aid-hyp110>3.0.co;2-q
- Baird, A. J., Surridge, B. W. J., & Money, R. P. (2004). An assessment of the piezometer method for measuring the hydraulic conductivity of a *Cladium mariscus*—*Phragmites australis* root mat in a Norfolk (UK) fen. *Hydrological Processes*, 18(2), 275-291. doi:10.1002/hyp.1375
- Basiliko, N., Moore, T. R., Jeannotte, R., & Bubier, J. L. (2006). Nutrient Input and Carbon and Microbial Dynamics in an Ombrotrophic Bog. *Geomicrobiology Journal*, 23, 531-534. doi:10.1080/01490450600897278
- Bayley, S. E., & Thormann, M. N. (2005). Nitrogen mineralization and decomposition in western boreal bog and fen peat. *Ecoscience*, 12(4), 455-465.
- Bear, J. (1972). *Dynamics of Fluids in Porous Media*. New York: Dover Publications, Inc. .
- Beckwith, C. W., Baird, A. J., & Heathwaite, A. L. (2003a). Anisotropy and depth-related heterogeneity of hydraulic conductivity in a bog peat. II: modelling the effects on groundwater flow. *Hydrological Processes*, 17(1), 103-113. doi:10.1002/hyp.1117
- Beckwith, C. W., Baird, A. J., & Heathwaite, A. L. (2003b). Anisotropy and depth-related heterogeneity of hydraulic conductivity in a bog peat. I: laboratory measurements. *Hydrological Processes*, 17(1), 89-101. doi:10.1002/hyp.1116
- Beltman, B., Rouwenhorst, T. G., Kerkhoven, M. B. V., Krift, T. V. D., & Verhoeven, J. T. A. (2000). Internal Eutrophication in Peat Soils through Competition between Chloride and Sulphate with Phosphate for Binding Sites. *Biogeochemistry*, 50(2), 183-194. doi:10.2307/1469376
- Bengtsson, F., Granath, G., & Rydin, H. (2016). Photosynthesis, growth, and decay traits in Sphagnum – a multispecies comparison. *Ecology and Evolution*, 6(10), 3325-3341. doi:10.1002/ece3.2119
- Blodau, C., Bauer, M., Regenspurg, S., & Macalady, D. (2009). Electron accepting capacity of dissolved organic matter as determined by reaction with metallic zinc. *Chemical Geology*, 260(3-4), 186-195. doi:<http://dx.doi.org/10.1016/j.chemgeo.2008.12.016>
- Boelter, D. H. (1969). Physical Properties of Peats as Related to Degree of Decomposition. *Soil Science Society of America Journal*, 33(4), 606-609. doi:10.2136/sssaj1969.03615995003300040033x

- Boeye, D., Verhagen, B., Haesebroeck, V. v., & El-Kahloun, M. (1999). Phosphorus Fertilization in a Phosphorus-Limited Fen: Effects of Timing. *Applied Vegetation Science*, 2(1), 71-78. doi:10.2307/1478883
- Boeye, D., & Verheyen, R. F. (1994). The Relation between Vegetation and Soil Chemistry Gradients in a Ground Water Discharge Fen. *Journal of Vegetation Science*, 5(4), 553-560. doi:10.2307/3235982
- Bonnett, S. A. F., Ostle, N., & Freeman, C. (2006). Seasonal variations in decomposition processes in a valley-bottom riparian peatland. *Science of The Total Environment*, 370(2-3), 561-573. doi:<http://dx.doi.org/10.1016/j.scitotenv.2006.08.032>
- Bottrell, S. H., Mortimer, R. J. G., Spence, M., Krom, M. D., Clark, J. M., & Chapman, P. J. (2007). Insights into redox cycling of sulfur and iron in peatlands using high-resolution diffusive equilibrium thin film (DET) gel probe sampling. *Chemical Geology*, 244, 409-420. doi:10.1016/j.chemgeo.2007.06.028
- Boucher, A. L. (2012). *PTTW for Open Pit Sump (Phase 1 Ditch) # 4640-89JHT2 (replaced #5254-6XWT3C) Annual 2012 Report*. Retrieved from Victor Mine, Ontario, Canada:
- Bouwer, H., & Rice, R. C. (1976). A slug test for determining hydraulic conductivity of unconfined aquifers with completely or partially penetrating wells. *Water Resources Research*, 12(3), 423-428. doi:10.1029/WR012i003p00423
- Brand, E. W., & Premchitt, J. (1980). Shape factors of cylindrical piezometers. *Géotechnique*, 30(4), 369-384. doi:10.1680/geot.1980.30.4.369
- Brand, E. W., & Premchitt, J. (1982). Response characteristics of cylindrical piezometers. *Géotechnique*, 32(3), 203-216. doi:10.1680/geot.1982.32.3.203
- Branfireun, B. A., Bishop, K., Roulet, N. T., Granberg, G., & Nilsson, M. (2001). Mercury cycling in boreal ecosystems: The long-term effect of acid rain constituents on peatland pore water methylmercury concentrations. *Geophysical Research Letters*, 28(7), 1227-1230.
- Branfireun, B. A., Roulet, N. T., Kelly, C. A., & Rudd, J. W. M. (1999). In situ sulphate stimulation of mercury methylation in a boreal peatland: Toward a link between acid rain and methylmercury contamination in remote environments. *Global Biogeochemical Cycles*, 13(3), 743-750. doi:10.1029/1999gb900033
- Brigham, M. E., Wentz, D. A., Aiken, G. R., & Krabbenhoft, D. P. (2009). Mercury cycling in stream ecosystems. 1. water column chemistry and transport. *Environmental Science & Technology*, 43(8), 2720-2725. doi:10.1021/es802694n
- Brown, K. A., & Macqueen, J. F. (1985). Sulphate uptake from surface water by peat. *Soil Biology and Biochemistry*, 17(4), 411-420. doi:[http://dx.doi.org/10.1016/0038-0717\(85\)90002-1](http://dx.doi.org/10.1016/0038-0717(85)90002-1)
- Bubier, J. L., Moore, T. R., & Bledzki, L. A. (2007). Effects of nutrient addition on vegetation and carbon cycling in an ombrotrophic bog. *Global Change Biology*, 13, 1168-1186. doi:10.1111/j.1365-2486.2007.01346.x
- Cabezas, A., Gelbrecht, J., & Zak, D. (2013). The effect of rewetting drained fens with nitrate-polluted water on dissolved organic carbon and phosphorus release. *Ecological Engineering*, 53(0), 79-88. doi:<http://dx.doi.org/10.1016/j.ecoleng.2012.12.016>
- Cabezas, A., Gelbrecht, J., Zwirnmann, E., Barth, M., & Zak, D. (2012). Effects of degree of peat decomposition, loading rate and temperature on dissolved nitrogen turnover in rewetted fens. *Soil Biology and Biochemistry*, 48(0), 182-191. doi:<http://dx.doi.org/10.1016/j.soilbio.2012.01.027>

- Campbell, D., & Bergeron, J. (2012). Natural Revegetation of Winter Roads on Peatlands in the Hudson Bay Lowlands, Canada. *Arctic, Antarctic, and Alpine Research*, 44(2), 155-163. doi:<http://dx.doi.org/10.1657/1938-4246-44.2.155>
- Carey, S. K., Quinton, W., & Goeller, N. T. (2007). Field and laboratory estimates of pore size properties and hydraulic characteristics for subarctic organic soils. *Hydrological Processes*, 21, 2560-2571. doi:10.1002/hyp.6795
- Caron, J., Létourneau, G., & Fortin, J. (2015). Electrical conductivity breakthrough experiment and immobile water estimation in organic substrates: Is $R = 1$ a realistic assumption? *Vadose Zone Journal*, 14(9). doi:10.2136/vzj2015.01.0014
- Chapin, C. T., Bridgham, S. D., Pastor, J., & Updegraff, K. (2003). Nitrogen, Phosphorus, and Carbon Mineralization in Response to Nutrient and Lime Additions in Peatlands. *Soil Science*, 168(6), 409-420.
- Chason, D. B., & Siegel, D. I. (1986). Hydraulic conductivity and related physical properties of peat, Lost River Peatland, northern Minnesota. *Soil Science*, 142(2), 91-99.
- Chenaf, D., & Chapuis, R. P. (2007). Seepage face height, water table position, and well efficiency at steady state. *Ground Water*, 45(2), 168-177. doi:10.1111/j.1745-6584.2006.00277.x
- Coleman Wasik, J. K., Engstrom, D. R., Mitchell, C. P. J., Swain, E. B., Monson, B. A., Balogh, S. J., . . . Almendinger, J. E. (2015). The effects of hydrologic fluctuation and sulfate regeneration on mercury cycling in an experimental peatland. *Journal of Geophysical Research: Biogeosciences*, 120(9), 1697-1715. doi:10.1002/2015JG002993
- Coleman Wasik, J. K., Mitchell, C. P. J., Engstrom, D. R., Swain, E. B., Monson, B. A., Balogh, S. J., . . . Almendinger, J. E. (2012). Methylmercury Declines in a Boreal Peatland When Experimental Sulfate Deposition Decreases. *Environmental Science & Technology*, 46(12), 6663-6671. doi:10.1021/es300865f
- Compeau, G., & Bartha, R. (1985). Sulfate-Reducing Bacteria: Principal Methylators of Mercury in Anoxic Estuarine Sediment. *Applied and Environmental Microbiology*, 50(2), 498-502.
- do Carmo Horta, M., & Torrent, J. (2007). Phosphorus desorption kinetics in relation to phosphorus forms and sorption properties of portuguese acid soils. *Soil Science*, 172(8), 631-638. doi:10.1097/ss.0b013e3180577270
- Dredge, L. A., & Cowan, W. R. (1989). Quaternary geology of the southwestern Canadian Shield. In R. J. Fulton (Ed.), *Quaternary Geology of Canada and Greenland* (Vol. Geology of Canada no. 1). Ottawa, Canada: Geological Survey of Canada.
- Environment Canada. (2015a). Canadian Climate Normals 1971-2000: Moosonee. Retrieved 23/03/2015, from Environment Canada http://www.climate.weatheroffice.gc.ca/climate_normals/
- Environment Canada. (2015b). Canadian Climate Normals 1971-2000: Lansdowne House. Retrieved 23/03/2015, from Environment Canada http://www.climate.weatheroffice.gc.ca/climate_normals/
- Eskelinen, R., Ronkanen, A.-K., Marttila, H., & Kløve, B. (2015). Purification efficiency of a peatland-based treatment wetland during snowmelt and runoff events. *Ecological Engineering*, 84, 169-179. doi:<http://dx.doi.org/10.1016/j.ecoleng.2015.08.004>
- Ferguson, J. F., Jenkins, D., & Eastman, J. (1973). Calcium Phosphate Precipitation at Slightly Alkaline pH Values. *Journal (Water Pollution Control Federation)*, 45(4), 620-631.
- Fleck, J. A., Gill, G., Bergamaschi, B. A., Kraus, T. E. C., Downing, B. D., & Alpers, C. N. (2014). Concurrent photolytic degradation of aqueous methylmercury and dissolved organic

- matter. *Science of The Total Environment*, 484, 263-275. doi:<http://dx.doi.org/10.1016/j.scitotenv.2013.03.107>
- Fraser, C., Roulet, N., & Moore, T. R. (2001). Hydrology and dissolved organic carbon biogeochemistry in an ombrotrophic bog. *Hydrological Processes*, 15(3151-3166), 3151-3166. doi:10.1002/hyp.322
- Gerke, J., & Hermann, R. (1992). Adsorption of Orthophosphate to Humic-Fe-Complexes and to Amorphous Fe-Oxide. *Zeitschrift für Pflanzenernährung und Bodenkunde*, 155(3), 233-236. doi:10.1002/jpln.19921550313
- Gilmour, C. C., & Henry, E. A. (1991). Mercury methylation in aquatic systems affected by acid deposition. *Environmental Pollution*, 71(2-4), 131-169. doi:10.1016/0269-7491(91)90031-Q
- Gilmour, C. C., Henry, E. A., & Mitchell, R. (1992). Sulfate stimulation of mercury methylation in freshwater sediments. *Environmental Science & Technology*, 26(11), 2281-2287. doi:10.1021/es00035a029
- Glaser, P. H., Hansen, B. C. S., Siegel, D. I., Reeve, A. S., & Morin, P. J. (2004). Rates, pathways and drivers for peatland development in the Hudson Bay Lowlands, Northern Ontario, Canada. *Journal of Ecology*, 92(6), 1036-1053. doi:10.2307/3599747
- Glaser, P. H., Wheeler, G. A., Gorham, E., & Wright, H. E., Jr. (1981). The patterned mires of the Red Lake Peatland, Northern Minnesota: vegetation, water chemistry and landforms. *Journal of Ecology*, 69(2), 575-599. doi:10.2307/2259685
- Gogo, S., Shreeve, T. G., & Pearce, D. M. E. (2010). Geochemistry of three contrasting British peatlands: Complex patterns of cation availability and implications for microbial metabolism. *Geoderma*, 158, 207-215. doi:10.1016/j.geoderma.2010.04.031
- Gorham, E. (1991). Northern Peatlands : Role in the Carbon Cycle and Probable Responses to Climatic Warming. *Ecological Applications*, 1(2), 182-195.
- Gorham, E. (2008). Northern Peatlands : Role in the Carbon Cycle and Probable Responses to Climatic Warming *Ecological Applications*, 1(2), 182-195.
- Heiberg, L., Koch, C. B., Kjaergaard, C., Jensen, H. S., & Hans Christian, B. H. (2012). Vivianite Precipitation and Phosphate Sorption following Iron Reduction in Anoxic Soils. *Journal of Environmental Quality*, 41(3), 938-949. doi:10.2134/jeq2011.0067
- Ho, Y. S., & McKay, G. (1999). Competitive sorption of copper and nickel ions from aqueous solution using peat. *Adsorption*, 5(4), 409-417. doi:10.1023/a:1008921002014
- Ho, Y. S., & McKay, G. (2000). The kinetics of sorption of divalent metal ions onto sphagnum moss peat. *Water Research*, 34(3), 735-742. doi:[http://dx.doi.org/10.1016/S0043-1354\(99\)00232-8](http://dx.doi.org/10.1016/S0043-1354(99)00232-8)
- Ho, Y. S., Porter, J. F., & McKay, G. (2002). Equilibrium isotherm studies for the sorption of divalent metal ions onto peat: copper, nickel and lead single component systems. *Water, Air, and Soil Pollution*, 141(1), 1-33. doi:10.1023/a:1021304828010
- Hoag, R. S., & Price, J. S. (1995). A field-scale, natural gradient solute transport experiment in peat at a Newfoundland blanket bog. *Journal of Hydrology*, 172, 171-184.
- Hoag, R. S., & Price, J. S. (1997). Effects of matrix diffusion on solute transport and retardation peat. *Journal of Contaminant Hydrology*, 28, 193-205.
- Hoggarth, C. G. J., Hall, B. D., & Mitchell, C. P. J. (2015). Mercury methylation in high and low-sulphate impacted wetland ponds within the prairie pothole region of North America. *Environmental Pollution*, 205, 269-277. doi:<http://dx.doi.org/10.1016/j.envpol.2015.05.046>

- Hvorslev, M. J. (1951). *Time lag and soil permeability in ground-water observations* (Vol. Waterways Experimental Station Bulletin 36). Vicksburg, Mississippi.: US Army Corps of Engineers.
- Juutinen, S., Bubier, J., & Moore, T. (2010). Responses of Vegetation and Ecosystem CO₂ Exchange to 9 Years of Nutrient Addition at Mer Bleue Bog. *Ecosystems*, 13(6), 874-887. doi:10.1007/s10021-010-9361-2
- Kadlec, R. H. (2009a). Wastewater treatment at the Houghton Lake wetland: Hydrology and water quality. *Ecological Engineering*, 35, 1287–1311. doi:10.1016/j.ecoleng.2008.10.001
- Kadlec, R. H. (2009b). Wastewater treatment at the Houghton lake wetland: Soils and sediments. *Ecological Engineering*, 35, 1333–1348. doi:10.1016/j.ecoleng.2009.03.004
- Kadlec, R. H., & Wallace, S. D. (2009). *Treatment Wetlands* (2nd ed.). Boca Raton, FL: CRC Press, Taylor & Francis Group.
- Kastelan-Macan, M., & Petrovic, M. (1996). The role of fulvic acids in phosphorus sorption and release from mineral particles. *Water Science and Technology*, 34(7-8), 259-265.
- Keller, J. K., & Bridgham, S. D. (2007). Pathways of anaerobic carbon cycling across an ombrotrophic-minerotrophic peatland gradient. *Limnology and Oceanography*, 52(1), 96-107. doi:10.4319/lo.2007.52.1.0096
- Kim, D.-G., Park, J., Lee, D., & Kang, H. (2011). Removal of nitrogen and phosphorus from effluent of a secondary wastewater treatment plant using a pond-marsh wetland system. *Water, Air, and Soil Pollution*, 214. doi:10.1007/s11270-010-0399-8
- Kirk, J. L., & St. Louis, V. L. (2009). Multiyear total and methyl mercury exports from two major sub-arctic rivers draining into Hudson Bay, Canada. *Environmental Science & Technology*, 43(7), 2254-2261. doi:10.1021/es803138z
- Kirkham, F. W., Mountford, J. O., & Wilkins, R. J. (1996). The Effects of Nitrogen, Potassium and Phosphorus Addition on the Vegetation of a Somerset Peat Moor Under Cutting Management. *Journal of Applied Ecology*, 33(5), 1013-1029. doi:10.2307/2404682
- Klute, A. (1986). *Methods of Soil Analysis. Part 1. Physical and Mineralogical Methods* (2 ed.). Madison, Wis., USA: American Society of Agronomy-Soil Science Society of America.
- Koerselman, W., Kerkhoven, M. B. V., & Verhoeven, J. T. A. (1993). Release of Inorganic N, P and K in Peat Soils; Effect of Temperature, Water Chemistry and Water Level. *Biogeochemistry*, 20(2), 63-81. doi:10.2307/1468907
- Koretsky, C. M., Haas, J. R., Ndenga, N. T., & Miller, D. (2006). Seasonal variations in vertical redox stratification and potential influence on trace metal speciation in minerotrophic peat sediments. *Water, Air, and Soil Pollution*, 179, 373-403. doi:10.1007/s11270-006-9089-y
- Kuhry, P., & Vitt, D. H. (1996). Fossil Carbon / Nitrogen Ratios as a Measure of Peat Decomposition *Ecology*, 77(1), 271-275.
- Kyzoil, J. (2002). Effect of Physical Properties and Cation Exchange Capacity on Sorption of Heavy Metals onto Peats. *Polish Journal of Environmental Studies*, 11(6), 713-718.
- Lagacé, R. (1986). *Auger hole test for very high and low hydraulic conductivity*. Paper presented at the American Society of Agricultural Engineers Winter Meeting, Chicago, IL.
- Lamers, L. P. M., van Diggelen, J. M. H., Op den Camp, H. J. M., Visser, E. J. W., Lucassen, E. C. H. E. T., Vile, M. A., . . . Roelofs, J. G. M. (2012). Microbial transformations of nitrogen, sulfur and iron dictate vegetation composition in wetlands: a review. *Frontiers in Microbiology*, 3, 1-12. doi:10.3389/fmicb.2012.00156

- Leclair, M., Whittington, P., & Price, J. (2015). Hydrological functions of a mine-impacted and natural peatland-dominated watershed, James Bay Lowland. *Journal of Hydrology: Regional Studies*, 4, Part B, 732-747. doi:<http://dx.doi.org/10.1016/j.ejrh.2015.10.006>
- Leclair, M. M. (2015). *The hydrological interactions within a mine impacted peatland, James Bay Lowland, Canada*. (Master of Science), University of Waterloo, Waterloo, Ontario.
- Lee, H. A. (1960). Late Glacial and Postglacial Hudson Bay Sea Episode. *Science*, 131(3413), 1609-1611. doi:10.1126/science.131.3413.1609
- Lee, S., Maniquiz, M. C., Choi, J., Kang, J.-H., Jeong, S., & Kim, L.-H. (2012). Seasonal treatment efficiency of surface flow constructed wetland receiving high nitrogen content wastewater. *Desalination and Water Treatment*, 48, 9-16. doi:10.1080/19443994.2012.698722
- Lens, P. N., De Poorter, M. P., Cronenberg, C. C., & Verstraete, W. H. (1995). Sulfate reducing and methane producing bacteria in aerobic wastewater treatment systems. *Water Research*, 29(3), 871-880. doi:[http://dx.doi.org/10.1016/0043-1354\(94\)00195-D](http://dx.doi.org/10.1016/0043-1354(94)00195-D)
- Limpens, J., Berendse, F., Blodau, C., Canadell, J. G., Freeman, C., Holden, J., . . . Schaepman-Strub, G. (2008). Peatlands and the carbon cycle: from local processes to global implications – a synthesis. *Biogeosciences*, 5(5), 1475-1491. doi:10.5194/bg-5-1475-2008
- Mastrocicco, M., Prommer, H., Pasti, L., Palpacelli, S., & Colombani, N. (2011). Evaluation of saline tracer performance during electrical conductivity groundwater monitoring. *Journal of Contaminant Hydrology*, 123(3-4), 157-166. doi:<http://dx.doi.org/10.1016/j.jconhyd.2011.01.001>
- Melamed, R., Trigueiro, F. E., & Villas Bôas, R. C. (2000). The effect of humic acid on mercury solubility and complexation. *Applied Organometallic Chemistry*, 14(9), 473-476. doi:10.1002/1099-0739(200009)14:9<473::AID-AOC25>3.0.CO;2-W
- Mitchell, C. P. J., Branfireun, B. A., & Kolka, R. K. (2008). Assessing sulfate and carbon controls on net methylmercury production in peatlands: An in situ mesocosm approach. *Applied Geochemistry*, 23(3), 503-518. doi:<http://dx.doi.org/10.1016/j.apgeochem.2007.12.020>
- Monninger, S. (2015). *De Beers Group of Companies Inc. Victor Mine Annual Groundwater and Subsidence Report as per condition 4.1.5 Permit to Take Water #1810-99FHAD (or amended)*.
- Moore, R. D. (2005). Slug injection using salt in solution. *Streamline Watershed Management Bulletin*, 9(2), 1-6.
- Moore, T. R., Trofymow, J. A., Siltanen, M., Prescott, C., & Group, C. W. (2005). Patterns of decomposition and carbon, nitrogen, and phosphorus dynamics of litter in upland forest and peatland sites in central Canada. *Canadian Journal of Forest Research*, 35, 133-142.
- Morris, A. J., & Hesterberg, D. L. (2012). Iron(III) Coordination and Phosphate Sorption in Peat Reacted with Ferric or Ferrous Iron. *Soil Science Society of America Journal*, 76(1), 101-109. doi:10.2136/sssaj2011.0097
- National Wetlands Working Group. (1997). *The Canadian Wetland Classification System* (Second Edition ed.). Waterloo, Ontario: University of Waterloo.
- Neuman, S. P. (1975). Analysis of pumping test data from anisotropic unconfined aquifers considering delayed gravity response. *Water Resources Research*, 11(2), 329-342. doi:10.1029/WR011i002p00329
- Niedermeier, A., & Robinson, J. S. (2007). Hydrological controls on soil redox dynamics in a peat-based , restored wetland. *Geoderma*, 137, 318 - 326.

- Nieminen, M., & Jarva, M. (1996). Phosphorus adsorption by peat from drained mires in southern Finland. *Scandinavian Journal of Forest Research*, 11(1-4), 321-326. doi:10.1080/02827589609382942
- Noe, G. B., Scinto, L. J., Taylor, J., Childers, D. L., & Jones, R. D. (2003). Phosphorus cycling and partitioning in an oligotrophic Everglades wetland ecosystem: a radioisotope tracing study. *Freshwater Biology*, 48(11), 1993-2008. doi:10.1046/j.1365-2427.2003.01143.x
- Oke, T. R. (1987). *Boundary Layer Climates* (2nd ed.). New York: Methuen & Co. Ltd.
- Olson, B. H., & Cooper, R. C. (1974). In situ methylation of mercury in estuarine sediments. *Nature*, 252, 682-683.
- Ours, D., Siegel, D. I., & Glaser, P. H. (1997). Chemical dilation and the dual porosity of humified bog peat. *Journal of Hydrology*, 196, 348-360.
- Palmer, K., Ronkanen, A.-K., & Kløve, B. (2015). Efficient removal of arsenic, antimony and nickel from mine wastewaters in Northern treatment peatlands and potential risks in their long-term use. *Ecological Engineering*, 75, 350-364. doi:<http://dx.doi.org/10.1016/j.ecoleng.2014.11.045>
- Penman, H. L. (1948). Natural evaporation from open water, bare soil and grass. *Proceedings of the Royal Society of London A: Mathematical, Physical and Engineering Sciences*, 193(1032), 120-145. doi:10.1098/rspa.1948.0037
- Perras, E. (2015). *Hydrological and geochemical implications of aquifer depressurization on expansive peatland systems in the Hudson/James Bay Lowlands*. (Master of Science), University of Waterloo, Waterloo, Ontario.
- Persson, J. (2000). The hydraulic performance of ponds of various layouts. *Urban Water Journal*, 2(3), 243-250. doi:[http://dx.doi.org/10.1016/S1462-0758\(00\)00059-5](http://dx.doi.org/10.1016/S1462-0758(00)00059-5)
- Persson, J., Somes, N. L. G., & Wong, T. H. F. (1999). Hydraulics efficiency of constructed wetlands and ponds. *Water Science and Technology*, 40(3), 291-300. doi:[http://dx.doi.org/10.1016/S0273-1223\(99\)00448-5](http://dx.doi.org/10.1016/S0273-1223(99)00448-5)
- Persson, J., & Wittgren, H. B. (2003). How hydrological and hydraulic conditions affect performance of ponds. *Ecological Engineering*, 21(4-5), 259-269. doi:<http://dx.doi.org/10.1016/j.ecoleng.2003.12.004>
- Pietro, K. C., Chimney, M. J., & Steinman, A. D. (2006). Phosphorus removal by the *Ceratophyllum*/periphyton complex in a south Florida (USA) freshwater marsh. *Ecological Engineering*, 27(4), 290-300. doi:10.1016/j.ecoleng.2006.05.014
- Polprasert, C., & Bhattarai, K. K. (1985). Dispersion model for waste stabilization ponds. *Journal of Environmental Engineering-ASCE*, 111(1), 45-59. doi:10.1061/(ASCE)0733-9372(1985)111:1(45)
- Postila, H., Ronkanen, A.-K., Marttila, H., & Kløve, B. (2015). Hydrology and hydraulics of treatment wetlands constructed on drained peatlands. *Ecological Engineering*, 75, 232-241. doi:<http://dx.doi.org/10.1016/j.ecoleng.2014.11.041>
- Price, J. S. (1991). On the occurrence of hypersaline sediments in James Bay coastal marshes. *Canadian Journal of Botany*, 69(10), 2328-2330. doi:10.1139/b91-293
- Price, J. S., & Maloney, D. A. (1994). Hydrology of a patterned bog-fen complex in southeastern Labrador, Canada. *Nordic Hydrology*, 25, 313-330.
- Price, J. S., & Woo, M. K. (1988). *Wetlands as waste repositories?: Solute transport in peat*. Paper presented at the Proc. National Student Conference on Northern Studies, Ottawa.
- Priestley, C. H. B., & Taylor, R. (1972). On the assessment of surface heat flux and evaporation using large-scale parameters. *Monthly Weather Review*, 100, 81-92.

- Quinton, W., Hayashi, M., & Pietroniro, A. (2003). Connectivity and storage functions of channel fens and flat bogs in northern basins. *Hydrological Processes*, 17, 3665-3684. doi:10.1002/hyp.1369
- Quinton, W. L., Gray, D. M., & Marsh, P. (2000). Subsurface drainage from hummock-covered hillslopes in the Arctic tundra. *Journal of Hydrology*, 237, 113-125.
- Quinton, W. L., Hayashi, M., & Carey, S. K. (2008). Peat hydraulic conductivity in cold regions and its relation to pore size and geometry. *Hydrological Processes*, 2837, 2829- 2837. doi:10.1002/hyp.7027
- Quinton, W. L., & Roulet, N. T. (1998). Spring and summer runoff hydrology of a subarctic patterned wetland. *Arctic and Alpine Research*, 30(3), 285-294. doi:10.2307/1551976
- Quinton, W. L., Shirazi, T., Carey, S. K., & Pomeroy, J. W. (2005). Soil water storage and active-layer development in a sub-alpine tundra hillslope, southern Yukon Territory, Canada. *Permafrost and Periglacial Processes*, 16(4), 369-382. doi:10.1002/ppp.543
- R Development Core Team. (2010). R: A language and environment for statistical computing. Vienna, Austria: R Foundation for Statistical Computing. Retrieved from <http://www.R-project.org>
- Reeve, A. S., Siegel, D. I., & Glaser, P. (2000). Simulating vertical flow in large peatlands. *Journal of Hydrology*, 227, 207-217.
- Reeve, A. S., Siegel, D. I., & Glaser, P. (2001). Simulating dispersive mixing in large peatlands. *Journal of Hydrology*, 242(103-114).
- Reeve, A. S., Siegel, D. I., & Glaser, P. H. (1996). Geochemical controls on peatland pore water from the Hudson Bay Lowland: a multivariate statistical approach. *Journal of Hydrology*, 181(1-4), 285-304. doi:[http://dx.doi.org/10.1016/0022-1694\(95\)02900-1](http://dx.doi.org/10.1016/0022-1694(95)02900-1)
- Rezanezhad, F., Price, J. S., & Craig, J. R. (2012). The effects of dual porosity on transport and retardation in peat: A laboratory experiment. *Canadian Journal of Soil Science*, 92(5), 723-732. doi:10.4141/cjss2011-050
- Richardson, C. J. (1985). Mechanisms Controlling Phosphorus Retention Capacity in Freshwater Wetlands. *Science*, 228(4706), 1424-1427.
- Richardson, M., Ketcheson, S., Whittington, P., & Price, J. (2012). The influences of catchment geomorphology and scale on runoff generation in a northern peatland complex. *Hydrological Processes*, 26(12), 1805-1817. doi:10.1002/hyp.9322
- Riley, J. L. (2011). *Wetlands of the Hudson Bay lowlands: A regional Overview*. Toronto, Ontario: Nature Conservancy of Canada.
- Rippy, J. F. M., & Nelson, P. V. (2007). Cation Exchange Capacity and Base Saturation Variation among Alberta, Canada, Moss Peats. *HortScience*, 42(2), 349-352.
- Ronkanen, A.-K., & Kløve, B. (2009). Long-term phosphorus and nitrogen removal processes and preferential flow paths in Northern constructed peatlands. *Ecological Engineering*, 35. doi:10.1016/j.ecoleng.2008.12.007
- Ronkanen, A.-K., & Kløve, B. (2007). Use of stable isotopes and tracers to detect preferential flow patterns in a peatland treating municipal wastewater. *Journal of Hydrology*, 347, 418-429. doi:10.1016/j.jhydrol.2007.09.029
- Ronkanen, A.-K., & Kløve, B. (2008). Hydraulics and flow modelling of water treatment wetlands constructed on peatlands in Northern Finland. *Water Research*, 42(14), 3826-3836. doi:<http://dx.doi.org/10.1016/j.watres.2008.05.008>
- Roulet, N. (1991). Surface level and water table fluctuations in a subarctic fen. *Arctic and Alpine Research*, 23(3), 303-310.

- Rubol, S., Silver, W. L., & Bellin, A. (2012). Hydrologic control on redox and nitrogen dynamics in a peatland soil. *Science of The Total Environment*, 432, 37-46. doi:10.1016/j.scitotenv.2012.05.073
- Rydin, H., & Jeglum, J. (2009). *The Biology of Peatlands*. New York, New York: Oxford University Press.
- Schlotzhauer, S., & Price, J. (1999). Soil water flow dynamics in a managed cutover peat field, Quebec: Field and laboratory investigation. *Water Resources Research*, 35(12), 3675-3683.
- Schneebeli, G. (1956). *Sur l'hydraulique des puits*. Paper presented at the Symposia Darcy, Gentbrugge, Belgium.
- Seo, D. C., Cho, J. S., Lee, H. J., & Heo, J. S. (2005). Phosphorus retention capacity of filter media for estimating the longevity of constructed wetland. *Water Research*, 39(11), 2445-2457. doi:<http://dx.doi.org/10.1016/j.watres.2005.04.032>
- Shaw, J. K. E., Watt, W. E., Marsalek, J., & Anderson, B. C. (1997). Flow pattern characterization in an urban stormwater detention pond and implications for water quality. *Journal of Water Quality Research*, 32(1), 53-71.
- Siegel, D. I., & Glaser, P. H. (1987). Groundwater flow in a bog-fen, Lost River Peatland, Northern Minnesota. *The Journal of Ecology*, 75, 743-754.
- Siegel, D. I., Reeve, A., Glaser, P., & Romanowicz, E. A. (1994). Climate-driven flushing of pore water in peatlands. *Nature*, 374, 531-533. doi:10.1038/374531a0
- Spence, C., & Woo, M.-k. (2003). Hydrology of subarctic Canadian shield: soil-filled valleys. *Journal of Hydrology*, 279(1-4), 151-166. doi:[http://dx.doi.org/10.1016/S0022-1694\(03\)00175-6](http://dx.doi.org/10.1016/S0022-1694(03)00175-6)
- Staunton, S., & Leprince, F. (1996). Effect of pH and some organic anions on the solubility of soil phosphate: implications for P bioavailability. *European Journal of Soil Science*, 47(2), 231-239. doi:10.1111/j.1365-2389.1996.tb01394.x
- Steinback, B. (2012a). *De Beers Canada Inc. Victor Mine Northeast Fen 2011 Annual Report per Condition 8(3) of Certificate of Approval No. 4056-6W8QBU*. Retrieved from Victor Mine, Ontario, Canada:
- Steinback, B. (2012b). *De Beers Canada Inc. Victor Mine PTTW for Open Pit Sump (Phase 1 Ditch) # 4640-89JHT2 (replaced #5254-6XWT3C) Annual 2012 Report*. Retrieved from Victor Mine, Ontario, Canada:
- Surridge, B. W. J., Baird, A. J., & Heathwaite, A. L. (2005). Evaluating the quality of hydraulic conductivity estimates from piezometer slug tests in peat. *Hydrological Processes*, 19(6), 1227-1244. doi:10.1002/hyp.5653
- Thackston, H. P. L., F. Douglas Shields, J., & Schroeder, P. R. (1987). Residence time distributions of shallow basins. *Journal of Environmental Engineering-ASCE*, 113(6), 1319-1332. doi:10.1061/(ASCE)0733-9372(1987)113:6(1319)
- Thornthwaite, C. W., & Holzman, B. (1939). The determination of evaporation from land and water surfaces. *Monthly Weather Review*, 67(1), 4-11. doi:10.1175/1520-0493(1939)67<4:TDOEFL>2.0.CO;2
- Ulanowski, T. A. (2014). *Hydrology and biogeochemistry of a bog-fen-tributary complex in the Hudson Bay Lowlands, Ontario, Canada*. (Master of Science), The University of Western Ontario, London, Ontario.

- Ulanowski, T. A., & Branfireun, B. A. (2013). Small-scale variability in peatland pore-water biogeochemistry, Hudson Bay Lowland, Canada. *Science of The Total Environment*, 454–455(0), 211-218. doi:<http://dx.doi.org/10.1016/j.scitotenv.2013.02.087>
- Vitt, D. H., Halsey, L. A., Bray, J., & Kinser, A. (2003). Patterns of Bryophyte Richness in a Complex Boreal Landscape: Identifying Key Habitats at McClelland Lake Wetland. *The Bryologist*, 106(3), 372-382.
- Vitt, D. H., Van Wirdum, G., Halsey, L., & Zoltai, S. (1993). The Effects of Water Chemistry on the Growth of *Scorpidium scorpioides* in Canada and The Netherlands. *The Bryologist*, 96(1), 106-111.
- Vymazal, J. (2007). Removal of nutrients in various types of constructed wetlands. *Science of The Total Environment*, 380(1–3), 48-65. doi:<http://dx.doi.org/10.1016/j.scitotenv.2006.09.014>
- Vymazal, J. (2014). Constructed wetlands for treatment of industrial wastewaters: A review. *Ecological Engineering*, 73, 724-751. doi:<http://dx.doi.org/10.1016/j.ecoleng.2014.09.034>
- Wallage, Z. E., & Holden, J. (2011). Near-surface macropore flow and saturated hydraulic conductivity in drained and restored blanket peatlands. *Soil Use and Management*, 27, 247-254. doi:10.1111/j.1475-2743.2011.00
- Whittington, P., & Price, J. (2012). Effect of mine dewatering on peatlands of the James Bay Lowland: the role of bioherms. *Hydrological Processes*, 26(12), 1818-1826. doi:10.1002/hyp.9266
- Whittington, P., & Price, J. (2013). Effect of mine dewatering on the peatlands of the James Bay Lowland: the role of marine sediments on mitigating peatland drainage. *Hydrological Processes*, 27(13), 1845-1853. doi:10.1002/hyp.9858
- Wind-Mulder, H. L., Rochefort, L., & Vitt, D. H. (1996). Water and peat chemistry comparisons of natural and post-harvested peatlands across Canada and their relevance to peatland restoration. *Ecological Engineering*, 7, 161-181.
- Woo, M.-k., Marsh, P., & Pomeroy, J. W. (2000). Snow, frozen soils and permafrost hydrology in Canada, 1995–1998. *Hydrological Processes*, 14(9), 1591-1611. doi:10.1002/1099-1085(20000630)14:9<1591::AID-HYP78>3.0.CO;2-W
- Xing, Y., Bubier, J. L., Moore, T. R., Murphy, M., Basiliko, N., Wendel, S., & Blodau, C. (2011). The fate of ¹⁵N-nitrate in a northern peatland impacted by long term experimental nitrogen, phosphorus and potassium fertilization. *Biogeochemistry*, 103, 281-296. doi:10.1007/s10533-010-9463-0
- Yates, C. N., Wootton, B. C., & Murphy, S. D. (2012). Performance assessment of arctic tundra municipal wastewater treatment wetlands through an arctic summer. *Ecological Engineering*, 44(0), 160-173. doi:<http://dx.doi.org/10.1016/j.ecoleng.2012.04.011>
- Zak, D., Wagner, C., Payer, B., Augustin, J., & Gelbrecht, J. (2010). Phosphorus mobilization in rewetted fens: the effect of altered peat properties and implications for their restoration. *Ecological Applications*, 20(5), 1336-1349. doi:10.2307/25680382

Appendix A

Rational

In remote regions, full scale pumping test to determine aquifer properties are costly and logistically challenging and potentially out of the budget of many researchers; yet, there remains a need for the rapid determination of these properties in these regions. Although the analytical methods for multiple monitoring point pumping tests are well known (Bouwer & Rice, 1976; Neuman, 1975), there is not yet a method for single well bail or slug tests in highly permeable anisotropic unconfined aquifers, such as peatlands. Traditionally, the in-situ estimation of peat hydraulic conductivity is determined using slug or bail tests performed on piezometers screened at specific depths (Baird, 1997; Baird & Gaffney, 1994; Baird *et al.*, 2004; Schlotzhauer & Price, 1999; Surridge *et al.*, 2005; Wallage & Holden, 2011); where, the hydraulic conductivity is determined by relating the head recovery in the standpipe of a piezometer and a well construction dependent shape factor (Baird & Gaffney, 1994; Baird *et al.*, 2004; Brand & Premchitt, 1980, 1982; Hvorslev, 1951). The Hvorslev (1951) time-lag solution is commonly used in peatlands and is suitable when the head recovery curve does not exhibit a sinusoidal function (time at 90 % head recovery / time at 50 % head recovery = 3.322) or when recovery is complete or near complete (99 % head recovery) (Baird & Gaffney, 1994; Brand & Premchitt, 1982; Hvorslev, 1951). Although complete recovery readily occurs in fully screened wells installed in peat (thus, negating the need to account of media compressibility), using the Hvorslev (1951) time-lag solution maybe incorrect as it assumes a constant screen length and water flow perpendicular to the well; neither of which occur during fully screened well bail tests. Unlike piezometers, where the region contributing to flow will remain approximately the same over the course of the test, during a bail test on a well the region contributing to flow will increase as the phreatic surface in the well increases; however, the variable head Hvorslev (1951) solution can account for this variation. The transmissivity of peat deposits has been estimated using multiple bail tests on fully screened wells at different water tables over an entire field season several months (cf. Price and Maloney, 1994) and solved using the time-lag method of Hvorslev (1951). This method requires significant field work and personal to achieve satisfactory results. Due to this, the goal of this study was to develop field methods and

analytical solution for a single well response test that could be performed over hours instead of months.

Methods

To determine the transmissivity of the peat profile, a series of bail tests were performed on 13 fully penetrating wells (0.052 m I.D., and 0.062 m O.D) with incrementally smaller screen lengths. The first bail test was performed on the entire fully penetrating well and the response was recorded. Once the first bail test was completed, an inflatable well packer (2” Inflatable Pipe Plug, Perma-Type Rubber) was lowered into the well and inflated 0.3 m above the bottom of the well to isolate that region from the rest of the well (i.e., if the well was 3 m long, 0 to 2.7 m of the well remained unblocked). Once inflated, a bail test was performed on the remaining non-isolated section of the well above the packer and the response recorded. This was repeated in 0.3 m increments until ~0.7 m below the water table when the increments were decreased to 0.1 m to gain higher data resolution in the upper peat profile; where, presumably the head recovery would vary the most. The resulting packer tests were then analysed separately using a modified Hvorslev (1951) time-lag variable head solution,

$$K_i = \frac{r^2 \ln(L_t/R)}{2L_t T_t} \quad \text{Equation A - 1}$$

where, K_i is the hydraulic conductivity for a given time period between each head recovery measurement, L_t (m) is the screen length at time t (hr), and

$$T_t = \frac{\log 0.37}{s_t} \quad \text{Equation A - 2}$$

where, s_t is the slope of the head recovery over time between each measurement point calculated by,

$$s_t = \frac{h_t - h_{t-1}}{t_t - t_{t-1}} \quad \text{Equation A - 3}$$

where, h_t (m) is the water level in the pipe at time t (hr), h_{t-1} (m) is the water level in the pipe at the time prior to t (hr), t_t (m) is the time (hr), and t_{t-1} (hr) is the time prior to t_t .

Given the expected exponential increase in hydraulic conductivity closer to the top of the water table (Leclair, 2015; Perras, 2015), seepage faces are likely to occur and need to be accounted for in estimations of K_i (Chenaf & Chapuis, 2007; Schneebeli, 1956). To account for potential seepage faces during bail tests, Schneebeli (1956) developed an analytical solution to estimate the seepage face height (h_{sf}) without additional monitoring wells (Chenaf & Chapuis, 2007; Schneebeli, 1956), where,

$$h_{sf} = \sqrt{h_w^2 + \left(\frac{Q_t}{\pi K_i}\right) \cdot \left[0.4343 \cdot \ln\left(\frac{Q_t}{\pi K_i r^2}\right)\right]} - 0.4 - h_w \quad \text{Equation A - 4}$$

and, h_w (m) is the water table at time t (hr) and Q_t ($\text{m}^3 \text{ day}^{-1}$) is the volumetric discharge into the well between time t_t and t_{t-1} . The seepage face estimation is added to the screen length in Equation A - 1 to calculate a hydraulic conductivity for the time period between each head recovery measurement. The geometric mean of the measured K_i for a given packer depth is then used to develop an average hydraulic conductivity for a given well screen length (K'). Plotting K' vs screen length results in a power function where,

$$K' = Ax^{-B} \quad \text{Equation A - 5}$$

and, A and B are fitting parameters and x is the screen length.

Assuming the aquifer was comprised of an infinite number of thin horizontal layers with constant hydraulic conductivity and finite layer thickness. Also it is assumed that the flow toward the borehole is horizontal and the main part of the flow is passing through the unblocked part of the well and that part of aquifer corresponding to that. The equivalent hydraulic conductivity (K') for horizontal layers in Cartesian coordinate can be written as,

$$K' = \frac{\int_0^x K_i \times \partial x}{\int_0^x \partial x} \quad \text{Equation A - 6}$$

where, x increases downward and is 0 at the surface. Equation A - 6 can be used for radial flow in cylindrical coordinates; thus, can be written as,

$$K' = \frac{[F]_0^x}{[x]_0^x} = \frac{[F]_0^x}{x} = \frac{F(x) - F(0)}{x} \quad \text{Equation A - 7}$$

$$x \times K' = F(d) - F(0) \quad \text{Equation A - 8}$$

where, $F(x)$ is the integration of hydraulic conductivity with respect to depth (d) and

$$K_y(d) = \frac{\partial F(d)}{\partial d} \quad \text{Equation A - 9}$$

where, $K_y(d)$ is the hydraulic conductivity in a given depth (d) or the hydraulic conductivity of the infinitely thin horizontal layer at a given depth. Therefore,

$$\frac{\partial(x \times K')}{\partial x} = \frac{\partial[F(x) - F(0)]}{\partial x} \quad \text{Equation A - 10}$$

Since $F(0)$ is a constant (0), Equation A - 10 can be written as,

$$\frac{\partial(x \times K')}{\partial x} = \frac{\partial[F(x)]}{\partial x} \quad \text{Equation A - 11}$$

thus,

$$\frac{\partial(x \times K')}{\partial x} = \frac{\partial(A \times x^{1-B})}{\partial d} = (1 - B) \times A \times d^{-B} \quad \text{Equation A - 12}$$

By combining Equation A - 11 and Equation A - 12, K_y was determined by taking the derivative of the K' -screen length power function (Equation A - 5), then solving for $K_y(d)$

$$K_y(d) = (1 - B)Ad^{-B} \quad \text{Equation A - 13}$$

and the K_y (m day⁻¹) of a given depth range (i.e., 0.25 – 0.50 m bgs) can be determined by

$$K_{y_{d_2-d_1}} = \frac{\int_{d_1}^{d_2} (1 - B)Ad^{-B}}{\int_{d_1}^{d_2} \partial d} \quad \text{Equation A - 14}$$

where, d_1 and d_2 is the depth range for which the hydraulic conductivity is determined and $\int_{d_1}^{d_2} \partial d$ is the length of the depth range.

To assess the validity of this new method five piezometers (0.25 m slotted intake, 0.025 m I.D., 0.034 m O.D.) were installed within 0.5 m of each fully screened well at 0.25, 0.50, 0.75, 1.25 m and directly above the mineral substrate. Bail tests were performed on each piezometer and the recovery was recorded using Slumberger micro-divers at 1 second intervals. The resulting response curves were then analysed using Hvorslev (1951) time-lag solution. The hydraulic conductivity determined from the piezometers were plotted against the integration of the same screen depth (Equation A - 7) from the transmissivity tests, where a 1:1 slope indicates perfect agreement. Due to the potential variability in temperature within the aquifer, temperature correction to 15 °C was applied to all data (Klute, 1986; Surridge *et al.*, 2005).

Results

The hydraulic conductivity typically followed an exponential increase as the packer progressively sampled closer to the surface in the peat profile (shorter screen lengths) and had good agreement with the observed values ($R^2 > 0.86$) (Figure A-1). Regression between hydraulic conductivity of the piezometer method and the packer method resulted in a slope of 1.7 (adj. $R^2 = 0.63$, df 32, $p < 0.001$) (Figure A-1); where, a 1:1 slope is ideal and a slope of 1 equals perfect

agreement between methods. However, a sharp decrease in fit is observed with hydraulic conductivities less than 1 m day^{-1} and when excluding those values a slope of 1.12 (adj. $R^2 = 0.79$, df 16, $p < 0.001$) was observed (Figure A-2), while below that threshold a slope of 0.5 was observed (adj. $R^2 = 0.10$, df 15, $p = 0.126$) (Figure A-2). Typically, hydraulic conductivities above 1 m day^{-1} were exclusively observed within the upper 0.5 m of the saturated peat aquifer (Figure A-3).

Discussion and Conclusions

Similar to Surridge *et al.* (2005), temperature correction resulted in a change of ~25 % in the hydraulic conductivities. The good agreement between the transmissivity tests and the piezometer measurements where hydraulic conductivity was above 1 m day^{-1} (slope near 1) indicates the potential for this method to determine the hydraulic conductivity of the upper layers in peatlands. The slope of the relationship between screen length and hydraulic conductivity when the

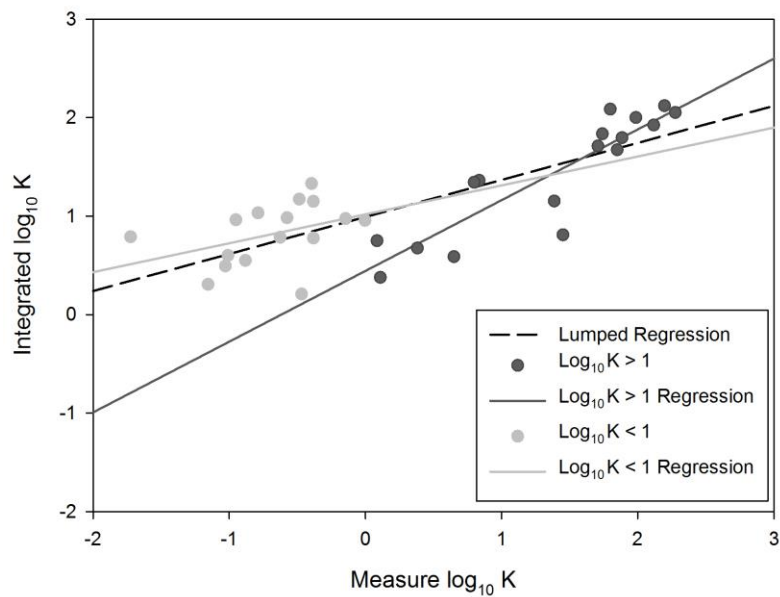


Figure A - 1 Linear regression between piezometer measured $\log_{10} K$ and the integrated $\log_{10} K$ determined by integrating the transmissivity curve over the piezometer screen opening depth. The lumped regression (dashed black line) accounts for all measurements, while hydraulic conductivities greater than 1 m day^{-1} (dark grey points and line) and less than 1 m day^{-1} (grey points and line) were separated.

latter is above 1 m day^{-1} indicates that the packer method slightly over-estimated (~12 %) hydraulic conductivity compared to the traditional Hvorslev (1951) time-lag solution for locations closest to the water table; it under-estimated (~46 %) further below the water table. Furthermore, previous work estimating the transmissivity of the peat aquifer in the EXP Fen ($0.07 - 43 \text{ m}^2 \text{ day}^{-1}$) (Perras, 2015) observed over a range of water tables ($-0.3 - 0.0 \text{ m bgs}$) agrees well with the estimated range in this study ($0.1 - 69.3 \text{ m}^2 \text{ day}^{-1}$). The method seems to be applicable for estimating both the hydraulic conductivity near the top of the water table (0.5 m) and the transmissivity of the highly

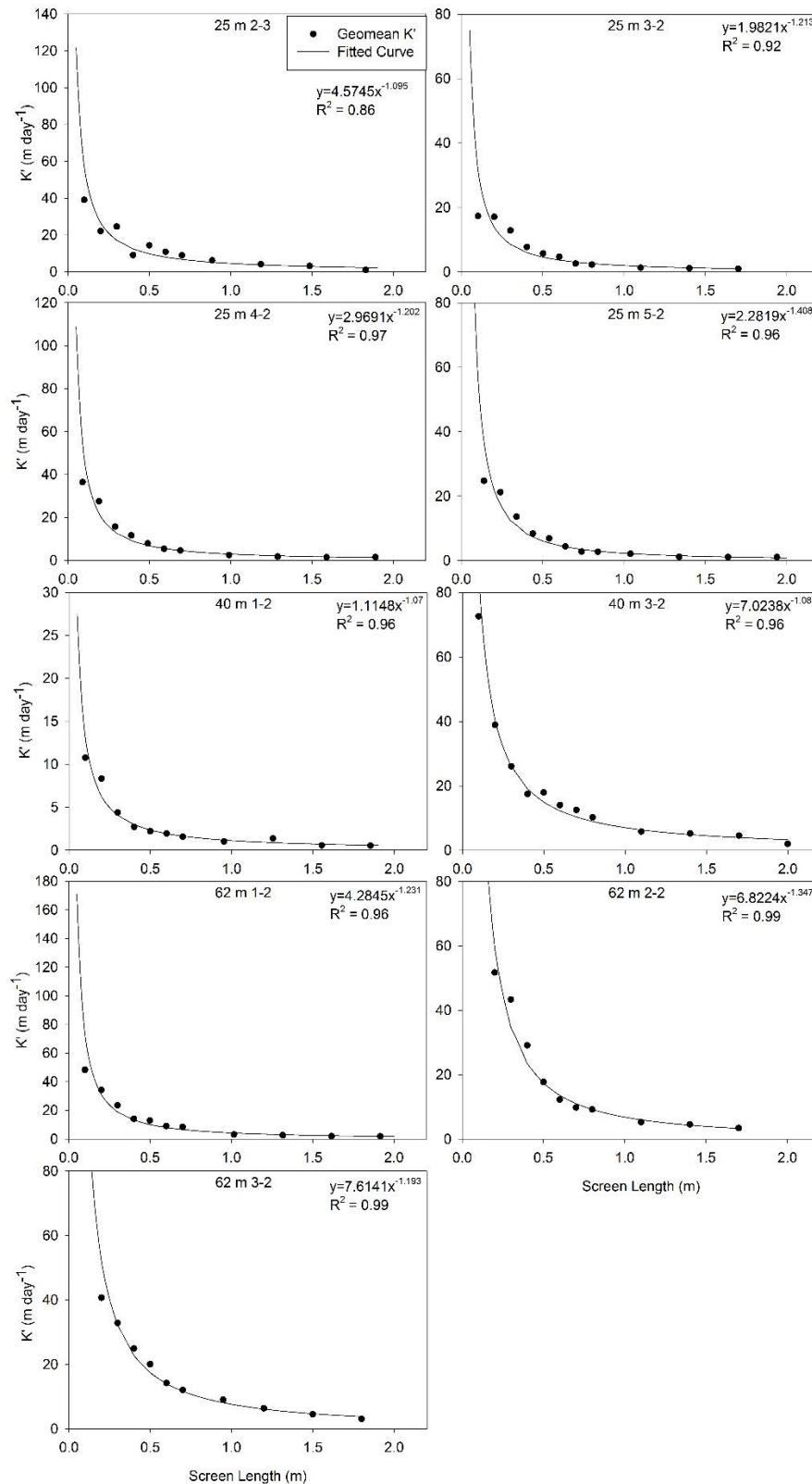


Figure A - 2 K' vs screen length for all nine tested wells.

anisotropic and heterogeneous aquifer. Unlike previous methods where bail or slug tests were performed at various water tables through the spring, summer and fall, this method requires only one test to be performed near or at the maximum water table and are typically completed within several hours. Thus, significantly less time is spent in the field and potentially decreasing overall costs associated with field work.

Notwithstanding the good agreement with measured data and previous studies (Perras, 2015), further refinement of this method is required to achieve greater accuracy

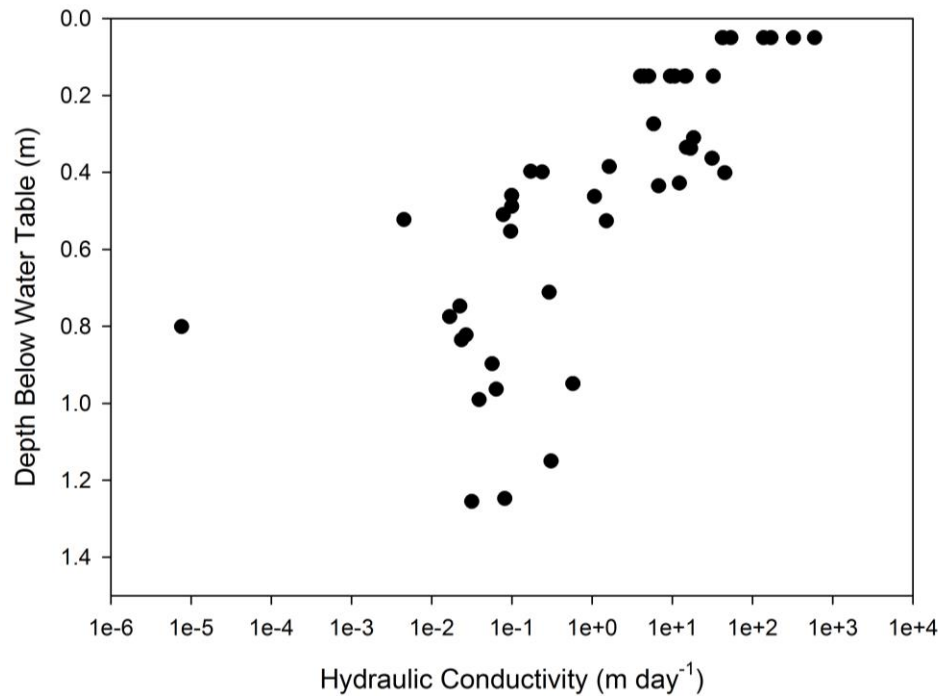


Figure A - 3 Hydraulic conductivity distribution at the EXP Fen. Above 0.3 m the hydraulic conductivity was determined through the packer method, while below 0.3 m the values were determined from the piezometer tests. The difference in maximum elevation is due to the differing surface elevations at the EXP Fen. Ribs 1-3 surface elevation is ~ 87.4 m asl, while the rest of the site is ~87.0 m asl.

within the low hydraulic conductivity peat layers. To achieve higher accuracy high temporal resolution pressure transducers could be used to better capture the entire recovery curve, as well as decreasing the packer interval to 0.1 m throughout the test instead of 0.3 m in the lower portion of the aquifer. Although

pressure transducers can provide high temporal resolution pressure data, they are subject to large fluctuations in pressure as noted by Surridge *et al.* (2005) and observed during an extremely wet year (2015, data not shown). This phenomena has been identified when the permeability of the substrate is extremely high, resulting in rapid flow into the well (Surridge *et al.*, 2005) and from seepage faces (Chenaf & Chapuis, 2007; Schneebeili, 1956). It is possible to capture these rapid rates using manual (i.e., blow sticks) measurements to gain an estimate of the recharge; however, for fully penetrating wells (2.3 m in this study) the length of the blow stick may impede the measurements. Utilizing a combination of decreased packer intervals (0.1 m), pressure transducers, and longer blow sticks may increase the sensitivity of the method to the low hydraulic conductivity layers at the bottom of the peat profile. Notwithstanding these potential improvements and limited sample size, the method presented in this study gives good approximations of both the transmissivity and the hydraulic conductivity of the upper peat layers. Additionally, this method also has the advantage over traditional transmissivity tests, which require multiple measurements

at different water table elevations because it requires one test performed near the peak water table to generate the transmissivity and hydraulic conductivity distribution.